



## **DC/AC Inverter based Switched Capacitor Topology**

---

**Department of Electronics and Computer Engineering  
College of Engineering, Design and Physical Sciences  
Brunel University, London, UK**

**By**

**Mohd Helmy Hakimie Bin Mohd Rozlan**

**A thesis Submitted for the degree of Doctor of Philosophy**

**Supervised**

**By:**

**Dr Mohamed Darwish**

**April, 2017**

## **Abstract**

This thesis presents a new DC/AC inverter circuit which is based on a switched-capacitor circuit topology with reduced components (power switch and capacitor) count for low power applications. The proposed circuit has distinct features of both voltage boost-up and near sinusoidal (multi-level/staircase) AC output voltage. The main idea is to utilise a simple circuit technique called resonant-based Double Switch Single Capacitor Switched-Capacitor (DSSC SCC) with variable duty cycle Pulse Width Modulation (PWM) control technique in such a way that multi-level voltage can be realised across a capacitor. In order to show the superiority of the applied technique, comparisons with other techniques/circuits configurations are presented. The circuit technique can significantly reduce the number of multiple stages of switched-capacitor circuit cells of the recent switched-capacitor multi-level inverter topology. The proposed inverter (with integrated DSSC SCC technique) can generate a line-frequency with 13-levels near sinusoidal AC output voltage with low total harmonics distortion. The output voltage can be achieved with the least number of components use and only a single DC source is used as an input. The proposed inverter topology is also reviewed against other inverter-based switched-capacitor circuit topology and the well-known multi-level inverter topology. The proposed inverter has shown a tremendous reduction in the total harmonics distortion and circuit component count in comparison with the recent Switched-Capacitor Boost multi-level inverter and the classical Cascaded H-Bridge multi-level inverter. Mathematical analysis shows the design of the proposed inverter and PSPICE simulation result to verify the design is also presented. The practical experiment implementation of the proposed system is presented and proves the correct operation of the proposed inverter topology by showing consistency between simulation results and practical results.

*I dedicate this thesis to*

*My Parents, Mohd Rozlan Abd Ghapar, Aznah Abdul Aziz,*

*lovely wife, Dr Nurul Syuhada Ramli*

*Son, Muhammad Ammar Harith,*

*Brothers and Sister, Afiq Azali, Afiq Farhan, Zarul Izham, Farra*

*Nadia,*

*& Humanity and My home country, Malaysia*

## **Acknowledgments**

First, I would like to thank Almighty Allah, the one who granted me a long life, and who always supported and blessed me with strength and good health. I also would like to thank my supervisor Dr Mohamed Darwish for his kindest guidance and assistance during my PhD study. He is a helpful advisor and the best instructor for the achievement of this thesis. I would like to special my thanks to Dr Christos Marouchos, Dr Michael Theoridis and Dr Maysam Abbod for their kind support and help.

I also thank the friendly staff and my research group colleagues at the Brunel Institute of Power Systems (BIPS) for their support and friendship.

Great thanks to my family, especially my fathers, my mothers, my brothers and sisters for their prayers, patience, and emotional support throughout conducting this research. Special thanks to my beloved wife, Dr Nurul Syuhada Ramli and son, Muhammad Ammar Harith, for their patience and emotional support.

# Table of Contents

<b>Abstract.....</b>	<b>II</b>
<b>Acknowledgments .....</b>	<b>IV</b>
<b>Table of Contents .....</b>	<b>V</b>
<b>List of Tables .....</b>	<b>VIII</b>
<b>List of Figures.....</b>	<b>X</b>
<b>List of Symbols .....</b>	<b>XIV</b>
<b>List of Abbreviations .....</b>	<b>XVII</b>
<b>Chapter 1 Introduction.....</b>	<b>1</b>
1.1    Overview .....	1
1.2    Research Question.....	4
1.3    Research Motivation .....	5
1.4    Research Aim and Objectives .....	6
1.4.1    Research Approach .....	7
1.4.2    Contributions to Knowledge .....	7
1.4.3    Thesis Overview and Structure .....	9
<b>Chapter 2 Literature Review of DC/AC Inverters .....</b>	<b>11</b>
2.1    Introduction .....	11
2.2    Classification of DC/AC Inverter Circuit.....	11
2.2.1    Voltage Source Inverter .....	14
2.2.2    Current Source Inverter.....	17
2.2.3    Impedance Source Inverter.....	19
2.2.4    Classical Multi-Level Inverter Topologies .....	23
2.2.5    Improving THD in CHB-MLI circuit topology .....	33
2.3    Summary of PWM Inverters & Multi-Level Inverter topologies .....	38
2.4    Summary .....	42

## **Chapter 3 Switched-Capacitor Circuit & Switched-Capacitor Multi-level DC/AC Inverter Topologies ..... 43**

3.1	Introduction .....	43
3.2	Overview of Voltage Boosting Technique.....	44
3.3	Switched Capacitor .....	46
3.3.1	Resonant-based Double Switch Single Capacitor (DSSC) circuit .....	50
3.3.2	Resonant-based Double Switch Double Capacitor (DSDC) circuit.....	65
3.3.3	Resonant-based Single Switch Single Capacitor (SSSC) circuit. ....	67
3.3.4	Resonant-based Triplen switch SCC circuit.....	68
3.3.5	Capacitor-based switched-capacitor circuit in series-parallel connection ....	70
3.4	Other Voltage Boosting Techniques .....	73
3.4.1	Magnetic Coupling.....	73
3.4.2	Multi-Stage Booster .....	74
3.5	General Comparison of Voltage Boosting Techniques.....	75
3.6	Selection of the SCC for the Proposed Inverter .....	76
3.7	Switched-Capacitor Multi-Level DC/AC Inverter Topologies .....	84
3.7.1	Cascaded-Boost Switched-Capacitor Multi-Level Inverter .....	86
3.7.2	Switched-Capacitor Boost-Multi-Level Inverter Using Partial Charging....	88
3.7.3	Switched-Inductor Multi-Level Inverter .....	92
3.7.4	Switched-Capacitor Inverter using Series/Parallel Conversion .....	94
3.7.5	Hybrid Multi-Level Inverter using Switched-Capacitor unit.....	96
3.8	Comparison of Different DC/AC Inverter Topologies .....	98
3.9	Summary .....	106

## **Chapter 4 Proposed DC/AC Inverter Circuit Topology and Control Technique..... 108**

4.1	Introduction .....	108
4.2	Proposed Inverter System.....	109
4.3	Operating Modes of the Proposed Inverter System .....	106
4.4	Design & Analysis .....	113
4.4.1	Design Procedure of the Proposed Inverter.....	114
4.4.2	Fourier Analysis .....	117
4.4.3	Design Example and Calculation of the Proposed Inverter .....	118
4.5	Proposed Control Technique .....	122
4.6	Summary .....	129

<b>Chapter 5 Simulation and Practical Implementation of the Proposed Inverter System .....</b>	<b>130</b>
5.1    Introduction .....	130
5.2    Choice of Simulation Modelling Package.....	131
5.3    Simulation of the Proposed Inverter Circuit using OrCAD PSPICE .....	132
5.4    Parameter of the Proposed Inverter Circuit.....	132
5.5    Simulation of the Designed Inverter System.....	134
5.5.1    Pure Resistive Load.....	137
5.5.2    High Inductive Load.....	143
5.6    Practical Implementation of the Proposed Inverter.....	146
5.7    Practical Comparison amongst DC/AC Inverter Topologies .....	155
5.8    Discussion .....	157
5.9    Summary .....	157
<b>Chapter 6 Conclusions and Future Work .....</b>	<b>159</b>
6.1    Conclusions .....	159
6.2    Future Works.....	165
<b>References .....</b>	<b>166</b>
<b>Appendix A .....</b>	<b>175</b>
Arduino C-language Program Code: Switching Control Pattern Generation .....	176
<b>Appendix B .....</b>	<b>182</b>
List of Publications .....	183

## List of Tables

Table 2.1 Single-Phase H-Bridge VSI Switching States .....	15
Table 2.2 Five-levels DC-MLI Switching States.....	26
Table 2.3 Five-levels FC-MLI Switching States.....	29
Table 2.4 Seven-level Symmetric CHB-MLI switching states.....	32
Table 3.1 Relationship between capacitor voltage level & duty cycle (Theoretical Calculation).....	64
Table 3.2 General comparison among voltage boosting techniques.....	78
Table 3.3 Comparison between SCC topologies/techniques for the performance selection criteria .....	82
Table 3.4 General Performance comparison of different multi-level DC/AC inverter topologies .....	104
Table 3.5 Comparison of different multi-level DC/AC inverter topologies to produce thirteen-levels output voltage.....	105
Table 4.1 Relationship between capacitor voltage level and duty cycle (Theoretical Calculation) .....	119
Table 4.2 Main switching angle or time (Theoretical Calculation) .....	120
Table 4.3 Variable amplitude modulation (or variable duty cycle) (Theoretical Calculation) .....	126
Table 5.1 Proposed inverter parameter for highly resistive load .....	133
Table 5.2 Proposed inverter parameter for highly inductive load.....	134
Table 5.3 Parameter component values (Experimental) .....	149
Table 5.4 Amplitude of output harmonics (purely resistive load) .....	152
Table 5.5 Amplitude of output harmonics (highly inductive load).....	154
Table 5.6 Experimental comparison between proposed inverter circuit topology and other inverter topologies performance for thirteen-levels output voltage.....	156

Table 5.7 Comparison between proposed inverter and other multi-level inverter topologies in term of components count for thirteen-levels output voltage..... 156

## List of Figures

Figure 2.1 Classification of DC/AC Inverters.....	13
Figure 2.2 Single-Phase H-bridge Voltage Source Inverter.....	15
Figure 2.3 Single-Phase Boost CSI Inverter .....	18
Figure 2.4 Three-Phase ISI Inverter.....	20
Figure 2.5 DC/AC inverter output waveforms.....	21
Figure 2.6 Diode-Clamped MLI circuit .....	26
Figure 2.7 Flying-Capacitor MLI circuit .....	28
Figure 2.8 Cascaded H-Bridge MLI circuit .....	32
Figure 2.9 Seven-level output voltage of the Symmetric CHB-MLI circuit.....	33
Figure 2.10 Seven-levels output voltage of the Symmetry CHB-MLI circuit (Equal step DC link voltage) .....	34
Figure 2.11 Harmonics spectrum of seven-levels CHB-MLI output voltage (before optimisation) .....	35
Figure 2.12 Optimised seven-levels CHB-MLI output voltage (Unequal step DC link source) .....	37
Figure 2.13 Harmonics spectrum of seven-levels CHB-MLI (more harmonics order eliminated). .....	37
Figure 3.1 Categorisation of voltage boosting technique.....	45
Figure 3.2 Categorisation of switched capacitor according voltage gain/ ability and the type of circuit topology/configuration .....	46
Figure 3.3 Basic configuration unit of the shunt-connected SCC.....	49
Figure 3.4 Resonant-based DSSC circuit.....	50
Figure 3.5 DSSC circuit identical to the effective capacitance.....	51
Figure 3.6 Relationship of effective capacitance and duty cycle (Theoretical).....	56
Figure 3.7 Resonant-based DSSC circuit in Mode 1 .....	58
Figure 3.8 Capacitor voltage during Mode 1 (Theoretical) .....	60

Figure 3.9 Capacitor current during Mode 1(Theoretical).....	61
Figure 3.10 Relationship between capacitor voltage and duty cycle with respect to S <sub>1</sub> for DSSC SCC circuit (Theoretical) .....	63
Figure 3.11 Resonant shunt-connected DSDC SCC circuit.....	65
Figure 3.12 Relationship between capacitor voltage and duty cycle with respect to S <sub>1</sub> (Theoretical) .....	66
Figure 3.13 Resonant-based Single Switch Single Capacitor circuit.....	67
Figure 3.14 Resonant shunt-connected Triplen switch circuit.....	68
Figure 3.15 Relationship between capacitor voltage and duty cycle with respect to S <sub>1</sub> for Triplen SCC circuit (Theoretical).....	70
Figure 3.16 Basic unit of S-C cell.....	71
Figure 3.17 SC cell operation: (a) Capacitor Charging and (b) Capacitor discharging .....	71
Figure 3.18 Buck Inverter with bulky line-frequency transformer .....	74
Figure 3.19 DC/DC Multi-Level Boost Converter .....	75
Figure 3.20 Classification of switched-capacitor multi-level inverter topologies .....	86
Figure 3.21 Five-levels Cascaded Boost-Switched-Capacitor Multi-Level Inverter circuit topology .....	87
Figure 3.22 Thirteen-levels Switched-Capacitor Boost-Multi-Level inverter circuit topology .....	88
Figure 3.23 Five-levels output voltage of the SCB-MLI circuit.....	89
Figure 3.24 Harmonics spectrum of five-levels SCB-MLI output voltage.....	90
Figure 3.25 Seven-levels output voltage of the SCB-MLI circuit .....	90
Figure 3.26 Harmonics spectrum of seven-levels SCB-MLI output voltage.....	91
Figure 3.27 Thirteen-levels output voltage of the SCB-MLI circuit .....	91
Figure 3.28 Harmonics spectrum of thirteen-levels SCB-MLI output voltage.....	92
Figure 3.29 Seven-levels Switched-Inductor Multi-Level Inverter circuit topology.	93
Figure 3.30 Seven-levels output voltage waveform of SI-MLI circuit.....	94

Figure 3.31 Frequency spectrum of output voltage of SI-MLI circuit.....	94
Figure 3.32 Seven-levels switched-capacitor inverter using series/parallel conversion .....	96
Figure 3.33 Hybrid Multi-Level Inverter using Switched-Capacitor Circuit unit ....	97
Figure 4.1 Circuit Block Diagram of Proposed Inverter System .....	111
Figure 4.2 Circuit diagram of the proposed inverter:.....	106
Figure 4.3 Equivalent Circuit for Mode 1 .....	109
Figure 4.4 Simplified Equivalent Circuit for Mode 1 .....	109
Figure 4.5 Equivalent Circuit for Mode 2 .....	111
Figure 4.6 Percentage of THD of output voltage $V_{THD}$ in terms of high switching frequency.....	121
Figure 4.7 Control logic circuit for DSSC circuit .....	124
Figure 4.8 Timing diagram of the control signal for a rectified staircase/multi-level waveform during period (0 to 10ms) (Theoretical).....	127
Figure 4.9 Timing diagram of the control signal for one cycle near AC output voltage waveform (0 to 20ms) (Theoretical) .....	128
Figure 5.1 Control Circuit .....	135
Figure 5.2 PSPICE switching pattern result: (a) carrier and reference signals & (b) to (e) control signals.....	136
Figure 5.3 Proposed inverter circuit with pure resistive load $R_o = 10 \Omega$ .....	137
Figure 5.4 Proposed inverter simulation result (for resistive load): (a) rectified voltage across H-Bridge, (b) output voltage and (a) output current .....	138
Figure 5.5 FFT analysis of the (a) output voltage and (b) output current spectrum (for resistive load) .....	139
Figure 5.6 FFT of the output voltage of the proposed inverter for purely resistive load (Simulation) .....	139
Figure 5.7 FFT of the output voltage of the proposed inverter for purely resistive load (Simulation) .....	140

Figure 5.8 Total power losses in the proposed inverter .....	142
Figure 5.9 losses in the proposed inverter system .....	143
Figure 5.10 Losses in MOSFETs Switches .....	143
Figure 5.11 The proposed inverter circuit with highly inductive load.....	144
Figure 5.12 Proposed inverter simulation result (for inductive load): (a) rectified voltage across H-Bridge, (b) output voltage and (a) output current .....	145
Figure 5.13 Proposed inverter simulation result (for inductive load): (a) output voltage and (b) output current.....	145
Figure 5.14 FFT of the output voltage of the proposed inverter for highly inductive load (Simulation).....	146
Figure 5.19 Switching pattern control signals.....	150
Figure 5.18 Measured output voltage waveform (resistive load) .....	151
Figure 5.19 Measured output current waveform (resistive load) .....	151
Figure 5.20 Measured output voltage harmonics spectrum (resistive load) .....	152
Figure 5.21 Measured output voltage waveform (highly inductive load).....	153
Figure 5.22 Measured output voltage harmonics spectrum (highly inductive load)	153

## List of Symbols

$\emptyset$	High frequency component of Switching Function
$\alpha$	Damping factor
$\Delta v_c$	Capacitor ripple voltage
$\omega_0$	Resonant frequency
$\omega_r$	Ringing frequency /damped resonant frequency
$\omega_s$	Angular switching frequency
$A_n, B_n, D_o$	Fourier Coefficient
C	Capacitance
Ceff	Effective capacitance
$D_o$	Duty cycle of switches
$D_k$	Varying duty cycle of the switches
D	Diode
$D_k$	Duty cycle
F <sub>car</sub>	Carrier signal frequency
F <sub>ref</sub>	Reference signal frequency
$F_s$	High Switching Frequency
$F_o$	Fundamental switching period
$F(t)$	Switching Function

$i(t)$	Instantaneous current
$I_{THD}$	Total harmonic distortion of current
$L$	Inductance
$m$	Number of voltage levels
$m_a$	Amplitude modulation
$m_f$	Frequency modulation
$n$	Number of harmonic order
$n$	Number of repeating switching cycle
$R_1$	Internal resistance of Inductor
$S$	Switch
$t_a, t_{on}$	ON Time switch duration
$t_b, t_{off}$	OFF Time switch duration
$t$	Time point
$T_s$	High Frequency Switching period
$T_o$	Fundamental switching period
$TX$	Transformer
$V_{dc_k}$	Multi-level DC amplitude of the reference signal
$V_{tri}$	Amplitude of the carrier signal
$V_{ref}$	Amplitude of the reference signal

$V_{THD}$	Total harmonic distortion of voltage
$V_{dc}$	DC Voltage
$V_{c_0}$	Initial capacitor voltage
$V_a, V_H, V_i$	DC link voltage or DC Bus Voltage
$V_{a0}, V_{an}$	Multi-level output voltage
$X_c$	Capacitive Reactance

## **List of Abbreviations**

ASD	Adjustable Speed Drive
AC	Alternating current
BJT	Bipolar Junction Transistor
CCM	Continuous conduction mode
CSI	Current Source Inverter
DC/AC	Direct Current to Alternating current
DC/DC	Direct Current to Direct Current
DC	Direct Current
DSSC	Double Switches Single Capacitor
DSDC	Double Switches Double Capacitor
EMI	Electromagnetic interference
ESR	Equivalent Series Resistance
IGBT	Insulated Gate Bipolar Transistor
ISI	Impedance Source Inverter
KVL	Kirchhoff's Voltage Law
MLI	Multi-level Inverter
MOSFET	Metal Oxide Semiconductor Field Effect Transistor
Op-Amp	Operational Amplifier

PWM	Pulse-width modulation
RS	Reference signals
RMS	Root Mean Square
S-C	Switched capacitor
SCC	Switched-Capacitor Circuit
SPWM	Sinusoidal Pulse-width modulation
SSSC	Single Switch Single Capacitor
SHE	Selective Harmonics Elimination
THD	Total Harmonics Distortion
UPS	Uninterruptable Power Supply
VSI	Voltage Source Inverter

# **Chapter 1 Introduction**

## **1.1 Overview**

The DC/AC inverter is one of the categories of power electronics technology that involves a conversion process and control in transferring electric power from an electrical DC source to an electrical AC output load, with a change in voltage magnitude, frequency, and number of output phases in a form that is suitable and efficient for the user electrical load (Rashid, 2006). The advances of semiconductor power switch devices, such as the Bipolar Junction Transistor (BJT), Metal Oxide Semiconductor Field Effect Transistor (MOSFET), and Insulated Gate Bipolar Transistor (IGBT) etc, have the capacity to improve power electronics DC/AC inverter performance.

Recently, power electronics DC/AC inverter has become an important device, and its relevance for many industrial and commercial as well as domestic applications, such as adjustable speed drives (ASD), renewable energy system conversion (RES), uninterruptable power supplies (UPS) (Luo and Ye, 2013), and home appliances is growing rapidly. The inverter systems in these applications should have low total harmonic distortion (THD), high efficiency, simplicity, and low cost (Rashid 2006, Luo and Ye, 2013). In addition, the inverters should be able to operate continuously without interruption. Many DC/AC inverter topologies and control methods are proposed in the literature survey, including conventional three-levels PWM DC/AC inverters, voltage source inverter (VSI), current source inverter (CSI) and impedance source inverter (ISI), and classical multi-level inverter (MLI) topologies.

Although conventional three-levels PWM inverters are reliable due to a lower number of power switches usage, the main disadvantage of the PWM inverter is high total harmonic distortion (THD) in output voltage and current. This is commonly reduced by modulating the power switches at higher switching frequencies. Therefore, achieving lower voltage THD is associated with high switching losses in power switches (Rashid 2006, Luo and Ye, 2013).

Many classical multi-level inverters (MLIs) topologies, such as Diode Clamped MLI (DC-MLI), Flying Capacitor MLI (FC-MLI), and Cascaded H-Bridge MLI (CHB-MLI) can achieve lower total harmonic distortion of the output voltage and current, and provide reduced power losses at the same time (Luo and Ye, 2013). They are still effective, with low-voltage stress on power switches and without requiring large passive filter at the output (Mecke 2011; Luo and Ye, 2013). However, the classical MLIs with fundamental low switching control require a large number of power switches and DC-link capacitors or isolated DC sources in achieving lower THD.

Apart from many extensive studies conducted in improving various aspects of the classical multi-level inverter, researchers continue to contribute towards the evolution of newer multi-level inverter circuit topology with reduced device count and simple control (Gupta et al. 2016). Many research efforts have begun to incorporate switched-capacitor circuits, which has had a significant impact on reducing the required number of isolated DC input source and power switches count (Luo and Ye, 2013, Babaei, Gowgani 2014, Barzegarkhoo et al. 2016). The recent switched-capacitor multi-level inverter topologies can generate more output voltage levels with a reduced number of isolated DC sources and reduced number of power switches usage, as compared to the classical ones (Barzegarkhoo et al. 2016). The multi-level

voltage output can be generated by controlling the capacitor charging and discharging in the multi-stage configuration of switched-capacitor circuit cells supplied from a minimum number of DC input sources (Babaei, Gowgani 2014). This switched-capacitor circuit cell can be controlled at a fundamental low switching frequency or at high switching frequency. However, to achieve low THD voltage, many newer switched-capacitor multi-level inverter topologies still have complex structures and control circuits that require many DC-link capacitors and power switches with associated gate drive units, protection units, and cooling units. In addition, unbalanced capacitor voltage problems can exist in these topologies and capacitor voltage balancing control techniques are required, which becomes more complicated when achieving a higher number of output voltage levels (Babaei, Gowgani 2014).

Therefore, appropriate switched-capacitor circuit configuration and control technique will be investigated to generate more numbers of output voltage levels, in order to achieve minimum THD voltage with minimum number of power switches and DC-link capacitors required, instead of requiring multiple stages configuration of switched-capacitor circuit cells in existing switched-capacitor multi-level inverter topologies. This will therefore minimise the overall inverter cost, size, and weight.

A new optimum DC/AC inverter circuit configuration is proposed, which is the main contribution of the thesis in the power electronics DC/AC inverter field. Such an inverter is desirable to produce AC output voltage with an acceptable amount of total harmonics distortion, efficiency, small size, and low cost. This proposed inverter could be used for low-voltage (270V- 600V) low-power (5-150kW) applications like in aircraft and electric vehicle systems where weight and size are critical requirements, and without constraints on the switch voltage stress.

## 1.2 Research Question

Traditional three-levels PWM inverter circuits are used to convert DC to AC voltage. However, this conversion process is associated with high distortion of voltage as well as current waveforms. In order to reduce distortion as well as output passive filter size, the conventional inverters should operate at higher switching frequencies. Obviously, the high switching frequencies are associated with high switching losses in power switches. One way to simultaneously reduce the harmonic distortion and switching losses is to use multi-level inverter circuit. The classical multi-level inverter topologies like DC-MLI, FC-MLI, and CHB-MLI, while effective, suffer from some limitations like a large number of isolated DC sources or a large number of DC-link capacitors, diodes, and power switches.

Recent switched-capacitor multi-level inverter topology has reduced the count of devices used to generate high multi-level AC voltage from a single DC source as compared to classical multi-level inverter circuit topology without using a transformer (Babaei, Gowgani 2014). This can increase the efficiency without having bulky inductors and can reduce system size and cost.

Yet, this circuit topology demands an increasing number of DC-link capacitors and power switches when constructing a higher number of voltage levels in order to achieve lower harmonics distortion. This still leads to having a bulky inverter circuit size and weight due to the complex control circuit. For low-voltage and low-power applications, such as in aerospace, marine applications, and electric vehicles, voltage quality and weight are the two of the critical requirements that are difficult to comply with conventional three-levels PWM inverters because of the need for heavy differential mode and common mode filters. This weight requirement could also be

difficult to meet in recent switched-capacitor multi-level inverter topologies. Therefore, the main challenge for the researcher is to design an optimum DC/AC inverter circuit that can generate acceptable sinusoidal AC output voltage waveform with a higher number of voltage levels so that a minimum THD voltage can be generated, using a minimum number of power switch, diodes and DC-link capacitors or separated DC input sources, and so that minimum associated control circuit components such as power switch gate drivers, protection units (opto-isolators), and cooling systems (heat-sinks).

### 1.3 Research Motivation

The research focuses on reducing the component (i.e. switches and capacitors) count required in switched-capacitor multi-level inverter circuit topology so that it can be used in low power applications. This topology has a minimum number of isolated DC source required and reduced number of power switches in comparison to the classical multi-level inverter topologies i.e. CHB-MLI, FC-MLI, and DC-MLI, when generating higher numbers of output voltage levels (Luo and Ye, 2013, Barzegarkhoo et al. 2016). However, generating a higher number of output voltage levels in order to achieve lower harmonics in output voltage waveform is associated with a multiple stage configuration of switch and capacitor components as well as a complex control circuit. This also can lead to unbalanced capacitor voltage issues between capacitors when connected in series.

For the past few years, efforts made to reduce the number of devices in the classical multi-level inverter topologies have been receiving wide attention in the field of multi-level DC/AC inverter research (Luo and Ye, 2013, Gupta et al. 2016,

Barzegarkhoo et al. 2016). Furthermore, the advance of power semiconductor switching device technology capable of working in high-speed helps to minimise the size of passive components (inductor and capacitor). Reducing the number of the power switches, passive components (inductor and capacitor), and harmonic filters as well as operating at higher switching frequency can lead to lower cost, smaller-in-size-yet-higher-in-reliability, and higher power conversion efficiency inverters. The contribution of switched-capacitor circuit technique in Darwish and Mehta, 1990 operating at high switching frequency could be helpful in reducing the size of the complex structure in existing switched-capacitor multi-level circuit topology.

## 1.4 Research Aim and Objectives

The aim of the thesis is to design a new DC/AC inverter topology with low harmonics distortion in output voltage using the least number of components for reducing the complexity and the cost of building the multi-level inverter for low power applications where size and weight are critical requirements.

The research aim is address through the following objectives:

- To review of the DC/AC inverters circuit; conventional PWM, classical and newly-evolved multi-level topologies and their modulation techniques.
- To review the available boosting voltage techniques.
- To review and investigate the different types of switched-capacitor circuit (SCC) topologies for voltage boosting and/or varying.
- To introduce a new type of circuit technique by modifying the existing DSSC SCC as a voltage regulator.

- To integrate the new circuit technique (voltage regulator) into the proposed DC/AC inverter system.
- To design and simulate the proposed inverter system.
- To validate the system design through practical hardware implementation.

#### **1.4.1 Research Approach**

The proposed inverter topology evolves from a single-phase current source inverter (CSI) topology. In the proposed inverter, a double switch single capacitor (DSSC) switched-capacitor circuit (SCC) technique is introduced. With a current source (DC voltage in series with an inductor and its internal resistance) applied at the proposed inverter input, the DSSC SCC can act as voltage controller where the capacitor voltage can be varied by controlling the switch duty cycle ratio at different values. The combination of a current source and DSSC SCC form a circuit which can also called ‘a resonant DSSC SCC circuit’. The introduction of the DSSC SCC technique in DC/AC inverter circuit is the main aspect in this research, as this has not yet been studied and implemented in the field of DC/AC inverters. The DSSC SCC technique is mainly used in the area of AC reactive high-power control and active power filters with AC voltage supplied from the input source.

#### **1.4.2 Contributions to Knowledge**

Many of new evolved switched-capacitor multi-level inverter topologies suffer from increasing multiple stages of switched-capacitor circuit cells (which consist of large numbers of power switches and DC-link capacitor components) to generate a

higher number of voltage levels, in order to achieve lower harmonic distortion at the output voltage and current and to achieve higher output power density.

In this thesis, a suitable circuit technique with the capability of reducing the number of required circuit components with less control complexity is investigated and a new DC/AC inverter circuit topology with a reduced count of power switches and capacitors is proposed. This is achieved by introducing a simple resonant-based DSSC switched capacitor circuit with variable duty cycle control technique which acts as voltage regulator. In such a way that a rectified stepped sinewave can be generated across a capacitor by applying variable duty cycle control to the associated power switches. This technique reduces the required number of capacitors with its associated power switch, which is far less when compared to the recent switched-capacitor multi-level inverter topologies.

The novelty of the research work is introducing the resonant-based DSSC switched capacitor circuit to the field of DC/AC inverter. The main applications of the switched capacitor circuits in electrical power field are in active filtering and AC reactive power compensation, while no research has been conducted to introduce it to the field of DC/AC inverter. The proposed inverter could be used in low-voltage and low-power applications such as aerospace and marine industries where voltage quality and weight are two critical requirements that need to be addressed.

### **1.4.3 Thesis Overview and Structure**

The thesis consists of six chapters, divided as follows: Chapter 1 provides an introduction including the aim, objectives, and outline of the thesis. Chapter 2 conducts an overview of traditional three-level PWM and classical multilevel DC/AC inverter circuit topologies and modulation techniques, which highlights the advantages and disadvantages of each topology and technique. In addition, an introduction of optimization techniques used to improve THD of the classical MLI and their advantages and disadvantages is provided.

Chapter 3 is divided into two sections. The first section conducts an overview of several voltage boosting technique in terms of the circuit configuration which highlights the advantages and disadvantages. Elaborates different techniques and topologies for voltage boosting and varying voltage using switched-capacitor circuit with critical comparison amongst them in terms of topologies and connections. In addition, a brief of overview of other famous voltage boosting techniques (magnetic couple and multi-stage booster). It also introduces new varying voltage technique using switched-capacitor circuit. It also conducts a comparative study of reviewed switched-capacitor circuit technique configuration in identifying an optimum configuration that has varying voltage or multi-level voltage ability with switch duty cycle control to be part of the proposed DC/AC inverter in this research effort. Following that, it presents mathematical analyses and derivations of the switched-capacitor circuit, showing its behaviour for a given duty cycle control as a variable capacitor and voltage regulator (varying voltage characteristic) ability. Selection performance criteria are set out for the decision to include the optimum switched-capacitor circuits as part of a new proposed DC/AC inverter circuit.

The second section presents reviews of recent multi-level DC/AC inverter based on switched-capacitor circuit topologies and control techniques in achieving staircase AC voltage waveform, which highlights the advantages and disadvantages of each topology and technique. This is to identify the gap or limitation as well as the merit of each recent switched-capacitor multi-level DC/AC inverter topologies.

Chapter 4 presents the proposed DC/AC inverter circuit system with a reduced component count which can be used for low power applications. The operating principle, design and analysis, and control techniques are elaborated on in detail. The author's main contribution is the integration of the optimum switched-capacitor circuit configuration assessed and selected in the previous chapter into a single-phase current source circuit topology leading to the introduction of a new DC/AC inverter circuit topology with reduced component count.

The simulation modelling of the proposed DC/AC inverter circuit using OrCAD PSPICE software and practical results are presented and discussed in Chapter 5. Finally, conclusions and further work are presented in Chapter 6. Appendices A and B present the Arduino microcontroller programming code and list of publications.

## **Chapter 2 Literature Review of DC/AC Inverters**

### **2.1 Introduction**

DC/AC inverters have garnered tremendous interest in past few years. Many references have been discussed on the development of DC/AC inverters techniques, including traditional three-levels PWM topologies as well as the classical multi-level topologies (Luo and Ye, 2013). The emphasis is on the inverter circuit configuration, particularly multi-level topology, due to their ability to generate near multi-level AC output with low harmonics distortion. This chapter classifies the available DC/AC inverter topologies according to the type of AC output waveforms. It also presents an overview of well-known DC/AC inverter circuits on the three-levels PWM topologies; VSI, CSI, ISI, and the classical MLI topologies surveyed in published literature in terms of circuit operating principle and modulation control technique (Luo and Ye, 2013, and Rashid 2006). It also highlights the techniques used to improve THD in CHB-MLI. A brief discussion on the advantages and disadvantages of each DC/AC inverter topology is presented.

### **2.2 Classification of DC/AC Inverter Circuit**

DC/AC inverter circuits are a type of power electronics converter that are used to convert DC voltage into sinusoidal AC voltage waveform with controllable amplitude, frequency, and phase that is suited for desired user loads application (Rashid 2006). It is mainly used in industrial and commercial applications such as AC motor adjustable speed drives (ASD), renewable energy conversion, and uninterruptable power supplies (UPS) (Luo and Ye, 2013). In low power applications, the inverters need to operate continuously without interruption. The inverter systems

should be efficient, reliable, inexpensive, and simple (Rashid 2006, Luo and Ye, 2013). The DC/AC inverters systems are desired to produce output voltage waveform with low total harmonic distortion (THD). The parameter used to measure the inverter performance is total harmonics distortion (THD) of its output voltage and current at an acceptable level as recommended in International Harmonics Standard guidelines IEEE Std 519 (IEEE Std 519 2014).

There are numerous DC/AC inverters with different circuit configurations and techniques that have been proposed in the literature. For the purpose of explaining the strengths and weaknesses of each circuit topology/technique, it is essential first to categorise the inverter topologies/techniques covered. Figure 2.1 shows a broad categorisation of the DC/AC inverters. The DC/AC inverter topologies/techniques can be categorised as three-levels PWM inverters and multi-level inverters. Each of these is presented in the following subsections, which are classified according to their type of circuit configuration and connection as well as their output waveform.

Figure 2.5 shows their type of output waveforms. These waveforms are generated by the DC/AC inverters circuit. PWM AC output waveforms can be generated by three-levels PWM inverters circuit configurations, which include VSI, CSI, and ISI.

The multi-level AC output waveform can be generated by multi-level inverter (MLI) circuit topologies, which includes the classical topologies and the newly evolve topologies with reduced number of device. The classical MLI topologies include Diode-Clamped MLI, Flying-Capacitor MLI and Cascaded H-Bridge MLI. Meanwhile, the newly evolve topologies (multi-level inverter based switched-capacitor circuit or also known as switched-capacitor MLI), which include the resonant-based switched-capacitor MLI and capacitor-based switched-capacitor MLI.

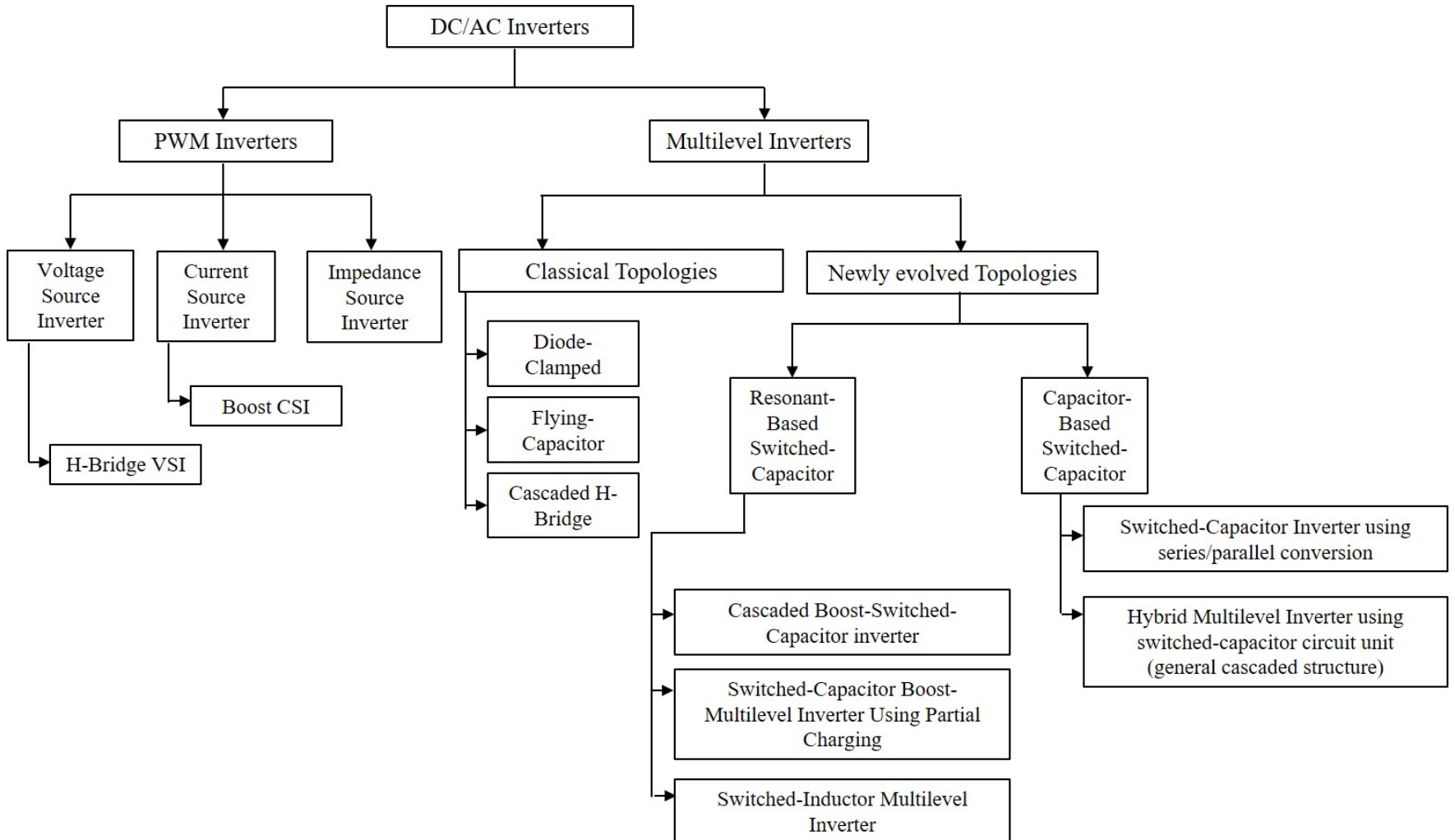


Figure 2.1 Classification of DC/AC Inverters

The following subsections present a review of each inverter circuit configuration surveyed and covered in this chapter showing their operation, technique, and advantages and disadvantages.

### **2.2.1 Voltage Source Inverter**

The voltage source inverter (VSI) generates an AC output voltage waveform. VSI has a buck function where its peak output voltage is lower than the input voltage (Xue et al. 2004). The output current is defined by the load which demands a good quality of output waveform in order to meet the application load requirement. In the medium-voltage ASD application market, VSI has proven to be efficient and have higher reliability (Luo and Ye, 2013). Meanwhile, in industrial applications and renewable energy systems, VSI are more famous and widely used than CSI. This is because VSI topology has a simple structure and control circuit (Luo and Ye, 2013). The following section describes the circuit operation and modulation control technique used.

A well-known Single-Phase H-bridge VSI circuit topology (Luo and Ye, 2013) also known as conventional three-levels Inverter or Square Wave Inverter is shown in Figure 2.2. This represents the basic principle of DC/AC conversion to obtain AC output waveform for given DC voltage at the input by commutating switches in appropriate switching signal pattern. It comprises of four switches where each leg has two switches. A VSI is supplied by a DC voltage source at input where the type of DC source at the input can be AC-DC rectifier and battery (Rashid 2006). The three output voltage levels waveform with the desired output frequency are synthesised from the DC source by commutating these switches (closing and opening) in appropriate gating signals (S1 to S4) pattern. The gating signals LOW (or logic 0) indicates the switch

OFF-state and HIGH (or logic 1) represents switch ON-state (Rashid 2006). The output voltage  $V_{an}$  can be generated as  $\{+1V_{dc}, -1V_{dc} \text{ or } 0 \text{ (zero)}\}$  voltage depending on which switches are closed.

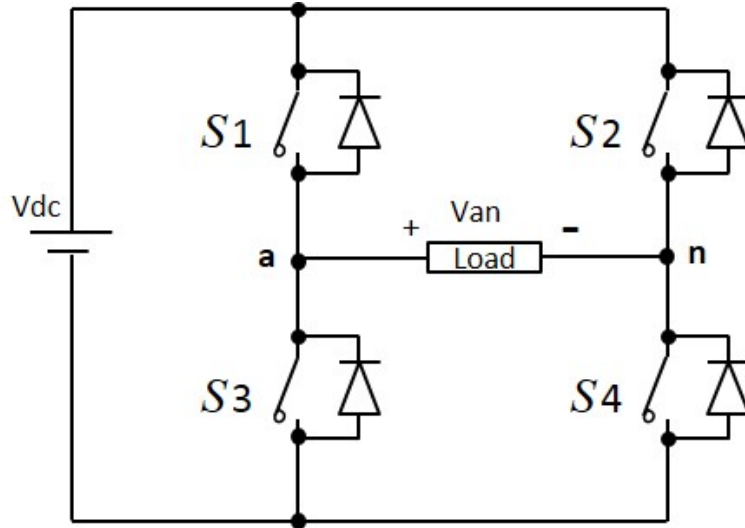


Figure 2.2 Single-Phase H-bridge Voltage Source Inverter (VSI)

Table 2.1 (Rashid 2006) shows four different switching state ( $S_a$  to  $S_d$ ) yields for three different output voltage levels (three-levels) as shown in Figure 2.5(a).

Table 2.1 Single-Phase H-Bridge VSI Switching States

Switching State	Gating Signals				Output Voltage, $V_{an}$
	$S_1$	$S_2$	$S_3$	$S_4$	
$S_a$	1	0	0	1	+1
$S_b$	1	1	0	0	0
$S_c$	0	0	1	1	0
$S_d$	0	1	1	0	-1

The two common types of modulation technique used to control H-bridge VSI power switches are low-frequency square wave PWM modulation and high carrier frequency PWM modulation (Arman, Darwish 2009). The switching operation of H-Bridge VSI as presented earlier in switching state Table 2.1 is known as low-frequency square

wave PWM modulation. The three levels of the output voltage waveform of the Single-Phase H-bridge VSI with low-frequency square wave PWM modulation is shown in Figure 2.5(a). This modulation method provides the simplest power switch control. However, the H-Bridge VSI inverter output voltage suffers from high harmonics content. Therefore, the large size of output filter is required at the inverter output to filter out the harmonics content (Lai et al. 2008) (Heldwein, Kolar 2009). The lower voltage harmonics output content of H-Bridge VSI can be achieved by modulating the power switches at higher carrier frequency PWM which also known as Sinusoidal Pulse-Width Modulation (SPWM) (Rashid 2006, Zhang & Zhang 2007, Luo and Ye, 2013).

The control signal switching pattern is obtained by comparing carrier signal (triangular wave) with a reference signal (sine wave). This carrier based PWM method can be classified into unipolar PWM and bipolar PWM operation (Luo and Ye, 2013). The three output voltage levels (three-levels) waveform of the Single-Phase H-bridge VSI with Unipolar PWM operation is shown in Figure 2.5(b). This carrier based Unipolar PWM is widely used in power inverter application (Arman, Darwish 2009, Luo and Ye, 2013) having the advantage of simple control circuit and operation. In addition to that, the low switch component count requirement results in low inverter cost. However, the power switch is associated with high switching losses. The power switches need to be operated at a high switching frequency which could degrade power conversion performance (Sanjeev, Jain 2013). The cooling unit (heat sink) is required which adds to the inverter size.

## 2.2.2 Current Source Inverter

The Current Source Inverter (Current Source Inverter (CSI)) generates an AC output current waveform. CSI is also famous in medium-voltage ASD application and renewable energy systems (RES) (Xue et al. 2004). This is due to the fact that it has a boosting voltage function where its peak output voltage is higher than the input voltage (Luo and Ye, 2013), which is very useful in RES applications with lower DC input resources. The variable-voltage and variable-frequency drive capability feature make CSI preferred in an ASD application (Takatsuka, Yamanaka & Hara 2013). The CSI also can be applied to low power application. In addition, CSI have simple structure and control circuit (Luo and Ye, 2013).

Figure 2.3 shows a single-phase CSI Boost DC/AC Inverter (Xue et al. 2004, Bai, Zhang & Zhang 2007). It is formed from a two-stage converter that connects the boost chopper circuit and full H-Bridge inverter circuit in cascade to perform a two-stage power conversion. It has a simple structure due to fewer power switches used, easy control, and low cost (Xue et al. 2004). The boost chopper circuit composes of inductor ( $L$ ) and single main power semiconductor switch ( $S_1$ ), while the full H-Bridge inverter circuit composes of DC link capacitor ( $C$ ) and power semiconductor switches ( $S_2$  to  $S_5$ ). The DC input voltage connects in series with an inductor formed current source at input circuit. This input current is maintained approximately constant by large inductor ( $L$ ).

To achieve sinewave-modulated AC output voltage as shown in Figure 2.5(c), the capacitor charging from the input current source must be controlled by main power switch ( $S_1$ ) through an appropriate modulation control, such as rectified sine wave appearing across capacitor (DC link). The main power switch can be modulated by applying an appropriate switching pulse pattern (varying frequency PWM train signal)

applied to the gate of power switches. Sinusoidal Pulse Width Modulation (SPWM) method is commonly used to obtain switching gate pattern where the sine reference signal is compared with triangular carrier wave (Bai, Zhang & Zhang 2007, Madouh, Ahmed & Al-Kandari 2012), (Alqarni, Darwish 2014). The full H-Bridge inverter is used to transform into line frequency AC output voltage. A low-pass filter is required at inverter output to smooth the output voltage waveform.

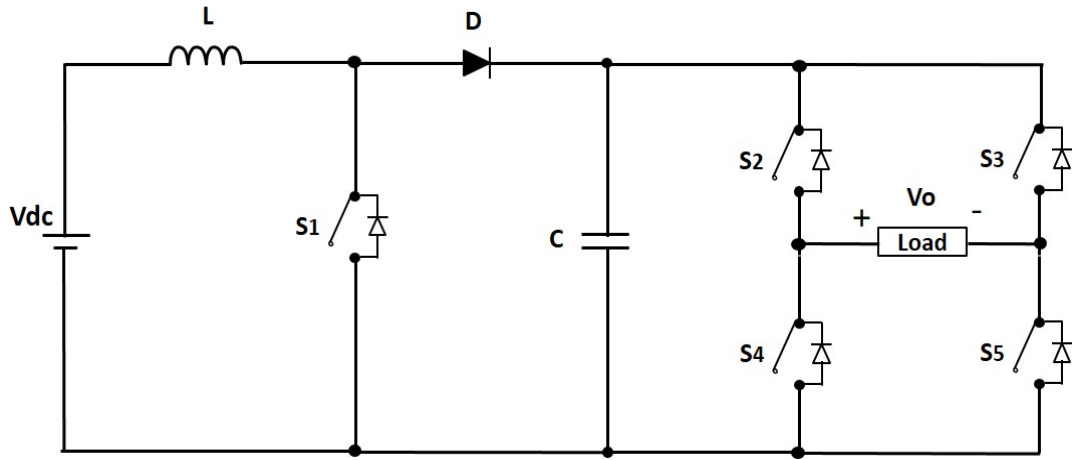


Figure 2.3 Single-Phase Boost CSI Inverter

However, the limitation of a Boost CSI DC/AC inverter is high switching losses in power semiconductor switches due to modulating operation at a high switching frequency in obtaining smooth output voltage waveform. Also, a low-pass filter is required to filter harmonics content at the output. These lead to increase overall size and cost due to filter and cooling unit requirements (Georgakas, Vovos & Vovos 2014). On the other hand, there is an issue on the formation of AC output voltage. The voltage does not reach zero voltage (voltage gap) when H-bridge inverter swap voltage polarity from positive to negative cycle voltage transition. Hence, lower-order harmonics are created at high amplitudes which contribute to high THD in output voltage (Madouh, Ahmed & Al-Kandari 2012, Georgakas, Vovos & Vovos 2014).

### 2.2.3 Impedance Source Inverter

Figure 2.4 shows three phases Impedance Source Inverter (ISI) (Anderson, Peng 2008, Bao et al. 2011). This circuit topology is composed of seven power semiconductor switches and a diode. Also, two inductors and two capacitors are configured in an x-shaped impedance network. Sinusoidal Pulse Width Modulation (SPWM) method is commonly used to obtain switching gate pattern so that to achieve sinewave-modulated AC output voltage as shown in Figure 2.5(c). ISI has a unique characteristic where it can become VSI if both inductors have zero inductance. On the other hand, if both capacitors have zero capacitance, this ISI can become CSI. This can provide buck-boost characteristics which are highly suitable for industrial applications, such as distributed generation (DG) and variable speed drive (VSD). Therefore, ISI has more flexibility in controlling AC output voltage than VSI and CSI. The output voltage adjusted higher or lower than the DC source voltage or DC link voltage. Traditional carrier-based Pulse Width Modulation (PWM) and Sinusoidal Pulse Width Modulation (SPWM) can be used to control this inverter.

Two capacitors and inductors can provide protection from overvoltage and overcurrent. This circuit is also robust from the shoot-through limitation which was caused by EMI noise due to the existence of these two inductors and two capacitors (Peng et al. 2013). Upper and lower bridge power switches controls can even operate simultaneously in overlap time without shoot-through issues during a very short period. Also, there is no need to set a short dead time control. The overall system cost is low and efficiency is high because of fewer components.

The disadvantages of VSI, CSI, and ISI three-levels PWM inverters are:

- The power switches in both VSI, CSI, and ISI PWM inverters need to be

switched at high switching frequency PWM in order to achieve low distortion in output voltage and current (Georgakas, Vovos & Vovos 2014, Carrasco et al. 2006, Madouh, Ahmed & Al-Kandari 2012).

- Switching losses are high due to high switching frequency operation. The VSI inverter is switched from a few kHz up to 100 kHz, while the CSI and ISI inverters are switched at 20kHz up and above to achieve low harmonics output distortion (Georgakas, Vovos & Vovos 2014 and Rozlan et al. 2015).
- The high switching frequency operation is useful in CSI, as smaller component size can be used. However, this can lead to increase power dissipation in power switch in both VSI and CSI inverter which also demand cooling systems (heat-sink). This adds to inverter size and offsets the advantage of high switching frequency operation.
- The output filter is required at both VSI and CSI inverter output can increase system size and cost.

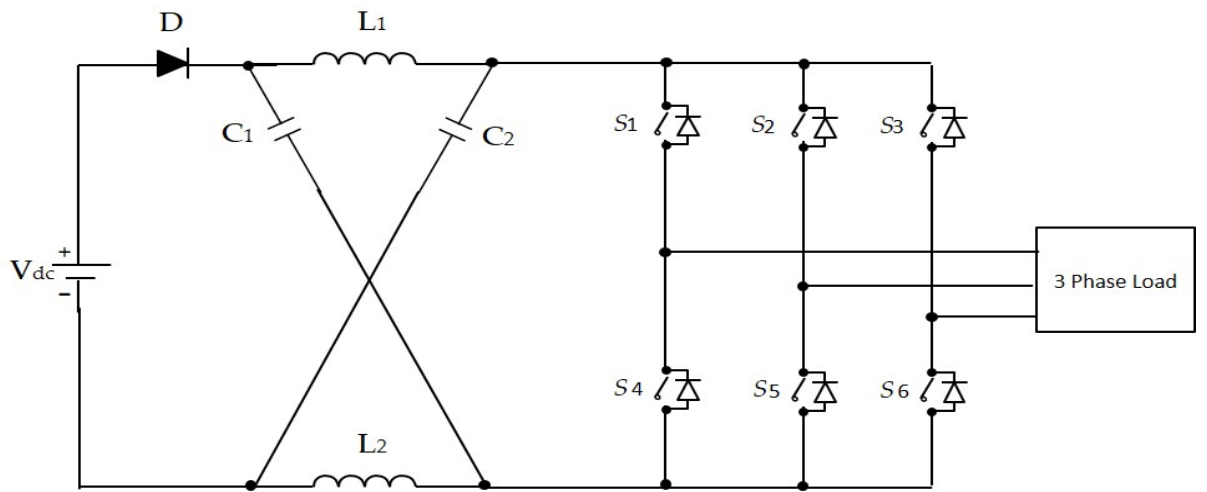


Figure 2.4 Three-Phase ISI Inverter

To achieve lower total harmonic distortion in output voltage and current waveform, the power semiconductor switch in each of VSI, CSI, and ISI PWM inverter circuits needs to operate at very high switching frequency i.e. 100 kHz. This high switching frequency operation is associated with high switching losses in power semiconductor switch which leads to reduce their efficiency when used in high power applications.

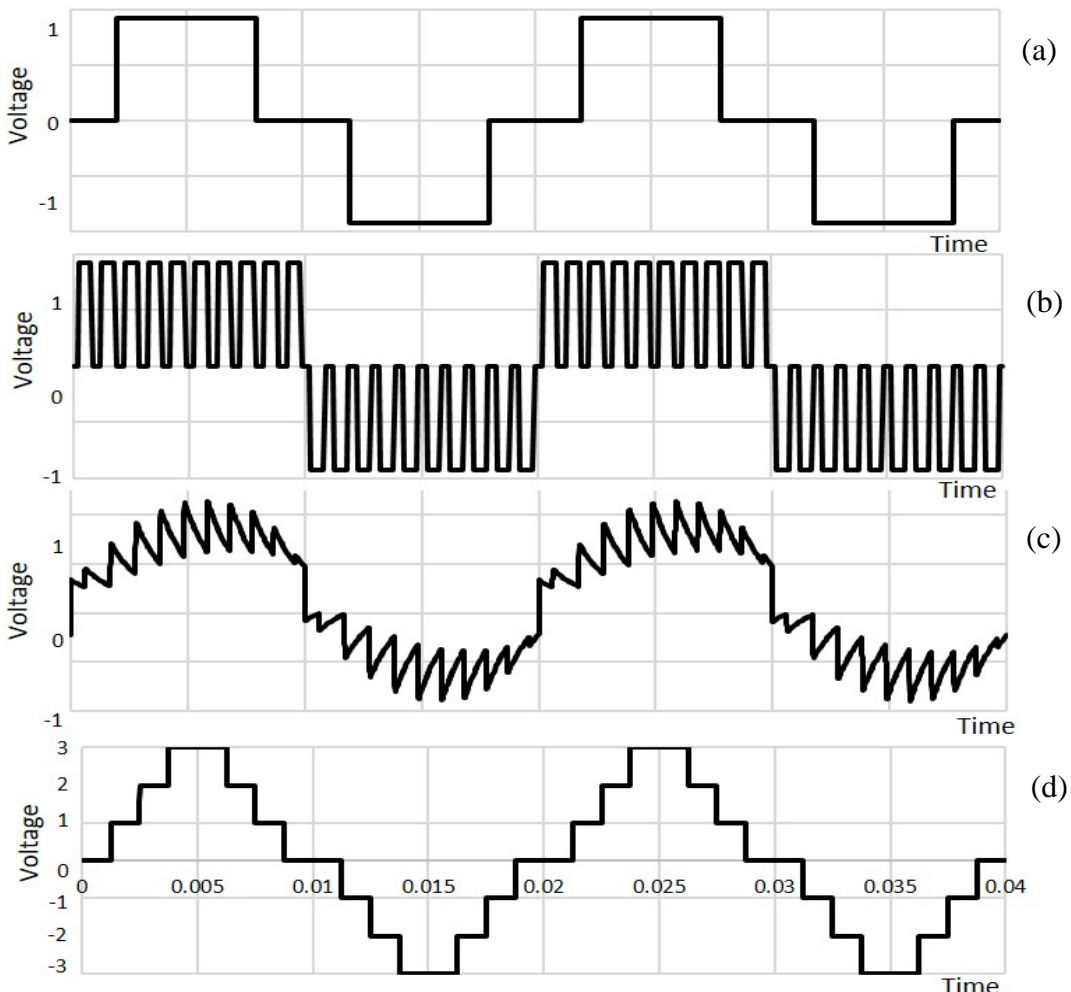


Figure 2.5 DC/AC inverter output waveforms: (a) Three-levels voltage waveform using low-frequency square wave PWM modulation. (b) Three-levels voltage waveform using unipolar high-frequency PWM modulation. (c) Sine-Modulated voltage waveform. (d) Seven-levels voltage waveform (multi-level)

Another inverter topology types called ‘multi-level inverter’ which can generate a near AC (multi-level/staircase) output voltage with reduced harmonics distortions and low power losses at the same time. This is explained in more detail in the following section 2.2.4.

## 2.2.4 Classical Multi-Level Inverter Topologies

Multi-level DC/AC inverter topology is an alternative DC/AC inverter configuration which is widely used in medium-voltage, high-power applications. It is less popular in low-voltage, low-power applications, but preferred to traditional three-levels PWM inverters (De, Banerjee, Gopakumar, Ramchand, & Patel, 2011). This method is known for simultaneously generating fewer harmonics in output voltage and current and smaller power losses. This technique also can overcome other problems of the conventional two-level inverter as mentioned in the previous section.

The multi-level DC/AC inverter technique is different from the previous conventional DC/AC inverter method, which vertically chops a reference sine voltage waveform into several pulses width, horizontally chops a reference sine voltage waveform into several pulses height, and synthesises these voltage levels to achieve near sinusoidal multi-level or staircase output waveform at inverter output (Jiang, Lipo 1998). The m-level of the near sinusoidal multi-level or staircase output voltage is usually synthesised from several lower DC voltage sources through low-voltage rated switch controls at low switching frequency. Considering m is the number of output phase voltage with respect to the negative terminal of the inverter. The harmonics distortion in multi-level inverter output voltage and current can be reduced by constructing a high number of levels or steps of inverter output voltage (Gupta et al. 2016). The higher the output voltage resolution, the closer to a sine waveform. This is because a pure sine waveform has zero total harmonic distortion (Luo and Ye, 2013). In achieving low harmonics output, the pulse width of the staircase waveform need to control the by appropriate switching modulation method which can be categorised into low-frequency modulation (Selective Harmonics Elimination, SHE) and high-

frequency modulation (Carrier-based PWM) (Luo and Ye, 2013, Arman, Darwish 2009). This refers to controlling the duration of the power switch to allow and block voltage using low-voltage rated power semiconductor switches (i.e. IGBTs or Power MOSFETs). The three main multi-level DC/AC converters have been reported in literature (Arman, Darwish 2009, Luo and Ye, 2013, Gupta et al. 2016) which can be referred as classical multi-level DC/AC inverter topology: Diode Clamped Multi-Level Inverter (DC-MLI), Capacitor Clamped Multi-level Inverter (FC-MLI) and Cascaded H-Bridge Multi-level Inverter (CHB-MLI). The following section describes an overview of each circuit topology features, circuit operation, advantages, and limitations.

#### **2.2.4.1 Diode-Clamped Multi-Level Inverters**

Diode-Clamped Multi-Level Inverters (DC-MLI) topology (Nabae, Takahashi & Akagi 1981, De et al. 2011, Mecke 2011) has been used such in renewable energy applications (Rashid 2006) where the PV is fed to input DC-link, as well as in adjustable speed motor drives (Luo and Ye, 2013). The DC bus voltage is divided into several voltage levels by several numbers of capacitors with a neutral point in the middle. This creates several inner voltages levels at a different magnitude which are clamped by either two extra diodes with different voltage ratings (Nabae, Takahashi & Akagi 1981). These two diodes block the switch voltage to the half level of the DC bus voltage. The near AC (multi-level/staircase) output voltage waveform is synthesised from several inner voltage levels through several switches connected in series which are controlled at the low-switching frequency. Figure 2.6 shows a three-levels and five-levels DC-MLI circuit topologies. The number of output voltage levels can also be extended from three-levels to five-levels or even more levels by adding

more power switches, capacitor and diodes components to generate a higher number of output voltage levels. Therefore, its structure needs to be expanded. The multi-level AC output voltage of DC-MLI ( $V_{a0}$ ) can be shaped by controlling the associated power switches in appropriate switching pattern sequence as shown in Table 2.2 for 5-level DC-MLI.

Advantages of DC-MLI circuit topology (Luo and Ye, 2013):

- For low fundamental switching frequency operation, small switching loss in power switches due to low switch commutation. Therefore, the efficiency is high.
- The DC link capacitors can be pre-charged as a group.

However, to obtain low output voltage harmonics, a number of output voltage levels need to be increased. This requires a large number of power switches control and clamp diode for blocking voltage, resulting in complex control circuits where each switch is associated with a control gate drive unit (Luo and Ye, 2013). For higher number of output voltage levels, the overall system can be bulky and expensive.

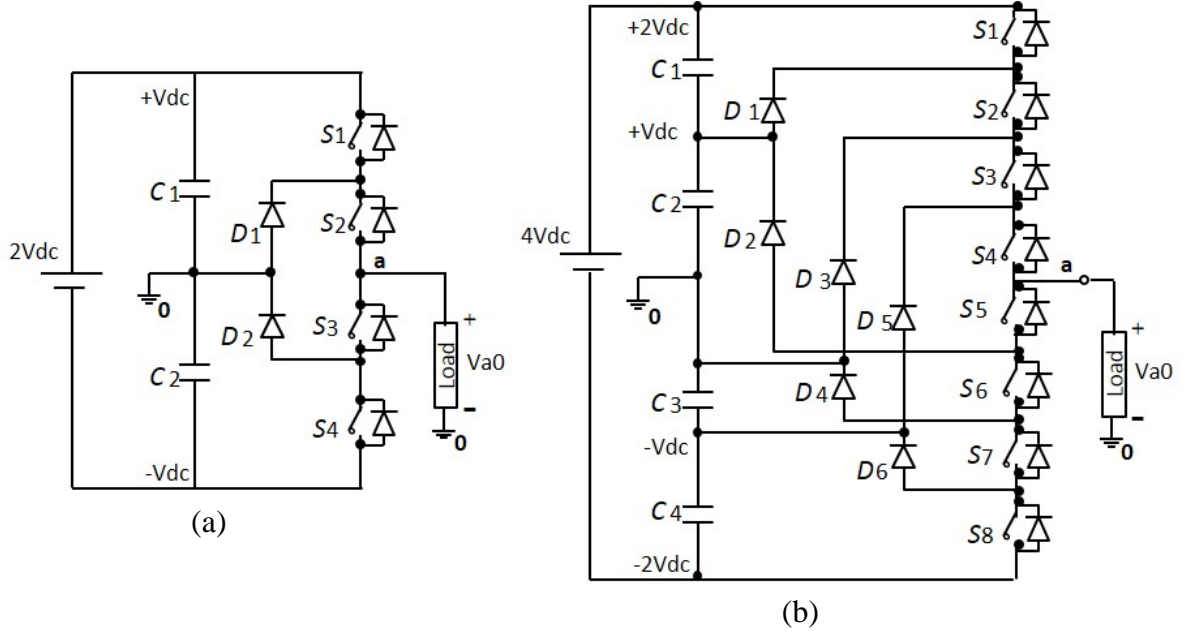


Figure 2.6 Diode-Clamped MLI circuit (a) Three-levels and (b) Five-levels

Table 2.2 Five-levels DC-MLI Switching States

DC bus voltage, (Vdc)	Switch State							
	S <sub>1</sub>	S <sub>2</sub>	S <sub>3</sub>	S <sub>4</sub>	S <sub>5</sub>	S <sub>6</sub>	S <sub>7</sub>	S <sub>8</sub>
V <sub>a0</sub> = 2Vdc	1	1	1	1	0	0	0	0
V <sub>a0</sub> = 1Vdc	0	1	1	1	1	0	0	0
V <sub>a0</sub> = 0	0	0	1	1	1	1	0	0
V <sub>a0</sub> = -1Vdc	0	0	0	1	1	1	1	0
V <sub>a0</sub> = -2Vdc	0	0	0	0	1	1	1	1

The generation of m-levels output voltage of DC-MLI inverter topology requires several units of component device, such as:

- Number of power semiconductor switches =  $2(m-1)$
- Number of semiconductor diodes =  $2(m-2)$
- Number of DC-Link Capacitors =  $m-1$

#### 2.2.4.2 Flying-Capacitor Multi-Level Inverter

Figure 2.7 shows a Three-level and Five-level Flying-Capacitor Multi-Level Inverter Flying-Capacitor Multi-Level Inverters circuit (Huang, Corzine 2004, He, Cheng 2016). The DC bus voltage is divided into several voltage levels by several numbers of capacitors with a neutral point in the middle. This creates several inner voltages levels at a different magnitude which then are clamped using clamping capacitors to one capacitor voltage levels. The multi-level or staircase AC voltage of FC-MLI is synthesised from several inner voltage levels through several switches connected in series. The conduction of the associated switches is controlled in appropriate switching pattern at the low switching frequency. The five-levels output voltages of FC-MLI and switching control pattern is shown in Table 2.3. The capacitor C1 is charged when switches (S1) and (S3) are turned ON and discharged when (S2) and (S3) are turned ON. The charge of C1 can be balanced by a proper selection of the zero-level switch combination.

Advantages of FC-MLI circuit topology (Luo and Ye, 2013):

- The voltage synthesised in FC-MLI has more flexibility than a Diode Clamped-MLI.
- A large number of clamping capacitors act like a capacitor bank which enables the inverter to act as short backup supply for a short duration during a power outage.

However, to obtain low output voltage harmonics, a number of output voltage levels need to be increased. Therefore, its structure needs to be expanded (i.e. five-five levels as shown in Figure 2.7 or more levels) to yield a higher number of output levels. This

requires a large number of power switches control and a bulk capacitor for clamping voltage, resulting in complex control circuit where each switch is associated with a control gate drive unit (Luo and Ye, 2013). For higher number of output voltage levels, the overall system can be bulky and expensive.

The generation of m-levels output voltage of FC-MLI inverter topology requires several units of component device, such as:

- Number of power semiconductor switches =  $2(m-1)$
- Number of clamping capacitors per phase =  $(m-1) \times (m-2)/2$
- Number of DC-link capacitors =  $m-1$

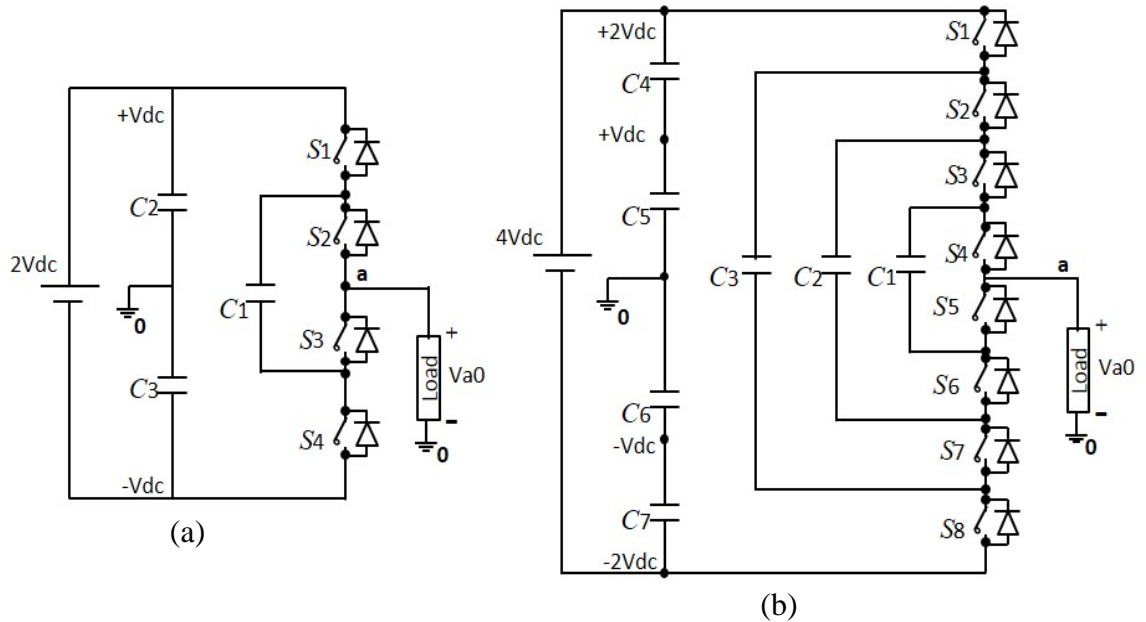


Figure 2.7 Flying-Capacitor MLI circuit (a) Three-levels and (b) Five-levels

Table 2.3 Five-levels FC-MLI Switching States

DC bus voltage, (Vdc)	Switch State							
	S <sub>1</sub>	S <sub>2</sub>	S <sub>3</sub>	S <sub>4</sub>	S <sub>5</sub>	S <sub>6</sub>	S <sub>7</sub>	S <sub>8</sub>
V <sub>a0</sub> = 2Vdc	1	1	1	1	0	0	0	0
V <sub>a0</sub> = 1Vdc	1	1	1	0	1	0	0	0
V <sub>a0</sub> = 0	0	0	1	1	0	0	1	1
V <sub>a0</sub> = -1Vdc	0	0	0	1	0	1	1	1
V <sub>a0</sub> = -2Vdc	0	0	0	0	1	1	1	1

#### 2.2.4.3 Cascaded H-Bridge multi-level inverter (CHB-MLI)

A five-levels and seven-levels cascaded H-Bridge multi-level inverter (CHB-MLI) circuit topologies are shown in Figure 2.8. This topology is the best possible for connecting a renewable energy source such as photovoltaics and fuel cells with an AC grid, because there is the need for a separate DC source in these applications (Luo and Ye, 2013). Figure 2.8 shows single-phase CHB-MLI topology consisting of multiple stages of full bridge inverter connected in cascade. The CHB-MLI topology with equal DC link voltage sources at the input of H-bridge circuit cell i.e. V<sub>dc1</sub> = V<sub>dc2</sub> = V<sub>dc3</sub> is known as ‘Symmetric CHB-MLI inverter’ (Beig, Dekka, 2012), while topology with unequal DC link voltage sources at the input of H-bridge circuit cell i.e. V<sub>dc1</sub> ≠ V<sub>dc2</sub> ≠ V<sub>dc3</sub> is known as ‘Asymmetric or Hybrid CHB-MLI inverter’. For given n-th H-bridge cells, the output voltage, V<sub>an</sub> is synthesised from n-th H-bridge phase voltage V<sub>Hn</sub> i.e. V<sub>an</sub> = V<sub>H1</sub> + V<sub>H2</sub> + ... + V<sub>Hn</sub>. The low-switching frequency method known as Step Modulation, which is also called Selective Harmonics Elimination (SHE) (Alamri, Darwish, 2015), is the common method used to modulate power

switches in Symmetric CHB-MLI. The seven-levels output voltage of CHB-MLI is shown in Figures 2.9 and 2.10 and the switching control pattern is shown in Table 2.4. This method allows several lower order harmonics to be eliminated while controlling the amplitude of the fundamental output voltage.

Advantages of CHB-MLI circuit topology (Luo and Ye, 2013,):

- Low switching loss due to all power switches operating at the low switching frequency.
- Low DC-link voltage means low rated-voltages power switch can be used (due to low peak voltage flow through power switch). Hence, low dv/dt and less electromagnetic interference (EMI).

Disadvantage of CHB-MLI circuit topology (Luo and Ye, 2013):

- Near sinusoidal output voltage with minimum THD can be achieved with a large number of isolated DC-link sources, power switches, and diodes to construct a high number of voltage levels.

In Hybrid or Asymmetric CHB-MLI inverter circuit topology, each DC link source of H-bridge switches cell can have different DC link voltage values or different DC link voltage integer ratio. It has hybrid modulation control which combines low and high-frequency switching operation to modulate the low-voltage rated and high- voltage rated power switches in Asymmetric/Hybrid CHB-MLI. The H-bridge power switch circuit cell can be divided into a lower number of commutation cells (low-side H-bridge cell) with high magnitude of DC link voltage sources and a higher number of commutation cells (high-side H-bridge cell) with a lower magnitude of DC link voltage sources. With an appropriate switching control pattern, a high number of output

voltage levels can be achieved with less number of power switches than symmetric CHB-MLI.

Advantages of Asymmetric/Hybrid CHB-MLI circuit topology (Luo and Ye, 2013):

- The number of voltage level can be increased without needing an increasing number of power switches. The higher number of levels gives higher output resolution (where the resolution is referred to the step size of the staircase/multi-level voltage) voltage, which is closer to a sine wave and low harmonics output can be achieved.
- Different commutation operation of H-bridge switches circuit cell allows using different types of power switches.

Disadvantage of Asymmetric/Hybrid CHB-MLI topology:

- Higher switching loss due to high-side power switches operating at high switching frequency.

Therefore, the generation of m-levels output voltage of Symmetry CHB-MLI inverter topology requires several units of component devices, such as:

- Number of power semiconductor switches =  $2m-2$
- Number of diodes =  $2m-2$
- Number of DC-link capacitors =  $(m-1)/2$

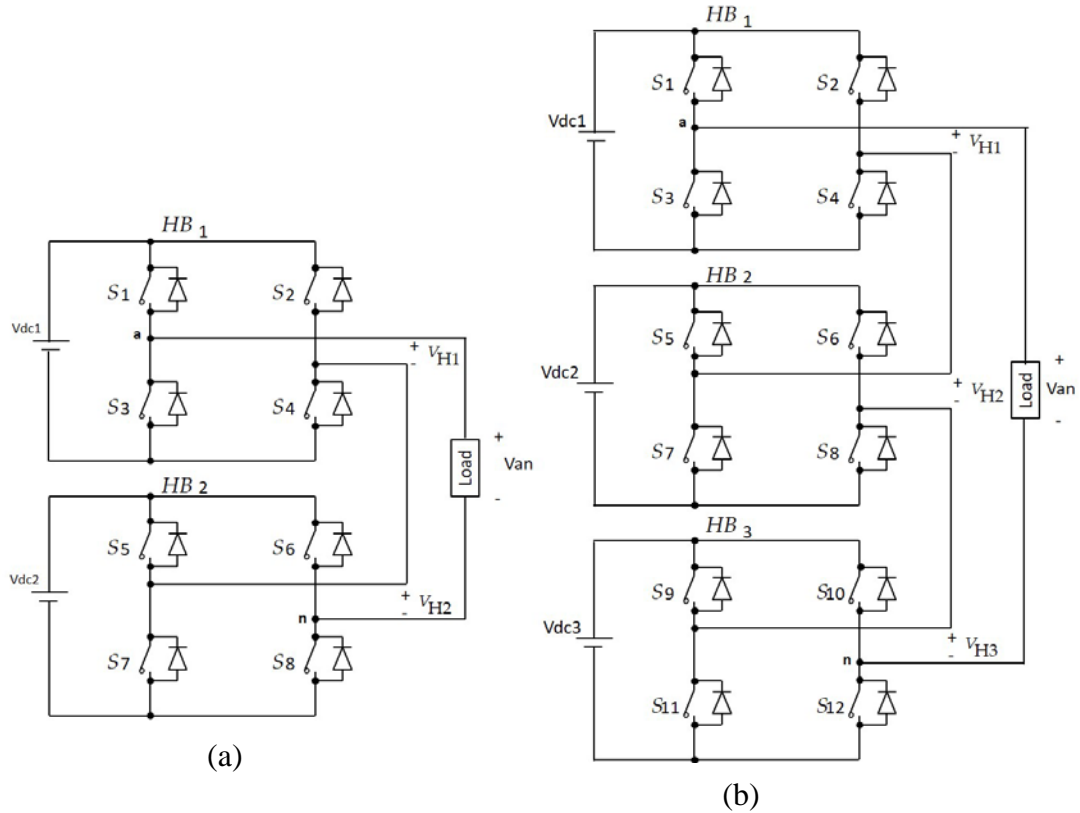


Figure 2.8 Cascaded H-Bridge MLI circuit (a) Five-level and (b) Seven-level

Table 2.4 Seven-level Symmetric CHB-MLI switching states

Output voltage, Van	Switch State											
	S <sub>1</sub>	S <sub>2</sub>	S <sub>3</sub>	S <sub>4</sub>	S <sub>5</sub>	S <sub>6</sub>	S <sub>7</sub>	S <sub>8</sub>	S <sub>9</sub>	S <sub>10</sub>	S <sub>11</sub>	S <sub>12</sub>
V <sub>H3</sub> = 3Vdc	1	0	0	1	1	0	0	1	1	0	0	1
V <sub>H2</sub> = 2Vdc	1	0	0	1	1	0	0	1	0	0	1	1
V <sub>H1</sub> = 1Vdc	1	0	0	1	0	0	1	1	0	0	1	1
V <sub>H0</sub> = 0	0	0	1	1	0	0	1	1	0	0	1	1
V <sub>H1</sub> = -1Vdc	0	1	1	0	1	1	0	0	1	1	0	0
V <sub>H2</sub> = -2Vdc	0	1	1	0	0	1	1	0	1	1	0	0
V <sub>H3</sub> = -3Vdc	0	1	1	0	0	1	1	0	0	1	1	0

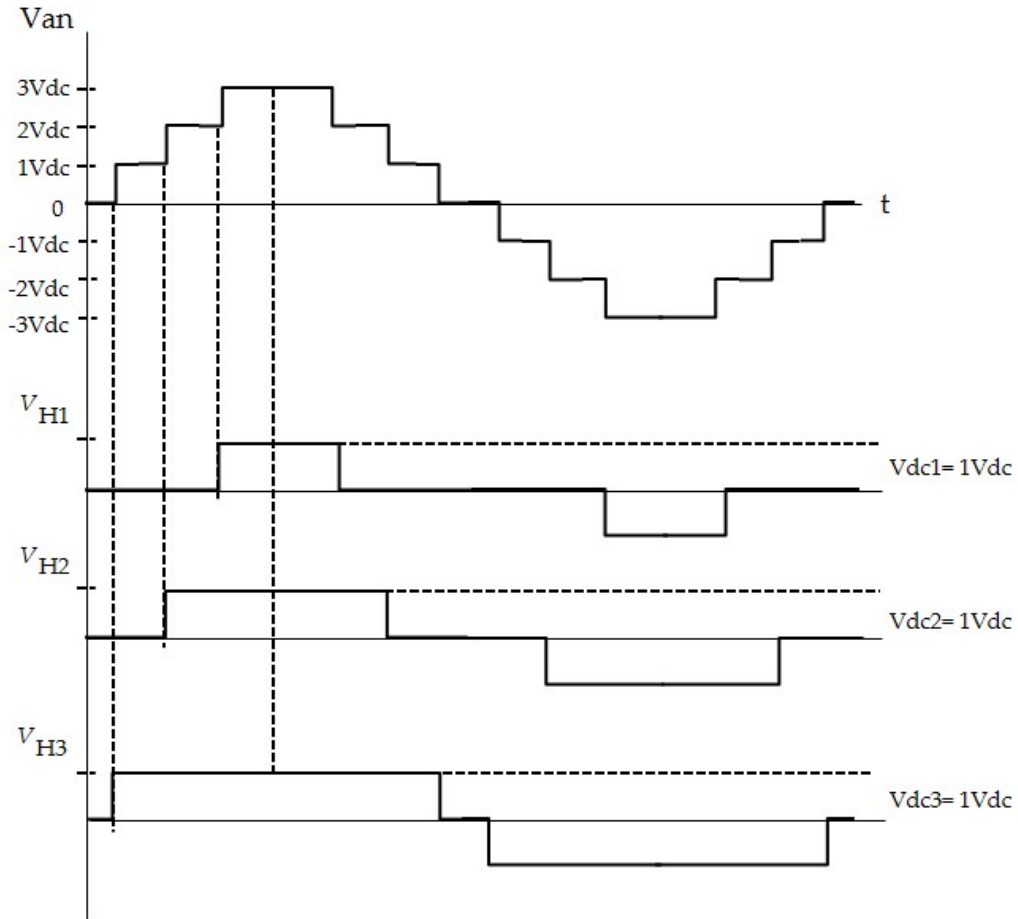


Figure 2.9 Seven-level output voltage of the Symmetric CHB-MLI circuit

### 2.2.5 Improving THD in CHB-MLI circuit topology

The trend of recent development of multi-level DC/AC inverter is receiving wider attention both in terms of topologies and modulation control technique (Gupta et al. 2016). In CHB-MLI circuit topology, near sinusoidal staircase output voltage can be generated from several low DC voltage levels. The higher number of voltage levels in staircase waveform can result in better quality resolution of output waveform which are close to a sinusoidal waveform. Hence, lower total harmonic distortion can be achieved with the reduced size of the filter is required at the output. A pure AC sinusoidal waveform has zero total harmonic distortion (Luo and Ye, 2013). The total

harmonic distortion in CHB-MLI can be improved by extending the number of output voltage levels and also by DC link voltage levels and or switching angle optimisation (Diong Sepahvand & Corzine 2013).

In order to track the sine waveform, the common method used to shape multi-level or staircase AC voltage waveform of CHB-MLI circuit topology is done by creating constant (equal step) voltage levels with respect to constant (equal step) switching angle intervals (Luo and Ye, 2013). Figure 2.10 shows seven-levels near AC output voltage waveform of the classical symmetric CHB-MLI circuit shown in Figure 2.8(b) with constant (equal step) DC link voltage with constant (equal interval) of switching angle. The harmonics spectrum of the output voltage waveform contains several higher lower order amplitudes (i.e.3<sup>rd</sup>, 5<sup>th</sup>, 7<sup>th</sup> and 9<sup>th</sup>) as shown in Figure 2.11. These lower orders harmonics have led to the high total harmonic distortion in 7-levels CHB-MLI output voltage.

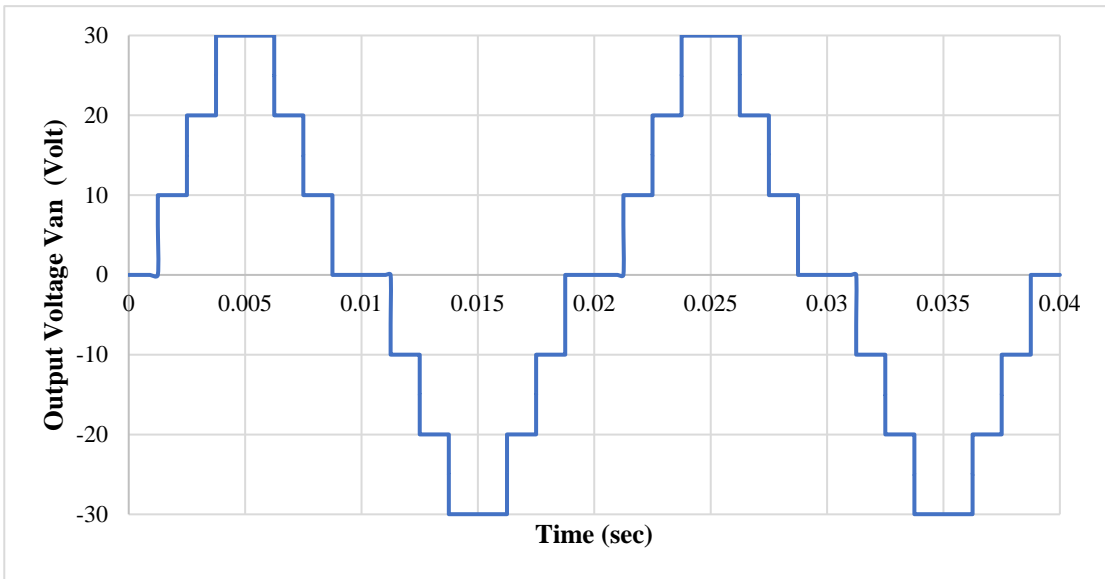


Figure 2.10 Seven-levels output voltage of the Symmetry CHB-MLI circuit (Equal step DC link voltage)

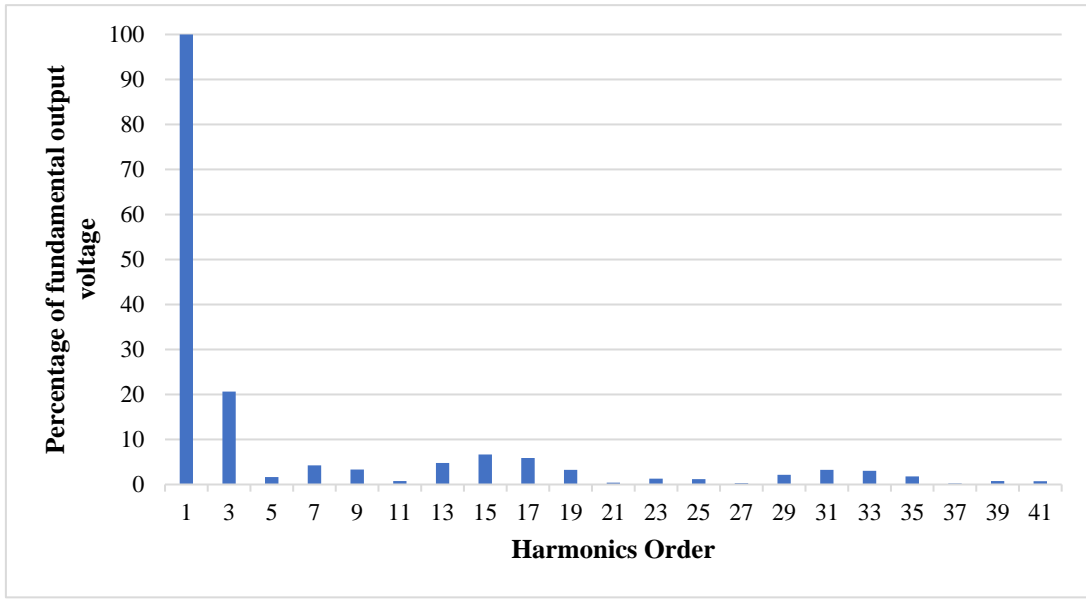


Figure 2.11 Harmonics spectrum of seven-levels CHB-MLI output voltage (before optimisation)

There are optimization techniques which are used to improve the THD in a Cascaded H-Bridge Multi-Level Inverter (CHB-MLI) as reported in literature (Jiang, Lipo 1998, Ziar et al. 2011, Diong Sepahvand & Corzine 2013). The techniques are used to eliminate some of the lower harmonics order in the output voltage of CHB-MLI circuit as shown in Figure 2.11. This can be achieved by optimising the DC link voltage levels and/or switching angle in multi-level/staircase output voltage waveform. The techniques are known as:

- 1) optimising switching angle with equal constant DC link voltage levels (Alamri, Darwish 2014) and/or
- 2) optimising the both DC link voltage levels and switching angle (Jiang and Lipo 1998, Ghasemi, Zare, 2012)

### **2.2.5.1 Optimising switching angle with equal constant DC link voltage levels**

For seven-levels symmetric CHB-MLI, there are two numbers of harmonics order can be eliminated in its output voltage spectrum (Alamri, Darwish 2014). To eliminate these specific harmonic orders, the switching angle must be determined first. The off-line calculation method called Selective Harmonics Elimination (SHE) is used to determine switching angles that can eliminate specific or selected harmonics order while controlling the magnitude of the fundamental voltage. The switching angle calculation can be determined by iterative mathematical method (Alamri, Darwish, 2014). However, only two harmonics order can be eliminated (i.e. 5<sup>th</sup> and 7<sup>th</sup> orders) (Alamri, Darwish, 2014).

### **2.2.5.2 Optimising both DC link voltage levels and switching angle.**

Eliminating more harmonics content can be achieved by optimising both voltage levels and switching angles as suggested in Jiang and Lipo 1998, Ghasemi, Zare, 2012, so that the multi-level/staircase AC waveform can be shaped more closely to sine waveform. This results in optimum DC link voltage steps and optimum switching angles. By optimizing both DC link voltage levels and switching angle technique, a near sinusoidal multi-level/staircase output voltage waveform is shaped. The optimum DC link voltage ratio is found to be 1.4054 Vdc: 1.0543 Vdc: 0.56 Vdc with 5<sup>th</sup>, 7<sup>th</sup>, 9<sup>th</sup>, 11<sup>th</sup>, 13<sup>th</sup> 15<sup>th</sup> and 17<sup>th</sup> harmonics orders eliminated as shown in frequency spectrum Figure 2.13 (Ghasemi, Zare, 2012). The 3<sup>rd</sup> harmonic can be easily eliminated in three-phase CHB-MLI inverter system configuration (Alamri, Darwish, 2014).

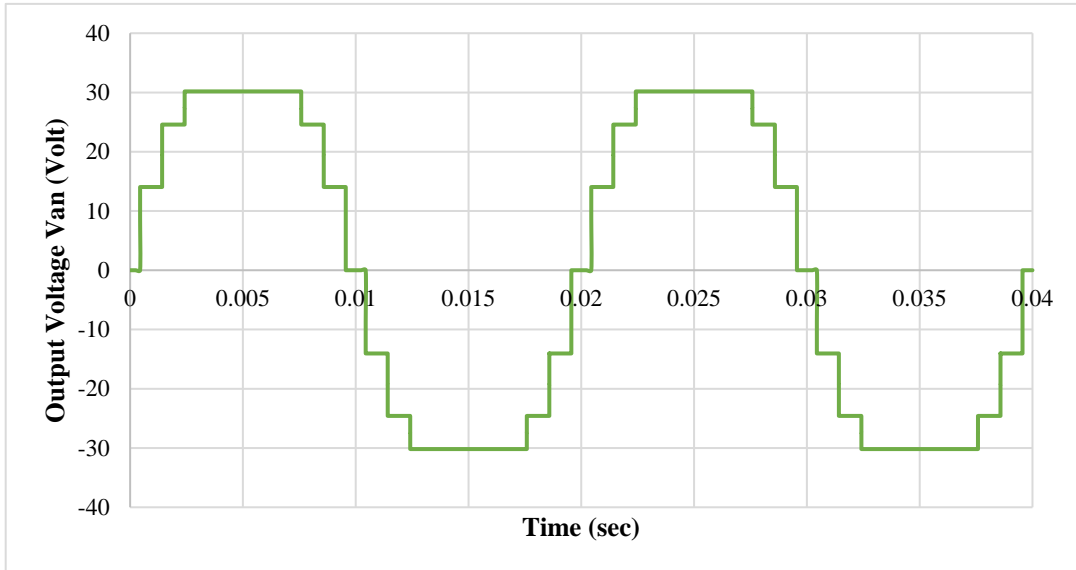


Figure 2.12 Optimised seven-levels CHB-MLI output voltage (Unequal step DC link source)

For both optimisation cases (a) and (b), the Genetic Algorithm (GA) optimisation method (Pandi, Devarajan, 2010) are used to solve the complicated non-linear transcendental equation where the optimum angles can faster to converge than the older Newton-Raphson Method. The GA optimisation tool in MATLAB was used for this purpose.

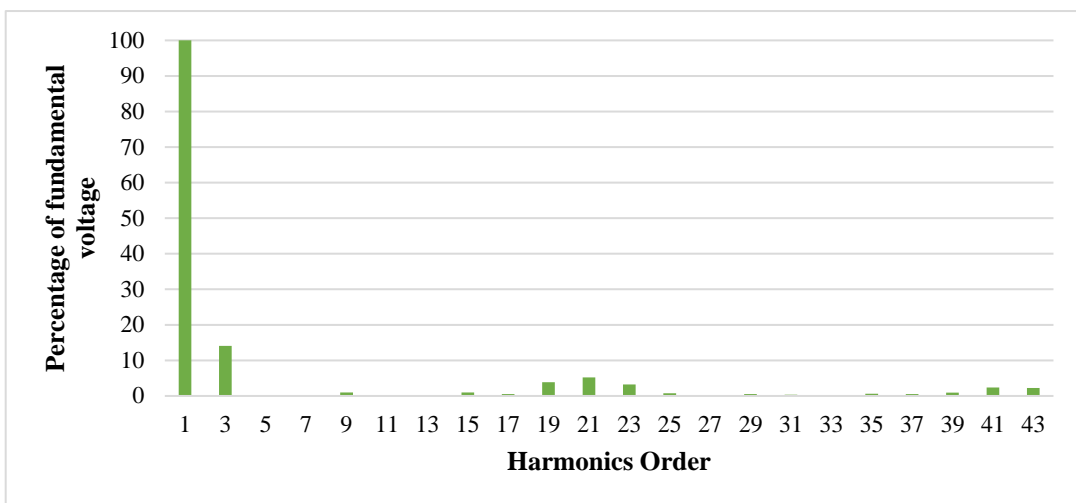


Figure 2.13 Harmonics spectrum of seven-levels CHB-MLI (more harmonics order eliminated).

The following section brief summarize the three-levels PWM inverter topologies and the classical multi-level inverter topologies which explain and compare the advantages and disadvantages of these two main DC/AC inverters as well as the improving THD technique in the classical multi-level inverter topologies.

### **2.3 Summary of PWM Inverters & Multi-Level Inverter topologies**

The main advantages of three-levels PWM inverter topologies for both PWM and SPWM modulation operation that make its relevant in low power domestic application and in high power industrial application such induction motor drives and renewable energy system application are:

- Simple structure due to less number of component (i.e. power switches, capacitor, inductor and diodes). The cost can be less.
- Simple control due to less number of power semiconductor switches used.
- Small size of passive components (i.e. capacitors and inductor) can be used when operating at very high switching frequency.
- Reliable system due to less number of components used.

The main disadvantages of three-levels PWM inverter topologies for both PWM and SPWM modulation operation are:

- Poor total harmonic distortion (THD)
- High switching losses in power semiconductor switches due to high switching frequency operation.
- High dv/dt of output voltage and di/dt of output current can result in high electromagnetic interference (EMI)

- Require of bulky and complex cooling system (heat-sink) can lead to bulky overall system size
- Require heavy common modes and differential mode filters at output
- Low efficiency at higher switching frequency

In medium-voltage high-power application, the classical multi-level inverters topologies are an attractive solution which much more preferred than three-levels inverter due to many advantages such:

- Low total harmonic distortion (THD)
- Can be operated at low switching frequency
- Low switching loss
- Low dv/dt can result in low EMI
- Low voltage rating device can be used.
- High efficiency

The multi-level inverter topologies are not so popular in low power applications. For low-power range, it can be preferred than three-levels PWM inverter topologies if the power semiconductor switches used in PWM inverter circuit are operated at very high frequency (i.e.  $>100$  kHz).

Although classical multi-level topologies (DC-MLI, FC-MLI, and CHB-MLI) are effective and can obtain minimum total harmonic distortion (THD). However, suffer from some disadvantageous when to construct higher number of voltage levels of the staircase/multi-level AC output waveform such:

- Require increasing number of power semiconductor switches, diodes and capacitors as well as the number of isolated DC sources. This is due to the fact that the multi-level inverter synthesized the higher output voltage levels from

several lower DC link voltages which are blocked/controlled by using several low-rated rating power semiconductor switch devices. The higher number of voltage levels means the lower the pulse height (DC linkage voltage). Lower pulse height (and also the pulse width) can cause fewer of harmonics in output spectrum which results in higher THD. The higher number of levels provides higher voltage resolution (smaller voltage step size) in staircase AC output voltage which can shape almost to the desired sinusoidal AC waveform.

- Although low-voltage rated of power semiconductor switches can be used which can be operated at the low fundamental switching frequency, however each switch requires gate driver control circuit, protection circuits, and cooling units (heat sink).
- Higher numbers of output voltage levels can have complicated control circuit and therefore the overall inverter system size can be bulky.
- The overall power losses in the inverter system can be high due to a large number of power semiconductor switches used. This can degrade the overall efficiency of the system (in transferring the real input power from source to the load).
- Commutating the power semiconductor switches at low fundamental switching frequency means the switches conduct in long conduction period so that allow the DC link capacitor current discharging. However, this can increase the conduction losses in the power switches and diodes.
- Inverter reliability can be decreased due to a large number of power switches used.
- Overall inverter system size can be bulky in size and expensive in cost due to many power switches used and associated control drive circuit.

In addition, the limitation of the optimization technique through Selective Harmonics Elimination (SHE) method that is used to reduce the total THD of the output voltage in the classical multi-level inverter (i.e. CHB-MLI) are:

- The need to undergo a complicated offline calculation of the transcendental non-linear equation to determine the optimum switching angle and/or DC link voltage that eliminates the specific lower harmonics orders.
- Only lower order harmonics order (which are located in the low-frequency sideband of the output voltage frequency spectrum) can be selectively eliminated by the optimum switching angle, while the passive output filter is required to remove the higher order harmonics (which is located in the high-frequency sideband of the output voltage frequency spectrum).

A summary of the above discussed inverter topologies, including three-levels PWM inverter topologies and multi-level inverter topologies, showing the advantages and disadvantages is presented. The selection of DC/AC inverter topologies depends on the factors the designer must compromise such as power quality; the number of levels and the total harmonics distortion (THD) of the AC output voltage and current, size and volume and cost. From the literature review and the above summary, it has been shown that the classical multi-level inverter topologies have a specific advantage over three-levels PWM inverter in the point of view of low THD, low switching loss and high efficiency. However, generating higher number of voltage levels using classical multi-level inverter topologies for the sake of improving THD demands high number of components (such as power switches, diodes and capacitors), complicated control circuit, bulky in size and expensive. Hence, it is important to look at different multi-level inverter topologies (newly-evolved) with reduced component count and

the current technologies that are used in designing inverter which have simple circuit configuration, straightforward control operations, and less complex control circuits.

## 2.4 Summary

This chapter presents a review of power electronics DC/AC inverter circuits on traditional three-levels PWM topologies and classical multi-level topologies surveyed in published literature. It sets out the operating principles, modulation control techniques, and harmonics elimination techniques. This chapter is important in identifying the weaknesses and strengths of each of the identified DC/AC inverter topologies. These points are very useful in providing a comparative study of available DC/AC inverter topologies surveyed in published literature. It has been shown that the classical multi-level inverters topologies have a specific advantage over conventional three-levels PWM inverters type. Therefore, the research need to emphasise on multi-level inverters topologies configuration type.

Over the last few years different multi-level inverter topologies/techniques (switched-capacitor based) have evolved. Some of these techniques need to be fully investigated in order to appreciate the proposed technique used in this thesis. Chapter 3 review some of the voltage boosting/varying techniques and their circuit topology configurations. Some of these techniques also need to be fully investigated in order to appreciate the selected technique used for the proposed inverter system. Also, critically reviews some of these recent topologies and highlights the gaps and the challenges in this field.

# **Chapter 3 Switched-Capacitor Circuit & Switched-Capacitor Multi-level DC/AC Inverter Topologies**

## **3.1 Introduction**

In Chapter 2, a general review of classical inverter type was presented. Over the last five years, new types of inverter circuits have evolved from the classical topologies (Luo and Ye, 2013, Gupta et al. 2016). Some of these techniques are investigated in this chapter, as it covers the basics of the proposed inverter topology presented in this thesis.

Many references have discussed the development of switched-capacitor circuit (SCC) techniques which can be operated at high switching frequency (Darwish, Mehta, 1990) and also operated at a hybrid switching frequency, which combines low and high-frequency operation for many power electronics applications. Recent reviews of published papers on DC/AC inverter topologies (Gupta et al. 2016) show the tremendous interest of integrating SCC into DC/AC inverter to achieve output voltage larger than the input voltage. The topic focuses on simple techniques and/or circuit configurations (low number of switches, capacitors, diodes, and isolated DC sources), which have the ability to boost and/or regulate/vary voltage.

In this chapter, an overview of voltage boosting/varying techniques is surveyed in the literature. The available techniques (switched capacitors technique, magnetic coupling, and multi-stage booster) are categorised. The available switched-capacitors techniques are categorised according to their type of circuit topology/configuration and connection. Some of these switched-capacitors techniques are investigated to appreciate the proposed technique used in this thesis. A brief discussion on the

advantages and disadvantages of each voltage boosting/varying technique and each type of switched-capacitor circuit's topology/configurations and connections are presented. A comparative study is conducted to help the author select an optimum circuit topology/configuration (voltage regulator) to be implemented/applied in the proposed inverter circuit (a new simple DC/AC inverter based switched capacitor topology), which is conducted in Chapter 4.

Furthermore, critical review of the recent switched-capacitor multi-level inverter topologies as reported in literature survey is also provided in this chapter. A brief discussion of the advantages and disadvantages of each circuit topology is presented. The gap and challenge in the recent multi-level DC/AC inverter based switched-capacitor circuit topologies is identified.

### **3.2 Overview of Voltage Boosting Technique**

Most renewable resources produce DC power sources, and inverters are used to interface to the AC grid. A DC/DC converter or/and a transformer is combined at DC or AC side in order to boost voltage to appropriate voltage levels. This is mainly due to low input DC voltage obtained from most renewable energy sources, such as domestic wind turbines, solar arrays, or fuel cells. In grid-connected inverter systems, boosting output voltage is one of the challenges. There are numerous voltage boost techniques with different circuit configurations that have been proposed in the literature (Forouzesh et al. 2017). Voltage boost technique is defined as the ability of circuit topology and technique to produce output voltage larger than the input voltage. It involves voltage multiplication and/or voltage regulation/varying voltage processes to the desired voltage levels. These processes are achieved by a combination of energy

storage elements (capacitors and inductors) and/or transformers in conjunction with power semiconductor switches and diodes in specific topology and using a specific technique. For the purpose of explaining the strength and weaknesses of each boosting circuit topology/configuration, it is essential first to categorise the voltage boosting techniques covered. Figure 3.1 shows the categorisation of the voltage boosting technique.

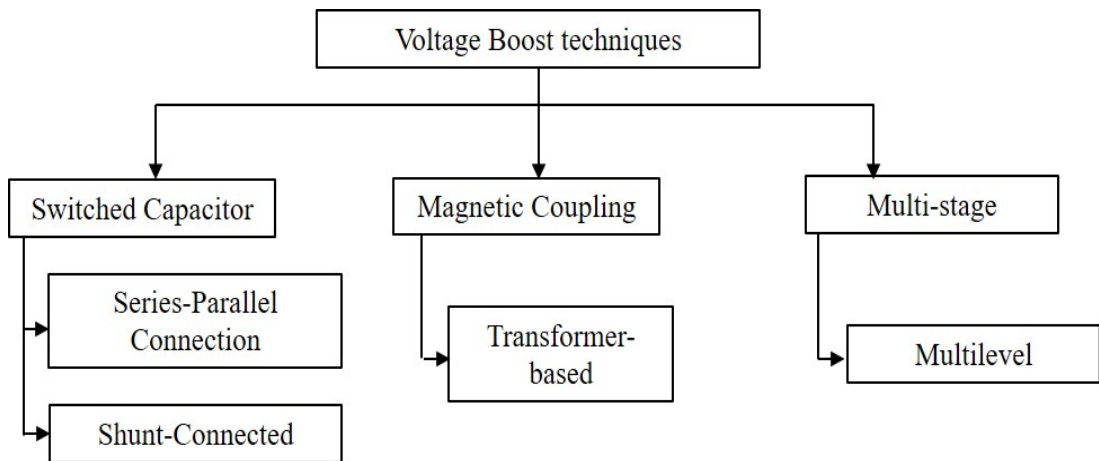


Figure 3.1 Categorisation of voltage boosting technique

Three main techniques are included, namely switched capacitor, magnetic coupling, and multi-stage booster. A review and investigation of the switched capacitor technique is discussed in addition to other voltage boosting techniques (magnetic coupling and multi-stage booster) conducted in literature. Upon this review and investigation, the desired technique and/or circuit configuration is adopted showing the justification of that selection. The following section discusses each of voltage boosting techniques covered in this chapter.

### 3.3 Switched Capacitor

Switched Capacitor is the most famous voltage boosting technique. This technique utilises energy storing elements such as capacitors and inductors in conjunction with power semiconductor switches. These elements are combined in a specific configuration to achieve high-voltage boost. The basic switched-capacitor (S-C) circuit cell consists of power semiconductor switches and diodes with DC voltage connected to input circuit. The most famous basic concept of S-C is known as charge pump where pump energy is moved from one capacitor to another through appropriate switching control technique. Its output voltage can reaches input voltage levels after several sequences of switching control cycles. This has been successfully utilised for power conversion in low power on chip DC-DC converter application.

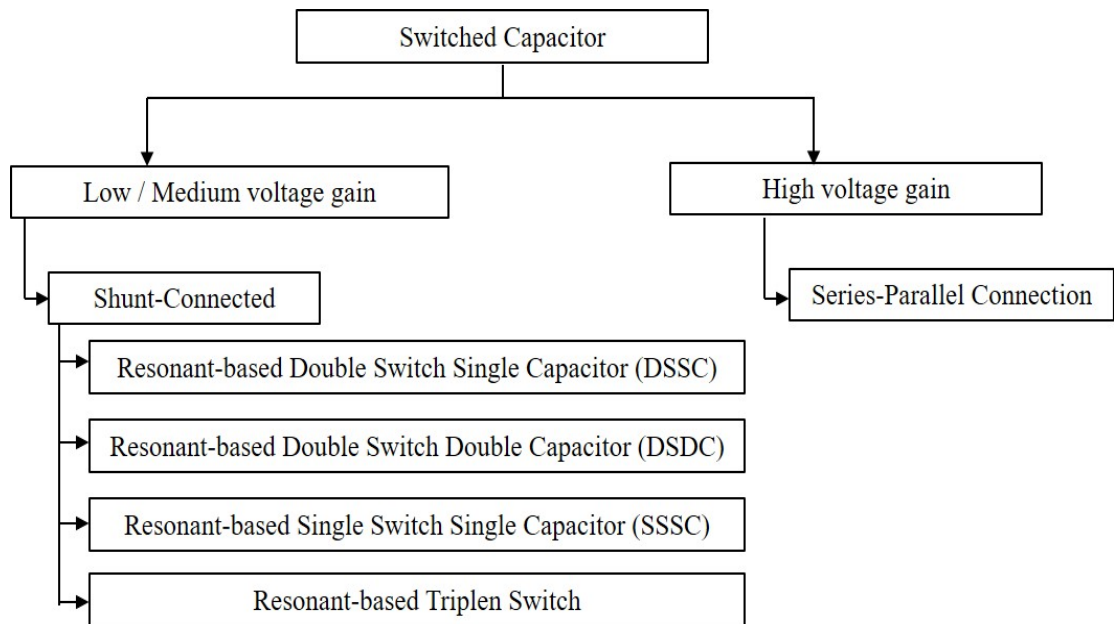


Figure 3.2 Categorisation of switched capacitor according voltage gain/ ability and the type of circuit topology/configuration

The switched-capacitor circuit (SCC) technique can be classified according to its voltage gain ability as well as its type of circuit topology/configuration connection as shown in Figure 3.2. Using different circuit configuration and connection, this S-C circuit can have low/medium-voltage gain or high-voltage gain. The low-voltage gain S-C circuits have a simple structure due to it containing fewer component (switch and capacitor) counts and simple control. Meanwhile, high-voltage gain S-C circuits have a large overall circuit structure due to the multi-stages cell. This utilises more switches and capacitor components. S-C has been applied for many other power electronic applications, such DC/AC inverters (Luo and Ye, 2013) and AC power system such active power filter and reactive power compensation (Darwish, Mehta, 1990, Arman, Darwish, 2009, Arman, Marouchos & Darwish, 2012). The switched-capacitor circuit (SCC) can also be classified according to the types of circuit topology/configuration connections as shunt-connected SCC and series-parallel connection SCC.

Shunt-connected SCC topology has been used in many AC power system applications. It is composed of capacitors, inductors, and power semiconductor switches which are configured in shunt-connected configuration. This topology is classified as low/medium-voltage gain/boost ability due to fewer numbers of capacitors used in conjunction with power switches. For reactive power compensation, it is incorporated with a thyristor in shunt-connected configuration to form Thyristor-Switched Capacitors (TSC). It is used for controlling bus voltage and prevents voltage collapse when high loading in AC power network systems is present (Mohan, 2002).

For active filter applications, this shunt-connected SCC technique has also been presented in Darwish, Mehta, 1990, El-Habrouk, Darwish & Mehta 2000, Arman, Darwish 2009 as a smoothly variable source of lagging and leading reactive power in reactive AC power control applications (Darwish, Mehta, 1990, Arman, Darwish 2009). Some of the shunt-connected SCC circuit topologies with varying switch duty cycle control technique were exhibits variable characteristic capabilities (Darwish, Mehta & Thomson 1988). In addition, these techniques were found to be effective for filtering harmonics applications such as automatically tuning impedance at any desired harmonics to filter out (Arman, Darwish 2009, Arman, Marouchos & Darwish, 2012).

The available basic unit configurations of the shunt-connected SCC circuits are shown in Figure 3.3 (a) Double Switch Single Capacitor (DSSC), (b) Double Switch Double Capacitor (DSDC), (c) Single Switch Single Capacitor (SSSC) and (d) Triplen Switch (Darwish, Mehta, 1990, Arman, Darwish 2009). A shunt-connected double switch single capacitor (DSSC) SCC circuit configurations has shown it unique variable capacitor features (Arman, Darwish 2009, Arman, Marouchos & Darwish, 2012). With an inductor is connected between AC voltage source and DSSC and/or DSDC circuits input, variable capacitor behavior can be obtained by applying varying switch duty cycle control technique in a specific switching pattern to the associated switches. However, from another point of view, this behaviour can also lead to providing varying voltage ability.

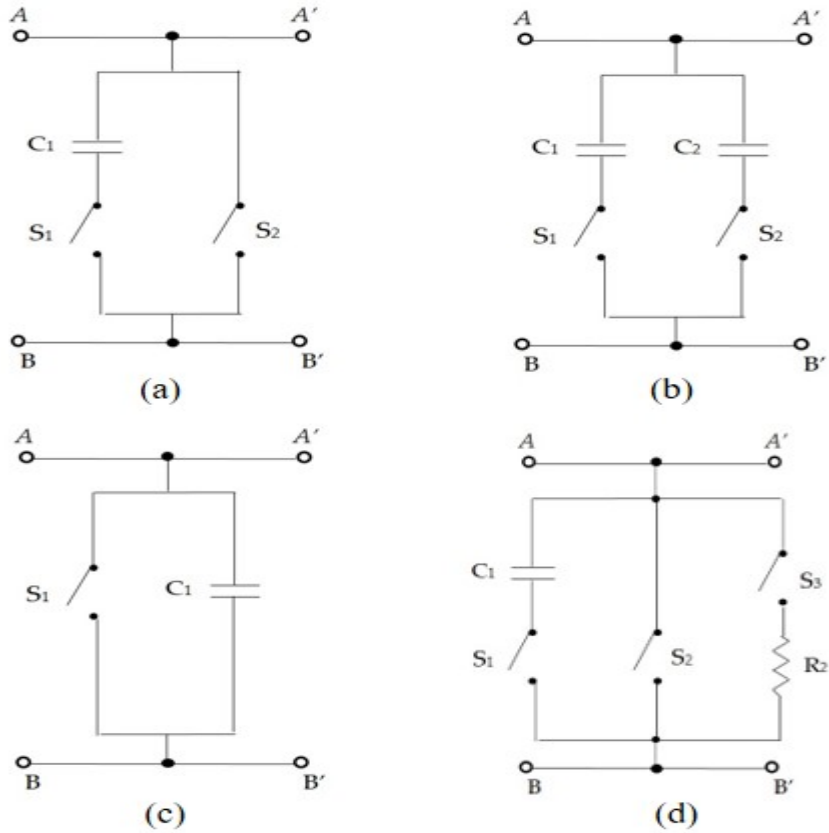


Figure 3.3 Basic configuration unit of the shunt-connected SCC

The following subsections review the operating principle of the shunt-connected switched-capacitor circuit (SCC) topology. An investigation of the main configuration of this topology is presented in addition to other configurations. This is to identify the possibility of obtaining variable capacitor behaviour among topologies with given DC source applied at the input that could provide voltage gain and/or varying/regulating voltage ability. Upon examination, the optimum is accepted based on its ability to comply with a strict set of criteria given as showing justification of that selection. The main configuration is DSSC. An outline of other configurations includes Single Switch Single Capacitor (SSSC), Double Switch Double Capacitor (DSDC), and Triplen Switch.

### 3.3.1 Resonant-based Double Switch Single Capacitor (DSSC) circuit

Basic DSSC circuit configuration (Darwish, Mehta, 1990) is shown in Figure 3.3(a). It is formed by one capacitor ( $C_1$ ), and two unidirectional power semiconductor switches ( $S_1$ ) and ( $S_2$ ). The two switches ( $S_1$ ) and ( $S_2$ ) operate in anti-parallel operation in order to prevent the capacitor ( $C_1$ ) from short-circuiting so that when ( $S_1$ ) is turned ON, ( $S_2$ ) is OFF instantaneously and vice versa. The switches can operate at high switching frequency (to smooth the ripple capacitor voltage but not too high in order to limit the switching losses i.e.  $<50$  kHz).

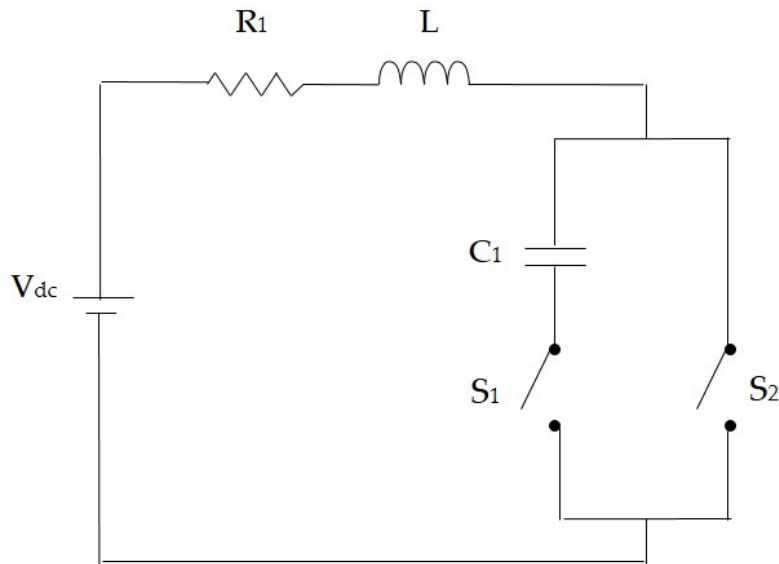


Figure 3.4 Resonant-based DSSC circuit

A current source consists of an inductor,  $L$  in series with the internal resistance of the inductor ( $R_1$ ), and DC voltage source ( $V_{dc}$ ) is inserted at the input of DSSC configuration as shown in Figure 3.4. The internal resistance of the inductor can limit the transient spike current flowing through power switches ( $S_1$ ) and ( $S_2$ ). This provides protection for power semiconductor switches.

Due to switch anti-parallel operation, DSSC circuit branches are alternately connected to the input DC supply. One branch forms a switched series resonance (R-L-C) circuit which is connected in series with switch ( $S_1$ ) with resonant current flowing through it. The other branch forms a series R-L circuit connected in series with a switch ( $S_2$ ) with transient current flowing through it. Therefore, a combination of a current source and DSSC configuration introduces a resonant-based DSSC circuit. This circuit configuration has fewer switching components which can reduce the power loss. It is composed of one capacitor ( $C_1$ ) and two semiconductor switches ( $S_1$ ) and ( $S_2$ ). However, instantaneous switching control transition between on and off switch ( $S_1$  &  $S_2$ ) states is required to avoid short-circuit problems which could occur for very short period of time. This could lead to high surge current which can damage the switches.

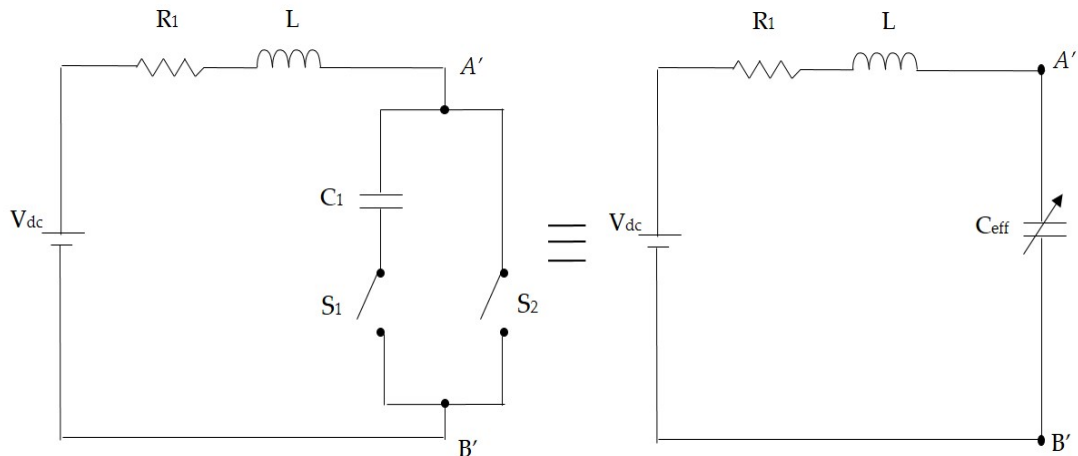


Figure 3.5 DSSC circuit identical to the effective capacitance

The following subsections present two mathematical analyses for proving purposes; switching function and transient analysis. The switching function analysis is conducted to prove that a DSSC circuit with a varying switch duty cycle control applied can introduce a variable capacitor. An inductor with its internal resistance is connected in series with DC voltage at input provides a current source for a DSSC

circuit. The value of effective capacitance ( $C_{eff}$ ) will be proven as it varies with varying the duty cycle of the power switches where  $C_{eff}$  can be measured across terminal (A'-B') as shown in Figure 3.5.

### 3.3.1.1 Switching function Analysis of the resonant-based DSSC circuit

Switching function principle (Marouchos 2006) is the process of commutating switches between turned on (1) and turned off (0) switch state in form of sequence of pulses. The varying switch duty cycle controlled technique involves the computations of power semiconductor switches ( $S_1$ ) and ( $S_2$ ) of the resonant-based DSSC SCC circuit configuration at high switching frequency ( $>10$  kHz). These switches are operated in anti-parallel operation.

The resonant-based DSSC SCC circuit configuration is shown in Figure 3.5. The circuit branches are alternately connected to the input DC supply. One branch forms a switched series resonance (R-L-C) circuit which connected in series with switch ( $S_1$ ) during its conduction period ( $D_o = 1$ ). The other branch form series (R-L) circuit connected in series with switch ( $S_2$ ) during its conduction period ( $D_o = 0$ ). The switch duty cycle  $D_o$  can have any value between 0 and 1. Varying switch duty cycle of the switches ( $D_k$ ) is the ratio of varying on-time switch duration  $t_{on}$  over the entire switch switching period  $T_s$ . The switching frequency of these switches can be assigned as  $f_s$ .

The switching function can be expressed as:

$$F(t) = D_o + \sum_{n=1}^{\infty} (A_n \cos(n\omega_s t) + B_n \sin(n\omega_s t)) \quad (3.1)$$

For the purpose of simplification, the switching instant is selected to be  $t_1 = -(t_{on}/2)$  which will simplify and reduced the previous equation to:

$$F(t) = D_o + 2 \sum_{n=1}^{\infty} K_n \cos(n\omega_s t) \quad (3.2)$$

where high switching period is  $T_s = 1/f_s$  and the angular switching frequency  $\omega_s = 2\pi F_s$  and  $K_n = \sin n \pi D_o / 2$ . Let,

$$\emptyset(t) = 2 \sum_{n=1}^{\infty} K_n \cos(n\omega_s t) \quad (3.3)$$

Hence,

$$F(t) = D_o + \emptyset(t) \quad (3.4)$$

where  $F(t)$  is the switching function of switch (S<sub>1</sub>). The switching function of (S<sub>2</sub>) will be the complementary of (S<sub>1</sub>),  $F'(t)$ ,

$$F'(t) = 1 - F(t) \quad (3.5)$$

The voltage across points A' - B' (DSSC SCC circuit branch as shown in Figure 3.5), is given by:

$$V_{dc} = R_1 i + L \frac{di}{dt} + V_{A'-B'} \quad (3.6)$$

$$V_{dc} = R_1 i + L \frac{di}{dt} + F(t) \cdot v_c(t) \quad (3.7)$$

where,

$$v_c(t) = \frac{1}{C_1} \int_0^t F(t) i(t) dt \quad (3.8)$$

$$v_c(t) = \frac{1}{C_1} \int_0^t D_o \cdot i(t) dt + \frac{1}{C_1} \int_0^t \emptyset(t) \cdot i(t) dt \quad (3.9)$$

Assuming the circuit is underdamped ( $\alpha < \omega_0$ ). The instantaneous current during

Mode 1 is

$$i_1(t) = \frac{V_{dc}}{\omega_r L} e^{-\alpha t} \sin(\omega_r t) \quad (3.10)$$

where the damping factor,

$$\alpha = \frac{R_1}{2L} \quad (3.11)$$

and the resonant frequency,

$$\omega_0 = \frac{1}{\sqrt{LC_1}} \quad (3.12)$$

and the ringing frequency (or damped resonant frequency),

$$\omega_r = \frac{1}{2} \sqrt{\frac{4L - C_1 R_1^2}{C_1 L^2}} \quad (3.13)$$

Consider only fundamental component frequency. So,  $F(t) = D_o$

$$v_c(t) = \frac{1}{C_1} \int_0^t D_o \cdot i_1(t) dt = \frac{D_o}{C_1} \left[ \frac{V_{dc}}{\omega_r L} e^{-\alpha t} \sin(\omega_r t) \right] \quad (3.14)$$

Hence, the capacitor voltage is

$$v_c(t) = -\frac{D_o V_{dc}}{\omega_r C_1} e^{-\alpha t} (\alpha \sin(\omega_r t) + \omega_r \cos(\omega_r t)) \quad (3.15)$$

The voltage across terminal point A' - B',

$$V_{xy} = F(t) \cdot v_c(t) \quad (3.16)$$

$$V_{xy} = [D_o + \emptyset(t)] \left[ -\frac{D_o V_{dc}}{\omega_r C_1} e^{-\alpha t} (\alpha \sin(\omega_r t) + \omega_r \cos(\omega_r t)) \right] \quad (3.17)$$

$$V_{xy} = D_o^2 \left[ \frac{1}{\omega_r C_1} \right] [-V_{dc} e^{-\alpha t} (\alpha \sin(\omega_r t) + \omega_r \cos(\omega_r t))] \quad (3.18)$$

Let,

$$I = -V_{dc} e^{-\alpha t} (\alpha \sin(\omega_r t) + \omega_r \cos(\omega_r t)) \quad (3.19)$$

Hence,

$$V_{xy} = D_o^2 [X_c] I \quad (3.20)$$

Since the effective capacitance (between terminal point A'-B' as shown in Figure 3.5) is given by:

$$X_{ceff} = \frac{V_{A'-B'}}{I} \quad (3.21)$$

Hence, the effective capacitance reactance can be calculated as follows:

$$X_{ceff} = D_o^2 X_c \quad (3.22)$$

$$C_{eff} = \frac{C_1}{D_o^2} \quad (3.23)$$

where  $C_1$  is the fixed capacitor of the DSSC switched-capacitor circuit.

$$C_{eff} = \frac{C_1}{D_o^2} \quad (3.24)$$

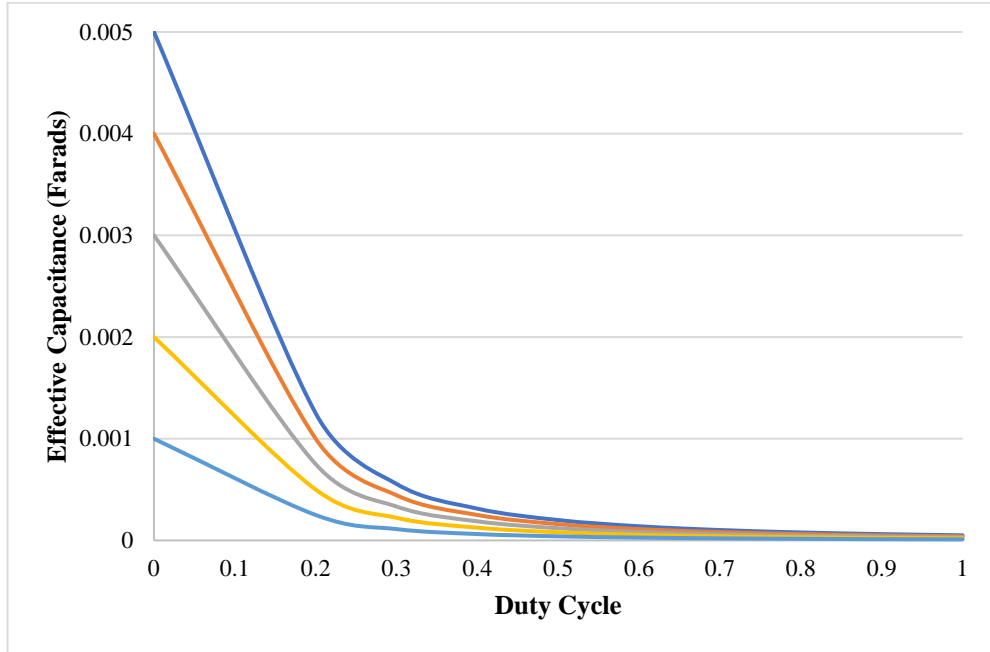


Figure 3.6 Relationship of effective capacitance and duty cycle (Theoretical)

The relation between effective capacitance ( $C_{eff}$ ) and switch duty cycle values is shown in Figure 3.6. This relation is obtained from equation (3.24) in switching function analysis. According to this analysis, the relationship shows that the value of capacitance (across terminal point A'- B') can be varied by controlling switch duty

cycle values (between  $D_o=0$  and  $D_o=1$ ) of the associated switch ( $S_1$ ) (and its complement switch ( $S_2$ )). At  $D_o=1$ , the capacitor branch is disconnected from the DSSC circuit as shown in Figure 3.5 and hence the circuit has zero capacitance. At  $D_o=0$ , the capacitor is connected to the circuit and the circuit has a fixed capacitor. Given a current source at input and varying switch duty cycle values control technique, which makes it clear that DSSC circuit configuration shows a variable capacitor behavior due to resonant frequency. By substituting  $C_1$  with  $C_{eff}$  in equation (3.30), this behavior can lead to varying voltage ability.

### 3.3.1.2 DC Transient Analysis

The resonant-based DSSC circuit with a varying switch duty cycle controlled has also been analysed using DC transient analysis (voltage - current characteristic). This is to investigate its ability to vary or regulate voltage. The voltage across the capacitor ( $C_1$ ) will be proven that it varies with varying switch duty cycle values. Due to anti-parallel switch operation, the DSSC circuit branches are alternately connected to the input DC supply via a current limiter (an inductor ( $L$ ) in series with its internal resistance ( $R_1$ )). This forms two modes of operations. During first mode (Mode 1), a switched series resonance ( $R-L-C$ ) circuit connection is formed on the left DSSC circuit branch, as shown in Figure 3.7. A current limiter is connected in series with a fixed capacitor ( $C_1$ ) to be controlled by a switch ( $S_1$ ). The resonant current flowing through it and capacitor ( $C_1$ ) is charging for duration  $t_a$ . During the second mode (Mode 2), series ( $R-L$ ) circuit connection is formed on the other branch where a current limiter is connected in series with switch ( $S_2$ ). The transient current flows through switch  $S_2$  and the capacitor is disconnected (holds its initial charge).

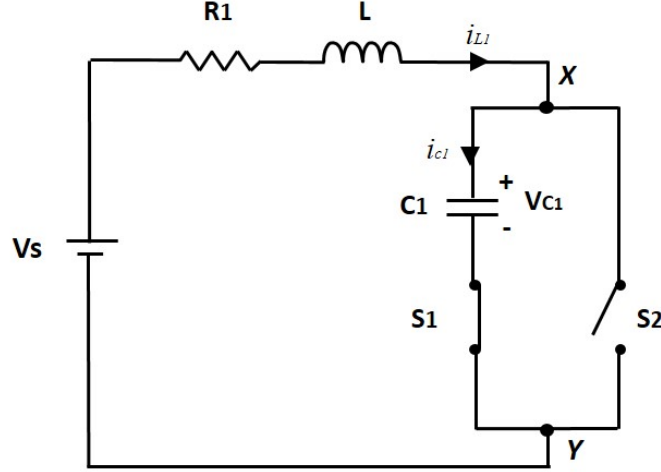


Figure 3.7 Resonant-based DSSC circuit in Mode 1

For simplification, the analysis is made during capacitor ( $C_1$ ) charging Mode 1 (Switch ( $S_1$ ) is closed and ( $S_2$ ) is open) as shown in Figure 3.7. Varying switch duty cycle control means varying on-time duration  $t_a$  of the associated switches. Assuming this circuit operates in continuous conduction mode (CCM), the inductor current never reach zero at every beginning of the capacitor charging interval.

Using Kirchhoff's Voltage Law (KVLs), the equation can be written as

$$R_1 i_{L1}(t) + L \frac{di_{L1}(t)}{dt} + \left( \frac{1}{C_1} \int i_{c1} dt + v_c(t=0) \right) = V_s \quad (3.25)$$

Assuming the circuit is underdamped ( $\alpha < \omega_0$ ). The instantaneous current during Mode 1 is

$$i(t) = i_{L1}(t) = i_{c1}(t) = \left( \frac{V_s - V_{c0}}{\omega_r L} \right) e^{-\alpha t} \sin(\omega_r t) \quad (3.26)$$

where the instantaneous charging current is equal to inductor current and capacitor current i.e.  $i(t) = i_{L_1}(t) = i_{c_1}(t)$ . Assuming the initial condition of inductor current is zero i.e.  $i_L(t = 0) = 0$  and the initial capacitor voltage is  $V_o$  i.e.  $v_c(t = 0) = V_{c_0}$ .

where the damping factor,

$$\alpha = \frac{R_1}{2L} \quad (3.27)$$

and the resonant frequency,

$$\omega_0 = \frac{1}{\sqrt{LC_1}} \quad (3.28)$$

and the ringing frequency (or damped resonant frequency),

$$\omega_r = \frac{1}{2} \sqrt{\frac{4L - C_1 R_1^2}{C_1 L^2}} \quad (3.29)$$

the peak-to-peak ripple voltage across fixed capacitor ( $C_1$ ) can be expressed as

$$\Delta v_c = v_c(t) - v(t = 0) = \frac{1}{C_1} \int_0^t i(t) dt \quad (3.30)$$

Or capacitor ripple voltage can also be expressed as

$$\Delta v_c = v_c(t) - V_{c_0} = -(V_s - V_{c_0}) e^{-\alpha(t)} \left( \frac{\alpha}{\omega_r} \sin(\omega_r t) - \cos(\omega_r t) \right) \quad (3.31)$$

The capacitor voltage equation during Mode 1

$$v_c(t) = -(V_s - V_{c_0}) e^{-\alpha(t)} \left( \frac{\alpha}{\omega_r} \sin(\omega_r t) - \cos(\omega_r t) \right) + V_{c_0} \quad (3.32)$$

where  $v_c(t)$  is the peak capacitor voltage,  $v(t = 0) = V_{c_0}$  is the initial capacitor voltage and  $i(t)$  is the instantaneous charging current.

Figure 3.8 and Figure 3.9 illustrates the peak capacitor voltage and peak capacitor current during Mode 1. This shows the characteristics of complete capacitor charge interchange. At initial start-up, this capacitor voltage and capacitor current oscillates and exponentially decreases amplitude under transient conditions. Once the steady-state condition is reached, the capacitor voltage is equal to DC input voltage ( $V_{dc}$ ). The capacitor current becomes resonant-type (sinusoidal).

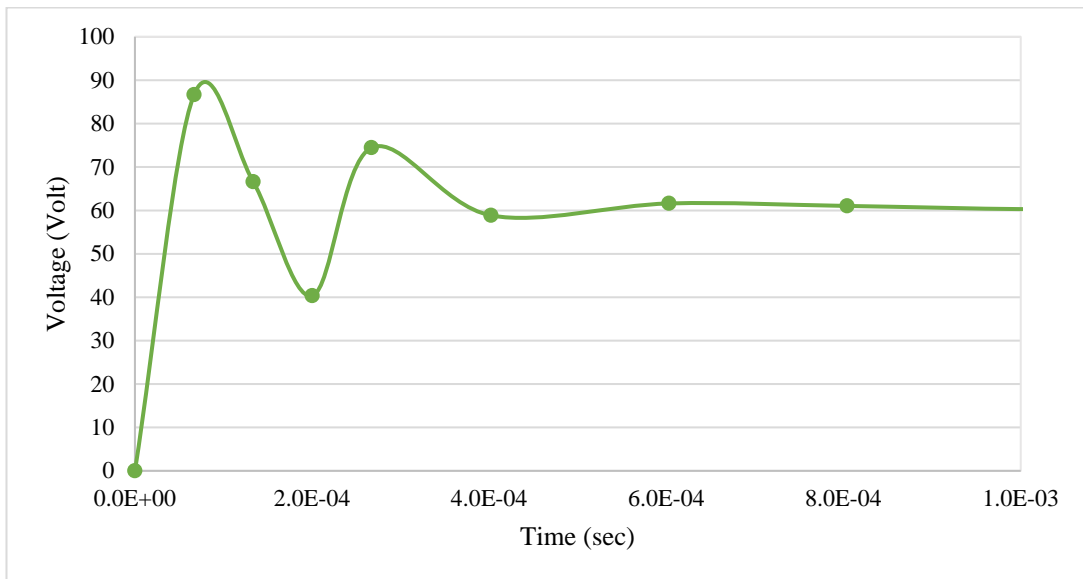


Figure 3.8 Capacitor voltage during Mode 1 (Theoretical)

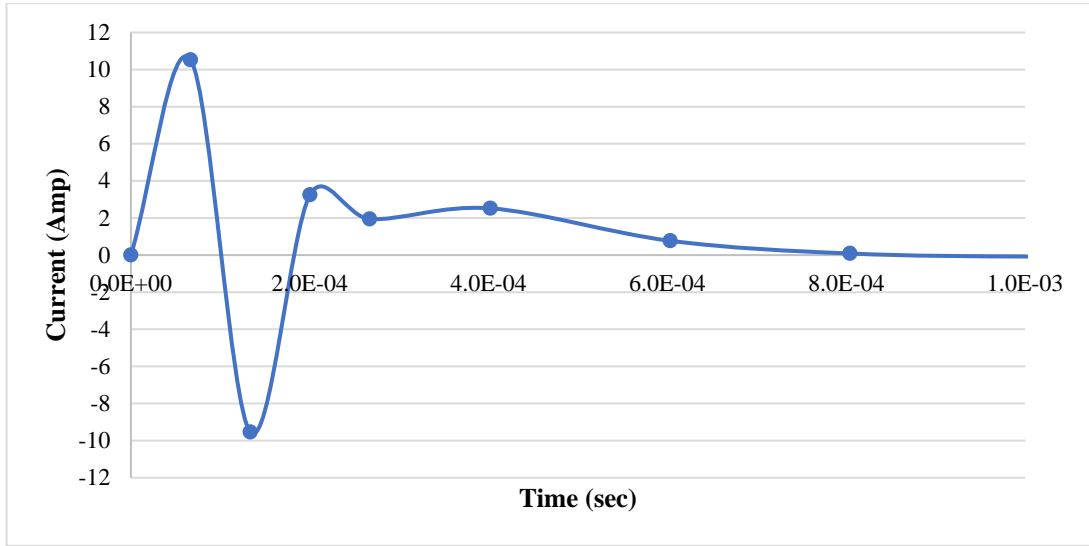


Figure 3.9 Capacitor current during Mode 1(Theoretical)

Due to switching action in such a way that capacitor ( $C_1$ ) is charged to peak maximum voltage value during Mode 1 and hold it charges (maintain constant initial voltage  $V_{c_0}$ ) in Mode 2. This capacitor voltage can be varied by varying the on-time switch  $t$  in equations (3.32 and 3.33). This can be done by varying the width of PWM square pulse control signal applied to switch ( $S_1$ ). The duty cycle ( $D_k$ ) of the switch ( $S_1$ ) is defined as the ratio of on-time switch  $t$  over entire high switching period,  $T_s$ .

$$D_k = \frac{t}{T_s} \quad (3.33)$$

During Mode 1 ( $0 \leq t_a \leq t_k (= D_k n T_s)$ ), duty cycle ( $D_k$ ) of the switch ( $S_1$ ) is the ratio of on-time switch ( $t_k$ ) takes to charge capacitor ( $C_1$ ) over entire  $n$  times repeating high switching period,  $n T_s$ .

$$D_k = \frac{t_k}{n T_s} \quad (3.34)$$

The longer charging duration time  $t_k = D_k nT_s$ ; the more charge can be stored and hence, the larger the capacitor voltage ( $v_c(t)$ ).

$$\Delta v_c = v_c(t_k) - v(t = 0) = \frac{1}{C_1} \int_0^{t_k} i(t) dt \quad (3.35)$$

With  $n$  times repeating switching period,  $nT_s$  of the PWM pulses signal applied to the associated switches causes the voltage across point X-Y to fluctuate from zero to maximum (peak capacitor voltage) creating large ripple voltage. In this case, low capacitance ( $C_1$ ) (i.e. 1uF or 10uF) can be used in achieving a large range of voltage across point X-Y (peak capacitor voltage). Therefore, the maximum peak amplitude of the staircase/multi-level output voltage can be determined by the value of capacitor chosen.

If  $k$ -th duty cycle value ( $D_k$ ) applied with increasing time point  $t_k$  can yield  $k$ -th capacitor voltage level ( $v_{c_k}(t_k)$ ) which can also be denoted as the voltage increment.

$$\Delta v_{c_k} = v_c(D_k nT_s) - v(t = 0) = \frac{1}{C_1} \int_0^{t_k} i(t) dt \quad (3.36)$$

$$v_{c_k}(t_k) = -(V_s - V_{c_0}) e^{-\alpha(t_k)} \left( \frac{\alpha}{\omega_r} \sin(\omega_r(t_k)) - \cos(\omega_r(t_k)) \right) + V_{c_0} \quad (3.37)$$

Hence, the relation between  $k$ -th capacitor voltage level ( $v_{c_k}(t_k)$ ) and duty cycle ( $D_k$ ) within appropriate switching time interval  $0 \leq D_k \leq t_k (= D_k nT_s)$  where  $k = 1, 2, \dots, N$  and  $N = \frac{m-1}{2}$  ( $k$  is the number of steps and  $m$  is the number of levels peak to peak output voltage) can be described by the following expression.

$$v_{c_k}(D_k) = \begin{cases} v_{c_1}(D_1), & 0 \leq D_1 \leq t_1 \\ \vdots & \vdots \\ \vdots & \vdots \\ \vdots & \vdots \\ v_{c_N}(D_N), & t_{N-1} \leq D_N \leq t_N \end{cases} \quad (3.38)$$

The following Figure 3.10 and Table 3.1 shows the relationship between capacitor voltage level or voltage increment and duty cycle. This illustrates the characteristic of the resonant-based DSSC switched-capacitor circuit with a switch duty cycle controlled technique, where the voltage across the fixed capacitor ( $C_1$ ) can be varied by controlling or varying the duty cycle value.

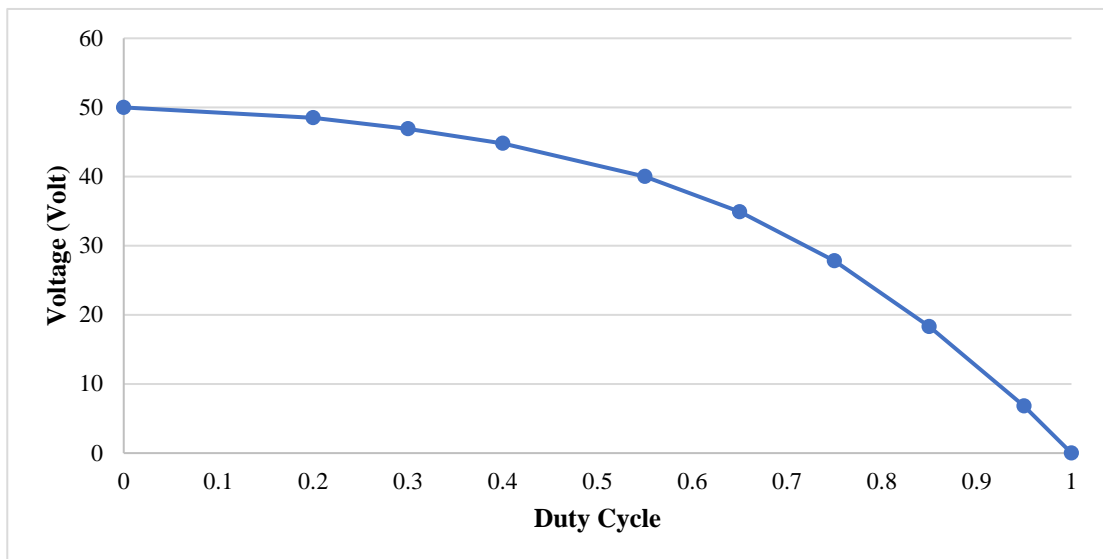


Figure 3.10 Relationship between capacitor voltage and duty cycle with respect to  $S_1$  for DSSC SCC circuit (Theoretical)

Table 3.1 Relationship between capacitor voltage level & duty cycle (Theoretical Calculation)

$k$	Duty Cycle Value $D_k$	Capacitor voltage level $v_{c_k}(D_k)$ (Volt)
0	1	0
1	0.95	6.8
2	0.85	18.3
3	0.75	27.8
4	0.65	34.9
5	0.55	40.0
6	0.4	44.8
7	0.3	46.9
8	0.2	48.5
9	0	50

As the duty cycle value of the switches is decreased, the magnitude of capacitor voltage level increase. According to this behaviour, this resonant-based DSSC circuit with switch duty cycle controlled technique has the ability to vary voltage across the capacitor ( $C_1$ ) due to resonant. The capacitor voltage level can be varied by controlling the duty cycle value of the switch  $S_1$ . The characteristic of this circuit configuration showed that it behaves like a voltage regulator. This can be considered as a new technique of regulating/varying voltage which can lead to producing multi-level voltage. Besides having voltage gain and/or varying voltage ability, it also contains low component count (one inductor ((where  $R_1$  represents an internal resistance of the inductor)), one capacitor, and two power semiconductor switches). An inductor with its internal resistance at input circuit can limit the spike/transient current flowing through power semiconductor switches. Due to this exhibited behaviour and low

component count, therefore the resonant-based DSSC circuit with varying switch duty cycle controlled technique will be used to implement a new optimum inverter topology, which is the aim of this research. This new technique is for the purpose of obtaining rectified multi-level or staircase voltage waveform in the first conversion stage of the proposed inverter by setting specific switching timing control to the associated switches.

### 3.3.2 Resonant-based Double Switch Double Capacitor (DSDC) circuit

Basic DSDC circuit configuration (Darwish, Mehta, 1990) is shown in Figure 3.3(b). It is composed of two capacitors ( $C_1$  and  $C_2$ ) and two semiconductor switches ( $S_1$ ) and ( $S_2$ ). These switches can be operated in the anti-parallel manner with a varying switch duty cycle controlled so that when ( $S_1$ ) is closed, ( $S_2$ ) is open instantaneously and vice versa. With a current source is applied at input, a resonant-based Double Switch Double Capacitor (DSDC) circuit is formed as shown in Figure 3.11.

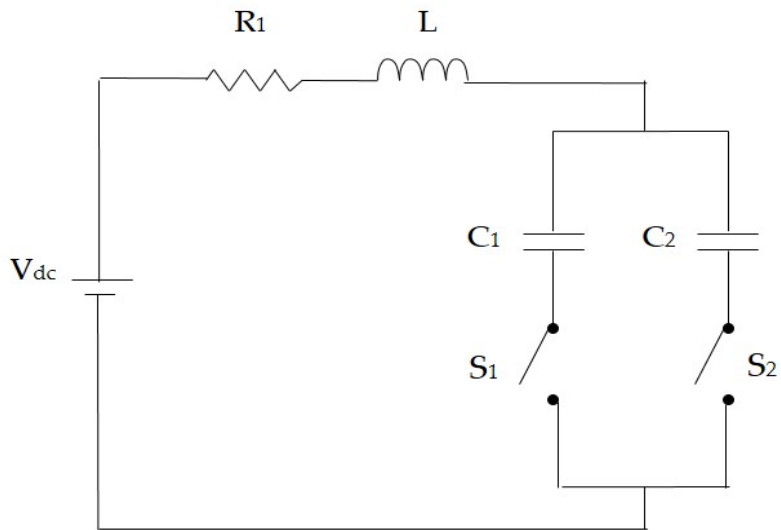


Figure 3.11 Resonant shunt-connected DSDC SCC circuit

By adopting the same approach used in DSSC circuit analysis, the voltage equation for DSDC SCC circuit can be written as follows:

During Mode 1, the voltage equation for  $C_1$  branch

$$R_1 i_{L1}(t) + L \frac{di_{L1}(t)}{dt} + v_{c1} = V_s \quad (3.39)$$

During Mode 2, the voltage equation for  $C_2$  branch

$$R_1 i_{L1}(t) + L \frac{di_{L1}(t)}{dt} + v_{c2} = V_s \quad (3.40)$$

The following Figure 3.12 shows the relationship between capacitor voltage level or voltage increment and duty cycle for DSDC circuit. This illustrates the characteristic of the resonant-based DSDC switched-capacitor circuit with switch duty cycle controlled technique. Each capacitor in DSDC circuit branch is alternately charged, repeating switching action such as continuously chopping the voltage across capacitors. This has no effect on varying capacitor voltage. Therefore, this can be concluded that the DSDC circuit topology does not have varying voltage ability. It also contains many components (two capacitors and two switches). More switches add power losses in the circuit.

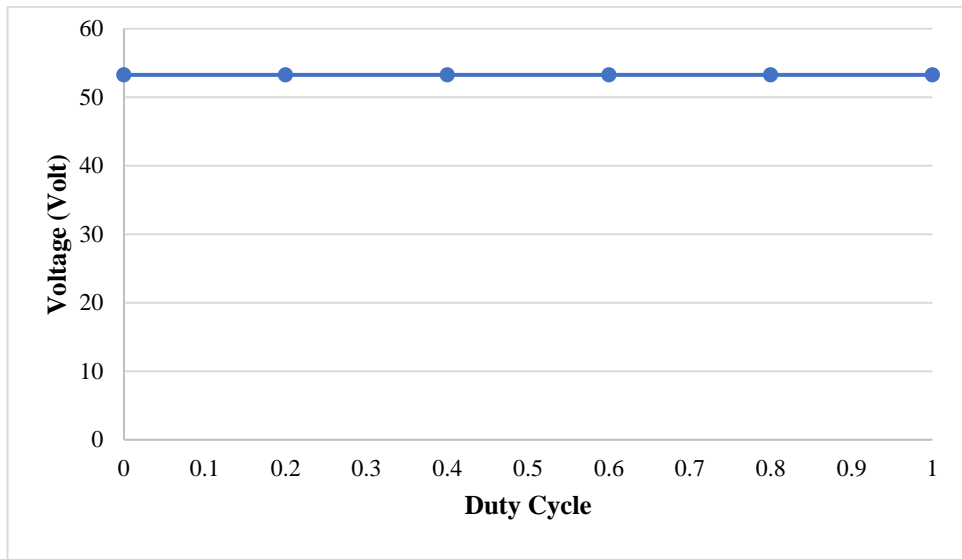


Figure 3.12 Relationship between capacitor voltage and duty cycle with respect to  $S_1$  (Theoretical)

### 3.3.3 Resonant-based Single Switch Single Capacitor (SSSC) circuit.

Basic SSSC circuit configuration (Darwish, Mehta, 1990) is shown in Figure 3.3(c). This is the simplest circuit configuration in shunt-connected switched-capacitor circuit topology. This circuit consists of single unidirectional switch ( $S_1$ ) connected in parallel with single fixed capacitor ( $C_1$ ). This combination is connected to the input of a current source which forms the resonant-based Single Switch Single Capacitor (SSSC) circuit as shown in Figure 3.13.

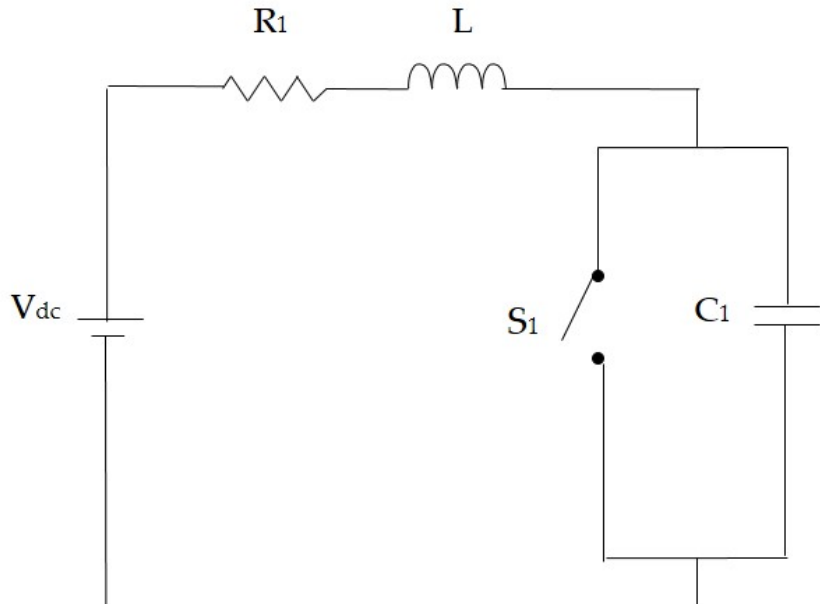


Figure 3.13 Resonant-based Single Switch Single Capacitor circuit

It has simple control operations due to few components used. Only a single switch is switched on and off at single switching frequency operation. Due to this operation, the branch is alternately connected to the input of a current source. One branch forms a series resonance (R-L-C) circuit during first half switching cycle of Switch ( $S_1$ ). During the other half switching cycle, the circuit forms series (R-L) circuit. However, this can have short-circuited problems if the switch is turned while the voltage across capacitor ( $C_1$ ) is not zero. In practice, the switch can only be closed when the voltage

across capacitors is very small (at least), which is close to zero, otherwise it will short-circuit the capacitor. Given that a current source at the input and varying switch duty cycle is controlled, a Single Switch Single Capacitor (SSSC) circuit configuration is unable to provide varying voltage behaviour.

### 3.3.4 Resonant-based Triplen switch SCC circuit

The resonant shunt-connected Triplen switch circuit is shown in Figure 3.14. A basic triplen switch configuration is shown in Figure 3.3(d). It is formed by a double switch single capacitor DSSC circuit with third switch branch connected in parallel. The third branch consists of a unidirectional switch in series with a resistor ( $R_2$ ).

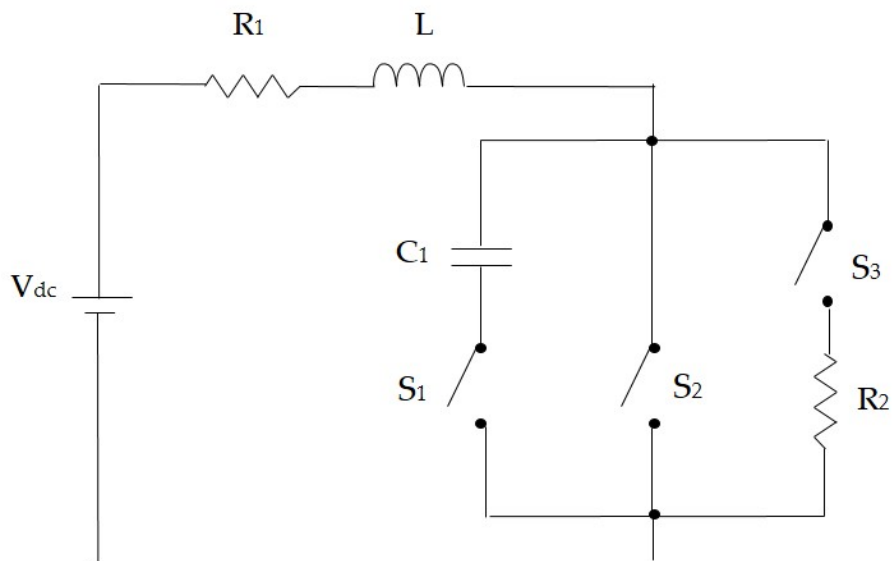


Figure 3.14 Resonant shunt-connected Triplen switch circuit

Introducing this auxiliary branch is to avoid a short-circuit condition during switching transition (between on and off) of anti-parallel switch operations, which was noticed in previous DSSC and DSDC circuits' operations. This is because the power semiconductor switching devices take a finite time to change from one state to another. During this transition action between ( $S_1$ ) and ( $S_2$ ), there is a very short period where

both switches are closed, leading to short-circuiting the capacitor ( $C_1$ ), and the switches are subjected to destructive surge current. The resistor ( $R_2$ ) in the third branch provides smooth transfer of current from one branch to another. The introduction of an additional switch branch in this circuit topology provides short-circuit protection for the switches from a dangerous surge current during the transition. Its operation and characteristics are quite similar to DSSC circuit but in this case the third modes (dead period mode) must be included. By adopting the same approach used in DSSC circuit analysis, the voltage equation for Triplen SCC.

During Mode 1, the voltage equation for  $C_1$  and  $S_1$  branch as follows:

$$R_1 i_{L1}(t) + L \frac{di_{L1}(t)}{dt} + v_{c1} = V_s \quad (3.41)$$

During Mode 2, the voltage equation for  $S_2$  branch as follows:

$$V_s = i_{L2}(t)R_1 + L \frac{di_{L2}(t)}{dt} \quad (3.42)$$

During Mode 3, the voltage equation for  $S_3$  branch as follows:

$$V_s = i_{L3}(t)(R_1 + R_2) + L \frac{di_{L3}(t)}{dt} \quad (3.43)$$

Given a current source at the input and varying switch duty cycle control, this circuit has varying voltage ability. The following Figure 3.15 shows the relationship between capacitor voltage and duty cycle. As the duty cycle value of the switches is decreased, the magnitude of capacitor voltage level increase. The capacitor voltage level can be varied by controlling the duty cycle value of the switch  $S_1$ . The characteristic of triple switch circuit configuration showed that it behaves like a voltage regulator. However, the operation is associated with complicated controls and

adds more components. The small resistance ( $R_2$ ) in series switch could be associated with high power dissipation, which could degrade the efficiency of transferring power from the input source to load. The additional switch could introduce more switching losses when operating at high switching frequency (the switch introduces losses due to their intrinsic characteristic of switching at high frequency).

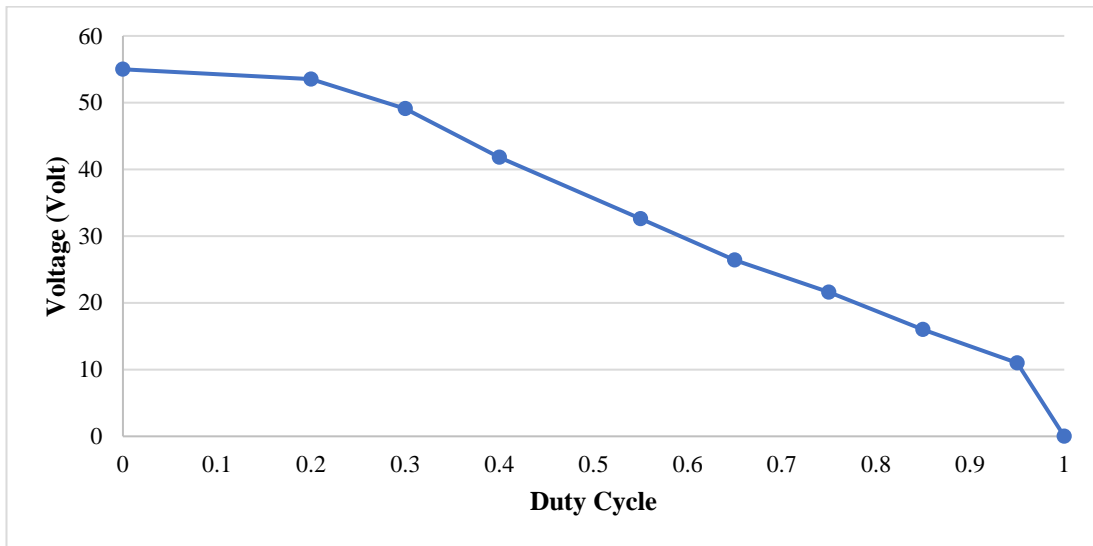


Figure 3.15 Relationship between capacitor voltage and duty cycle with respect to  $S_1$  for Triplen SCC circuit (Theoretical)

### 3.3.5 Capacitor-based switched-capacitor circuit in series-parallel connection

The series-parallel connection is other types of circuit connection used in the switched-capacitor technique. The switched-capacitor (S-C) circuit cells can be configured in series-parallel connection so that they (S-C cells) can perform energy transfer from one to another to obtain voltage multiplication. These cells can be expanded to multi-stages to generate higher voltage level/gain. The basic cell is composed of power semiconductor switches, diodes and capacitors as shown in Figure 3.16. This circuit configuration can be considered as a capacitor-based switched-

capacitor circuit (Luo and Ye, 2013). This has been used in DC/DC converter to accomplish energy transfer and voltage conversion.

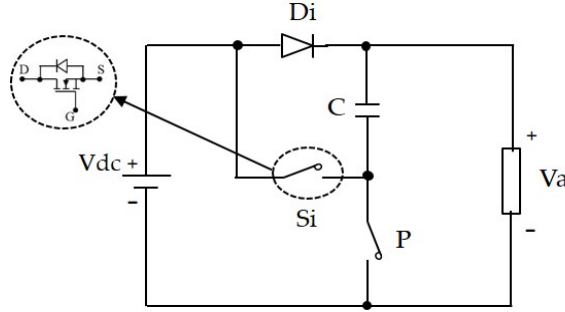


Figure 3.16 Basic unit of S-C cell

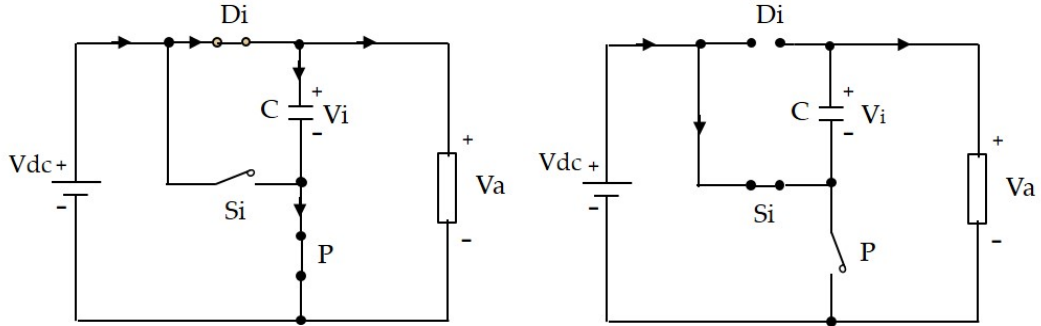


Figure 3.17 SC cell operation: (a) Capacitor Charging and (b) Capacitor discharging

Figure 3.16 shows a basic unit of switched-capacitor circuit cell (Luo and Ye, 2013). The switches Si and P connect a capacitor C in series and parallel with DC voltage. The switches Si and P have a complementary operation which means when switch Si is switched on, switch P must be switched off and vice versa. Otherwise, short-circuiting occurs across DC voltage. Figures 3.17(a) and (b) shows the operation mode of the basic unit of the switched-capacitor circuit. When switch P is switched on during the first half of the switching cycle, the capacitor C is charged to DC voltage i.e.  $V_a = V_i = V_{dc}$  via conducting diode, Di. During the second half of the switching cycle, Switch Si is switched on and capacitor start to discharge. The diode Di becomes reverse-biased to prevent back discharging to DC voltage source. The DC voltage source is connected in series with the charged capacitor C, and therefore these voltages

can be added i.e.  $V_a = V_{dc} + V_i$  while the capacitor C current flows to the load. To achieve a higher number of voltage levels (multi-level voltage), multiple stages of S-C circuit must be connected in cascaded. Series-parallel S-C circuit topologies are popular owing to their structure modularity and capability for bulk integration. Small capacitor size can be used with high switching frequency operations. They utilise capacitors efficiently without having a magnetic element. Hence, no issues related to magnetic, such as electromagnetic interference (EMI), are problems.

However, this type of S-C has high transient current (also known as spike current) which can degrade power density and efficiency. For high power levels (high power applications), spike current waveform is exhibited among capacitors. In addition, multiple stages of S-C circuit are required to achieve high-voltage gain. This demands a large number of power switches, diodes, and capacitors. In synthesising the output voltage, unbalance capacitor voltage problem can occur when more than one capacitor is connected in series. High switching frequency operation can diminish this problem. Yet, this can lower the converter efficiency due to increased switching losses across power switches. The large numbers of power switches used also adds to the power losses.

### **3.4 Other Voltage Boosting Techniques**

The other types of voltage boosting techniques are also briefly discussed. These techniques include magnetic coupling and multi-stage booster. The presentation of these techniques aims to justify the selection of the circuit topology/technique to be adopted for the new proposed inverter system.

#### **3.4.1 Magnetic Coupling**

Magnetic coupling is one of well-known voltage boost method which is used in isolated and non-isolated DC/DC converters. Transformer-based boost (Forouzesh et al. 2017) is popular among the voltage boosting techniques due to flexibility in boost voltage ability. It has been used in DC/DC converters for long to accomplish voltage boosting by turns ratio or/and to provide isolation protection between low-level voltage side and high-level voltage side. This transformer can be added at the DC or AC side of the power electronics converters. In high-power ( $>10$  kW) wind energy system application, traditional full-bridge buck inverters (Xue et al. 2004) are used with line frequency transformers as shown in Figure 3.18. These line frequency transformers are used to step-up voltage and provide galvanic isolation. However, they are bulky in size, heavy in weight, and costly due to the heavy magnetic core (the bulkiest component in transformer) to sustain high power.

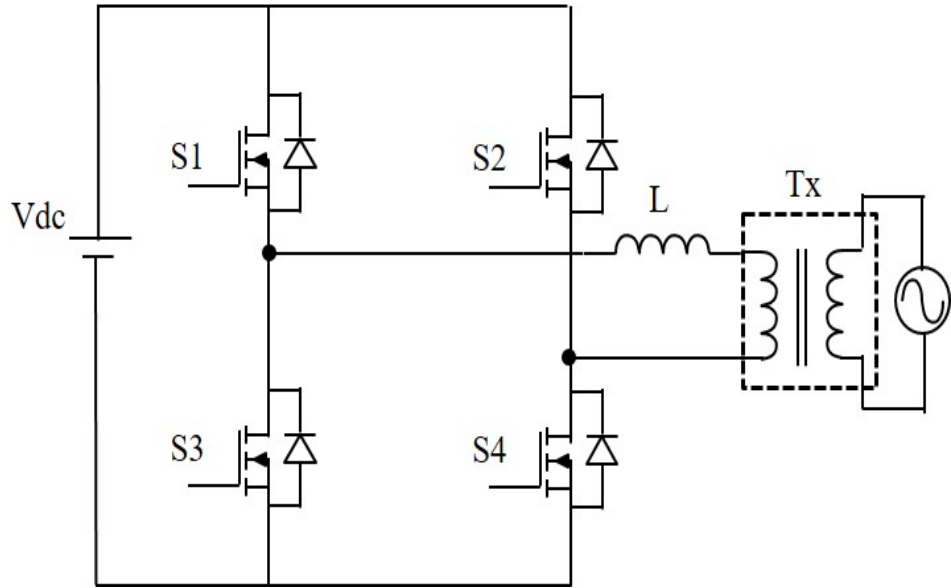


Figure 3.18 Buck Inverter with bulky line-frequency transformer

### 3.4.2 Multi-Stage Booster

Multi-stage booster, also known as multi-level, technique is gaining attention to achieve higher output voltage using multiple stage cells. The cells contain capacitors and diodes (as blocking voltage) in conjunction with power switches (as blocking voltage) which are configured in modular stack structures. This technique has been implemented in DC/DC Multi-Level Boost converters for high power DC supply (Rosas-Caro et al. 2010) as shown in Figure 3.19. In renewable energy system applications, multiple DC sources are obtained from distributed energy sources (batteries, photovoltaics, and fuel cells). These sources are fed into numbers of H-bridge cells in cascaded (modular) multi-level DC/AC topology order to synthesise higher number of AC output voltage levels. The modular structure can ease maintenance and save time such in replacement/swap of the faulty module.

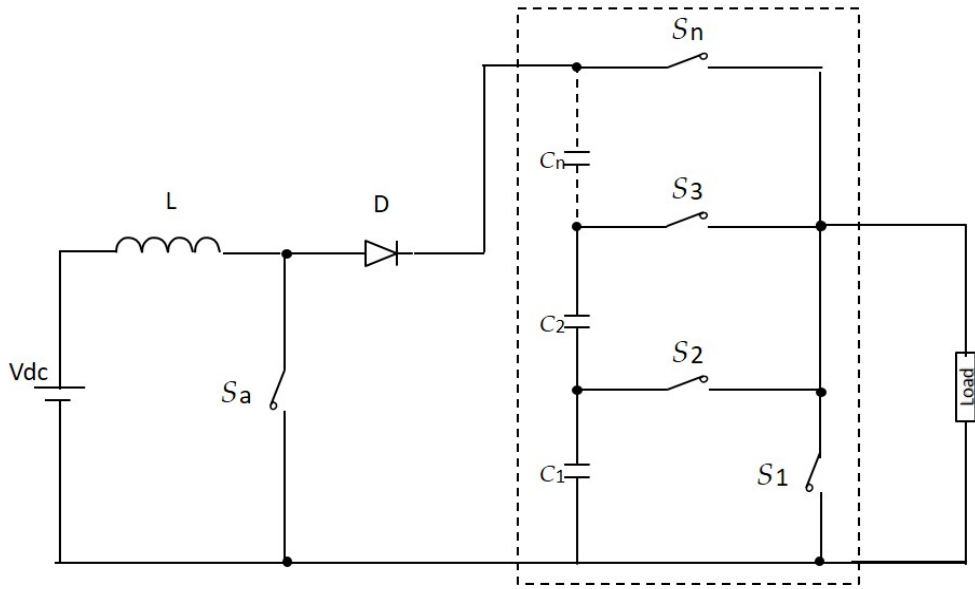


Figure 3.19 DC/DC Multi-Level Boost Converter

High-power density can be achieved by simply adding more cells. High output voltage can be obtained efficiently without transformer at output. However, this requires a large number of components (power switches, diodes, and capacitors) which increases the system size (as it is bulky) and cost.

The following section presents a comparative study of different voltage boosting techniques, as well as different SCC topologies/techniques covered in this thesis. This leads to the selection of an optimum topology/technique to be applied in the proposed inverter system

### 3.5 General Comparison of Voltage Boosting Techniques

It is apparent from the preceding review of voltage boosting techniques (switched capacitor, magnetic coupling, and multi-stage booster) that high-voltage gain and/or varying voltage can be achieved by using the step-up converter circuits.

The step-up converter (switched capacitor, transformer-based, and multi-level) circuits are used to implement these techniques in many DC/DC converters. Each of these circuits has their own advantages and disadvantages. Table 3.2 shows a general comparison of the discussed voltage boosting techniques, showing the advantages and disadvantages according to the type of circuit topology/configuration and connection. The selection of the boosting technique to be applied for the proposed inverter depends on factors such voltage boost/gain and varying voltage ability, low component use (power switches, diodes, and capacitors), switching frequency, and capability for integration. The literature review and the general comparison of the boosting techniques show that the switched-capacitor circuit (SCC) technique has a specific advantage over the others. This is due to the fact that it has a cell-based structure which is easy to integrate into various circuit structure and high-voltage gain/step up ability. Therefore, the SCC technique is given special attention in this chapter.

### **3.6 Selection of the SCC for the Proposed Inverter**

It is apparent from the preceding comparison that the switched-Capacitor Circuit (SCC) technique is superior to the others. This SCC is classified according to the type of circuit topologies/configurations and connections. Two major SCC topologies/techniques covered in literature, namely capacitor-based SCC (in series-parallel connection) and resonant-based SCC (in shunt connection) configurations, were reviewed and investigated.

These topology/techniques need to be carefully chosen before they can be integrated into the proposed inverter system leading to the introduction of a new inverter topology. This is to ensure minimum shortcomings in the overall proposed

inverter system performance. The selected SCC topology/technique configuration should satisfy the following criteria:

1. Voltage gain/boost ability and/or varying/regulating voltage technique;
2. Low component count (power switches, diodes, and capacitors);
3. Ability to operate at high switching frequency; and
4. Capability of integration (circuit cell easy to be integrated into various circuits).

The aim of the multiple-stage inverters system is to have boost voltage/varying voltage and/or isolation carried out in the first circuit stage and inversion in the second stage (Xue et al. 2004). However, this system is bulky due to many voltage multiplier cells and/or transformers.

The selected SCC topologies/techniques of the new proposed optimum inverter topology should provide voltage boost and/or varying/regulating voltage technique ability in order to step up the low-voltage at the input. This can diminish the requirement of huge multiple stages of cells for voltage multiplication or bulky and heavy transformers for a step-up voltage. The voltage boost and/or varying voltage ability technique is required to step up the low input voltage and/or to produce different magnitude voltage levels (multi-level).

The selected technique should have low component count (power switches, capacitors, and diodes). This is to reduce the overall system structure and control complexity. The reduction of the number of power switches can lead to reducing the switching losses which helps to reduce overall power losses in the proposed inverter system.

Table 3.2 General comparison among voltage boosting techniques

Voltage Boosting Techniques	Type of circuit topology/configuration and connection	Advantages	Disadvantages
Switched-Capacitor Circuit (SCC)	Capacitor-based SCC in series-parallel connection	<ul style="list-style-type: none"> <li>- high-voltage gain</li> <li>- can operate without inductors (capacitor-based)</li> <li>- can be integrated to other structure</li> </ul>	<ul style="list-style-type: none"> <li>- high spike current at initial start-up can increase switching losses and decrease system efficiency</li> <li>- high components (power switches, diodes and capacitors) due to huge multiple stages of cells</li> </ul>
	Resonant-based SCC (with inductor) in shunt connection	<ul style="list-style-type: none"> <li>- low or medium-voltage gain.</li> <li>- Low component use</li> <li>- can limit the spike current</li> <li>- can be integrated to other structure</li> </ul>	<ul style="list-style-type: none"> <li>- need more passive components (capacitors and inductors)</li> <li>- sensitive to internal resistance of the inductor</li> </ul>
Magnetic Coupling	Transformer-based	<ul style="list-style-type: none"> <li>- the high-voltage boost</li> </ul>	<ul style="list-style-type: none"> <li>- effect of leakage inductance such as a large voltage spike</li> </ul>

		<ul style="list-style-type: none"> <li>- flexible in boost ability due to changeable turn ratio</li> </ul>	<ul style="list-style-type: none"> <li>- bulky and costly due to the heavy magnetic core to sustain high power</li> </ul>
Multi-stage Booster	Multi-level	<ul style="list-style-type: none"> <li>- high power density</li> <li>- modular structure</li> <li>- can be integrated to other structures</li> </ul>	<ul style="list-style-type: none"> <li>- large number of components</li> <li>- heavy bulky and costly</li> </ul>

Also, the selected technique should be able to operate at high switching frequency PWM operation to smooth the voltage waveform (which is high enough i.e. <50 kHz to limit the switching losses across power switches), and a small size capacitor and inductor can be used. This high switching frequency PWM can cause the PWM control pulse to narrow so that to smooth (narrow ripple) the voltage waveform. In the frequency spectrum of the voltage, the lower order harmonics content (located in the lower frequency side band) can be suppressed to a higher frequency side band. This higher order harmonics content could be easily filtered by small output filter size at the proposed inverter output.

Finally, the selected SCC topologies/technique should have a structure that can be easily integrated into various circuit structures. The trade-off is between harmonics in voltage and switching losses, and switching losses which must be compromised. These sets of criteria are important for the author in deciding the adopted optimum switched-capacitor circuit.

Table 3.3 illustrates a comparison between SCC topologies/techniques in terms of the performance criteria and fair comment set. This was a guideline for the author to decide an optimum SCC topology/technique to be integrated into the proposed inverter circuit. The attractive SCC topologies/techniques configurations are found to be; capacitor-based (series-parallel connection) circuits, resonant-based DSSC, and resonant-based triplen switch circuits. These configurations are capable of producing varying voltage with switch duty cycle controlled and/or multi-level voltage. Capacitor-based can achieve high-voltage gain by employing multiple stages of S-C cells. It can be operated without an inductor (as inductors are large and heavy compared with other components in the circuit).

However, it has the drawback of high transient current (or spike current) which can lead to high losses across power switches and degrade the system efficiency. Meanwhile, resonant-based SCC (with inductor) in shunt connection topology has the advantage of limiting this spike current by the internal resistance of the inductor. This can decrease the switching losses across semiconductor switches as well as provide high surge current protection for switches in this topology.

Both capacitor-based and resonant-based triplen switch configurations contain more components which can increase switching losses. Despite many components and complex control, the triplen switch configuration can avoid the short-circuiting problem by the third auxiliary branch (a resistor in series with a power switch). However, high power dissipation in the auxiliary resistor. Meanwhile, resonant-based DSSC configuration with varying switch duty cycle control can perform varying/regulating voltage ability. This new technique evolved after conducting the investigation above. An investigation has been conducted through mathematical transient analysis. This can be considered as a new technique of varying voltage using switched capacitor technique. This circuit configuration has a low power switch count. The power losses could be less. The associated high switching frequency operation allows using small passive component sizes.

Therefore, this comparative study directed the author to select resonant-based SCC DSSC as the optimum technique. This technique aimed to produce rectified sine (staircase/multi-level) voltage waveform in the first stage of the proposed inverter design. The proposed inverter will be applied in low power applications (i.e. aircraft and marine applications). The formation of this waveform is explained in detail in Chapter 4.

Table 3.3 Comparison between SCC topologies/techniques for the performance selection criteria

Topology	Circuit configuration/connection	Criteria	Comment
Capacitor-based switched-capacitor circuit	Series-parallel connection	<ul style="list-style-type: none"> <li>- high-voltage gain / voltage multiplication ability</li> <li>- can operate without inductors (as inductors are bulky and heavy compared with other components in the circuit)</li> <li>- modular structure which can be integrated into various structure</li> </ul>	<ul style="list-style-type: none"> <li>- Suitable to generate high multi-level voltage for high power application by adding stage of S-C cells, but this needs large number of components and huge circuit layout</li> <li>- high power loss (switching losses) due to a large number of power switches which are required</li> <li>- high transient current (spike current) in the capacitor can degrade system efficiency</li> </ul>
Resonant-based switched-	Double Switch Double Capacitor (DSSC)	<ul style="list-style-type: none"> <li>- varying/regulating voltage technique (showing ability to vary voltage with a varying duty cycle controlled)</li> <li>- need to be operated at high switching frequency (<math>F_s &gt; 5 \text{ kHz}</math>)</li> <li>- needs five components</li> </ul>	<ul style="list-style-type: none"> <li>- spike current is limited</li> <li>- suitable for varying voltage</li> <li>- high switching losses</li> <li>- medium component count</li> </ul>

capacitor circuit		<ul style="list-style-type: none"> <li>- can be integrated into various structures</li> </ul>	
	Double Switch Double Capacitor (DSDC)	<ul style="list-style-type: none"> <li>- needs six components</li> <li>- can be integrated into various structures</li> </ul>	<ul style="list-style-type: none"> <li>- spike current is limited</li> <li>- not showing varying/regulating voltage</li> <li>- high switching losses</li> <li>- medium component count</li> </ul>
	Single Switch Single Capacitor (SSSC)	<ul style="list-style-type: none"> <li>- not showing varying/regulating voltage</li> <li>- needs four components</li> <li>- can be integrated into various structures</li> </ul>	<ul style="list-style-type: none"> <li>- spike current is limited</li> <li>- not suitable for varying voltage due to short-circuited problem</li> <li>- low switching losses</li> <li>- low component count</li> </ul>
	Triplen Switch Circuit	<ul style="list-style-type: none"> <li>- able to vary voltage with a duty cycle controlled</li> <li>- needs to be operated at high switching frequency (<math>F_s &gt; 5 \text{ kHz}</math>)</li> <li>- needs seven or eight components</li> <li>- can be integrated into various structures</li> </ul>	<ul style="list-style-type: none"> <li>- spike current is limited</li> <li>- suitable for varying voltage</li> <li>- high power dissipation and switching losses</li> <li>- high component count</li> <li>- complex control</li> </ul>

The following section presents critical reviews some of the recent switched-capacitor multi-level inverter topologies as reported in literature survey. A brief discussion is presented on the advantages and disadvantages of each circuit topology. It also highlights the gaps and the challenges required in this field.

### **3.7 Switched-Capacitor Multi-Level DC/AC Inverter Topologies**

Producing an acceptable sinusoidal output voltage waveform and boosting the output voltage are two challenges (Rahim et al. 2011) in DC/AC inverters. The transformer can be used to accomplish voltage step-up and/or provide isolation. However, this increases the size and cost of the inverter. The efficiency of the inverter system can decrease due to the bulky magnetic element.

Over, the last few years another family group of multi-level DC/AC inverter topologies/techniques have evolved which are known as switched-capacitor multi-level inverter topologies. These topologies/techniques contain components (capacitors and power semiconductor switches) arranged in a specific configuration. The switching control can be fundamental low-frequency modulation or high-frequency carrier-based pulse-width modulation (PWM). They can generate a high number of AC output voltage levels (high-voltage gain) from single DC input source using less number of power semiconductor switches and isolated DC source usage than the classical multi-level inverter circuits (Gupta et al. 2016). They have simple circuit configuration (due to low power semiconductor switch count), straightforward control operations, and less complex control circuits (Luo and Ye, 2013, Gupta et al. 2016). They have been used in renewable energy sources and industrial applications (Luo and Ye, 2013).

These new evolved multi-level DC/AC inverter topologies accomplish two-stage power conversion. The first stage comprises of Switched-Capacitor Circuit (SCC) which is used to boost DC input voltage to the desired voltage levels (voltage appears across a series of capacitors). The associated power switches are controlled in such a way that rectified sine multi-level/staircase waveform is shaped during the positive cycle of AC output. The second stage is H-bridge circuit which changes the polarity of magnitude output voltage between positive and negative and vice versa. These topologies have a voltage boosting feature; the low input voltage can be step-up to produce higher AC output voltage levels.

There are numerous switched-capacitor multi-level inverter topologies with different SCC configurations that have been proposed in the literature (Luo and Ye, 2013, Gupta et al. 2016). For the purpose of explaining the strengths and weaknesses of each circuit topology, it is essential first to categorise the circuit topology covered. Figure 3.20 shows the categorisation of the switched-capacitor multi-level inverter topologies. These topologies can be classified according to the component/element used as; resonant-based (with inductor) SCC, and capacitor-based (without inductor) SCC surveyed in published literature. For resonant-based SCC, three configuration type are included namely; Cascaded Boost-Switched-Capacitor Multi-Level Inverter (CBSC-MLI), Switched-Capacitor Boost Multi-level Inverter Using Partial Charging (SCM-MLI), and Switched-Inductor Multi-Level Inverter (SI-MLI). For capacitor-based SCC, two configuration types are included namely; Switched-Capacitor inverter using Series/Parallel Conversion (SCI-S/P), and Hybrid Multi-level Inverter using Switched-Capacitor unit (HSC-MLI).

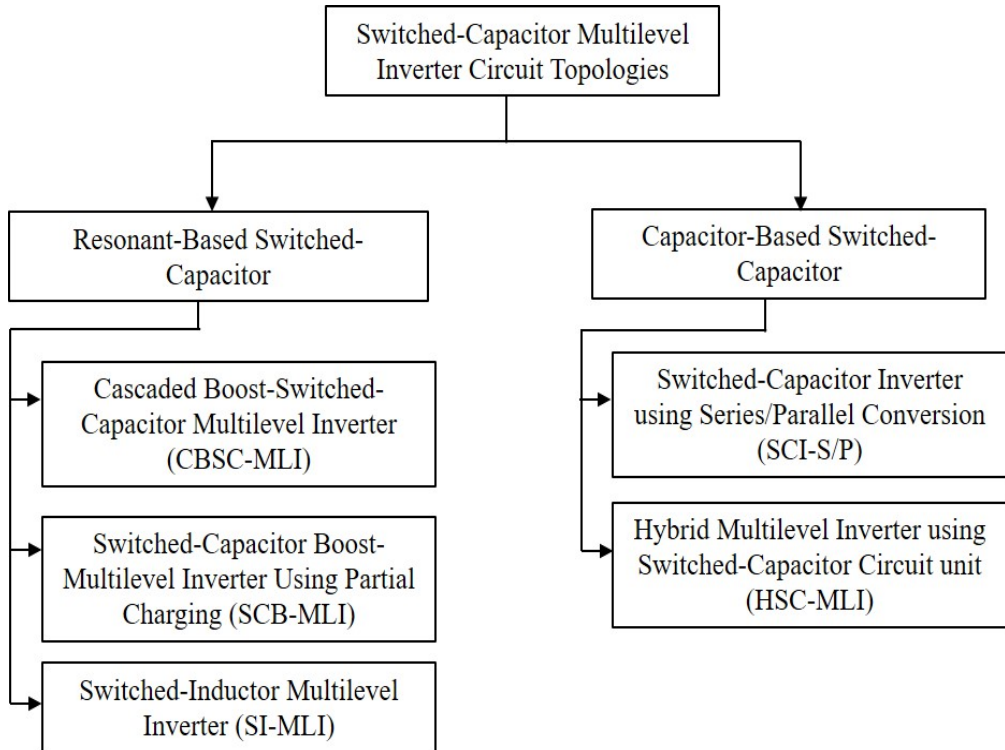


Figure 3.20 Classification of switched-capacitor multi-level inverter topologies

The following sections review different circuit configurations of the switched-capacitor multi-level inverter topologies covered in this chapter. This shows the merits and limitation of each technique.

### 3.7.1 Cascaded-Boost Switched-Capacitor Multi-Level Inverter

Figure 3.21 shows five-levels output voltage of Single-phase Cascaded Boost-Switched-Capacitor Multi-Level Inverter (CBSC-MLI) circuit topology (Axelrod, Berkovich and Ioinovici 2005). It is two-stage inverter which is formed by switched-capacitor boost converter and conventional H-bridge circuit. The switched-capacitor (S-C) boost circuit stage composes of the switched-capacitor unit, diodes, and an inductor element. The DC input voltage can be stepped up to obtain multi-level DC

voltage waveform by adding multiple stages of switched-capacitor (S-C). The control switches are operated at a fundamental low-frequency (fundamental low-frequency modulation method). The multi-level voltage is applied to the input of full H-bridge inverter to generate staircase AC voltage waveform without a transformer at output load. It has the advantage that the input voltage can be stepped up to achieve higher output voltage without demanding multiple separate DC sources at input. This topology inverter suffers from fundamental low-frequency operating of the control switch. Low harmonics can be achieved by increasing number of output voltage levels. This consequently requires a large number of switch and capacitor components that act as voltage gain in this case.

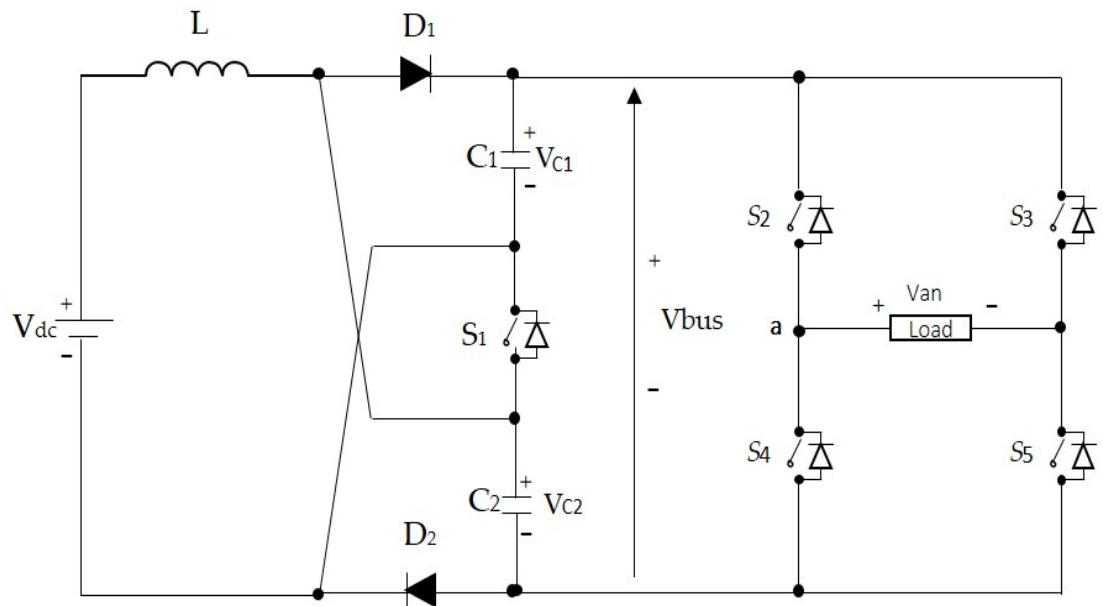


Figure 3.21 Five-level Cascaded Boost-Switched-Capacitor Multi-Level Inverter circuit topology

### 3.7.2 Switched-Capacitor Boost-Multi-Level Inverter Using Partial Charging

Figure 3.22 shows Single-Phase Switched-Capacitor Boost-Multi-level Inverter Using Partial Charging (SCB-MLI) circuit topology that generates 13-levels multi-level output voltage through partial capacitor charging technique (Chan and Chau 2007). It is formed by a two-stage circuit, switched-capacitor (S-C) boost, and full H-bridge.

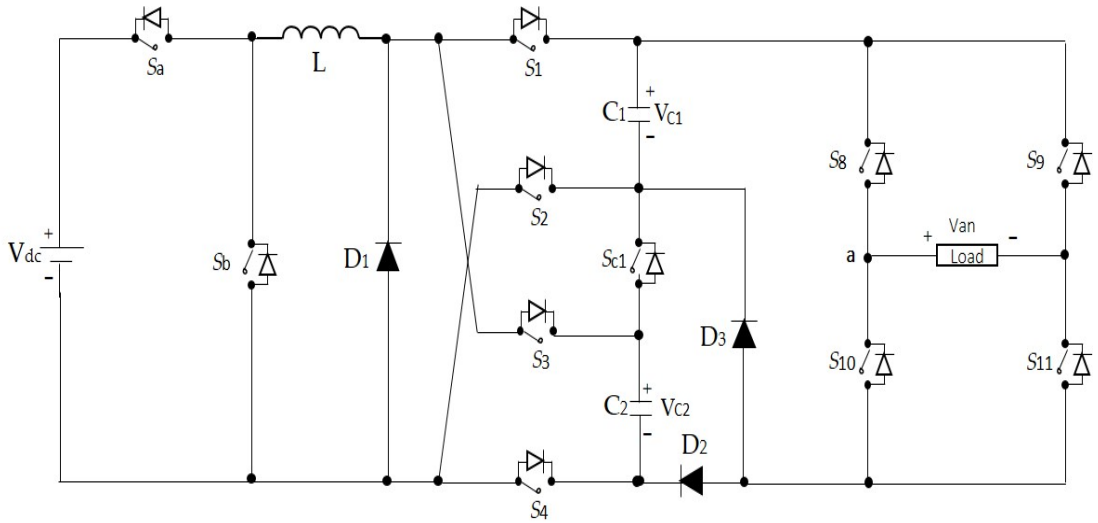


Figure 3.22 Thirteen-levels Switched-Capacitor Boost-Multi-Level inverter circuit topology

This topology has similar features to previous inverter topology which was proposed by Axelrod, Berkovich and Ioinovici (2005) where the low input DC voltage can be stepped up to produce higher staircase AC output voltage without requiring a number of isolated DC sources. The multi-level output voltage and the frequency spectrum of output voltage; five, seven and thirteen-levels, as shown in Figure 2.23 to 2.27 can be obtained by using switched-capacitor (S-C) boost circuit operating in partial charging technique. The switched-capacitor (S-C) boost circuit is controlled by applying specific switching pulse pattern to switches controlling capacitors. The

partial charging works in such a way that each capacitor is step-by-step charged to three different voltage levels. The voltage levels can have an equal step ( $V_{c1} = V_{c2} = V_{c3}$ ) or unequal step ( $V_{c1} \neq V_{c2} \neq V_{c3}$ ). A higher number of voltage levels can be achieved by adding a number of capacitors with its associated control switches. The capacitor may act as voltage gain. The partial charging technique may realise multi-level voltage step per capacitor. This may in turn reduce the number of switches and component count usage. However, to obtain low harmonics in output voltage, the number of voltage levels need to be increased, which demands a large number of capacitors and switch components to be used. This may cause the overall system to be highly expensive, bulky, complex controlled, and less reliable due to many switch and capacitor usages.

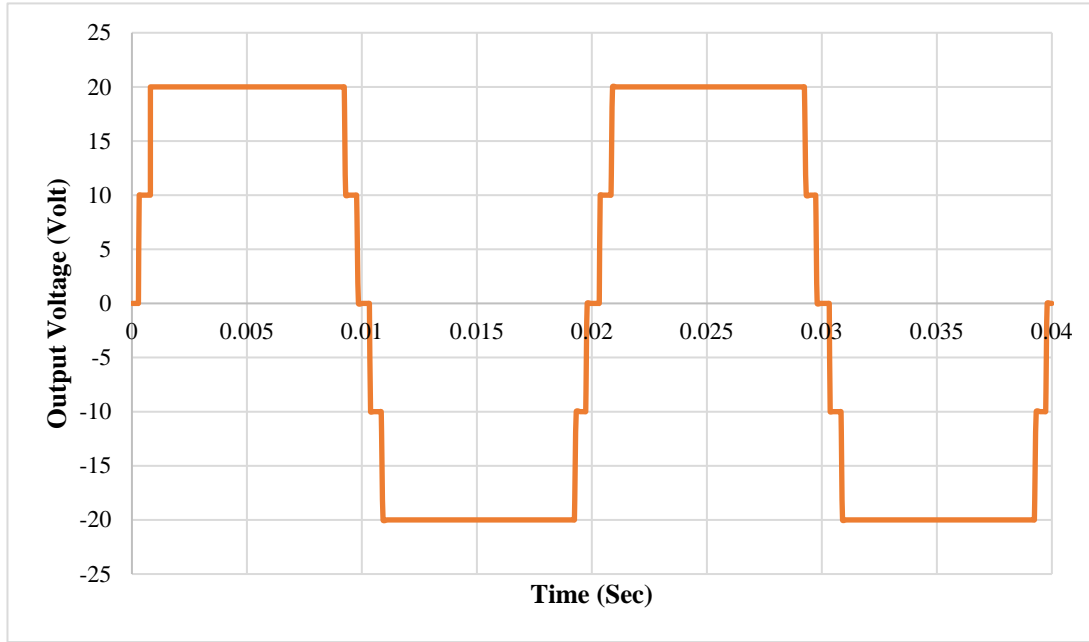


Figure 23 Five-levels output voltage of the SCB-MLI circuit

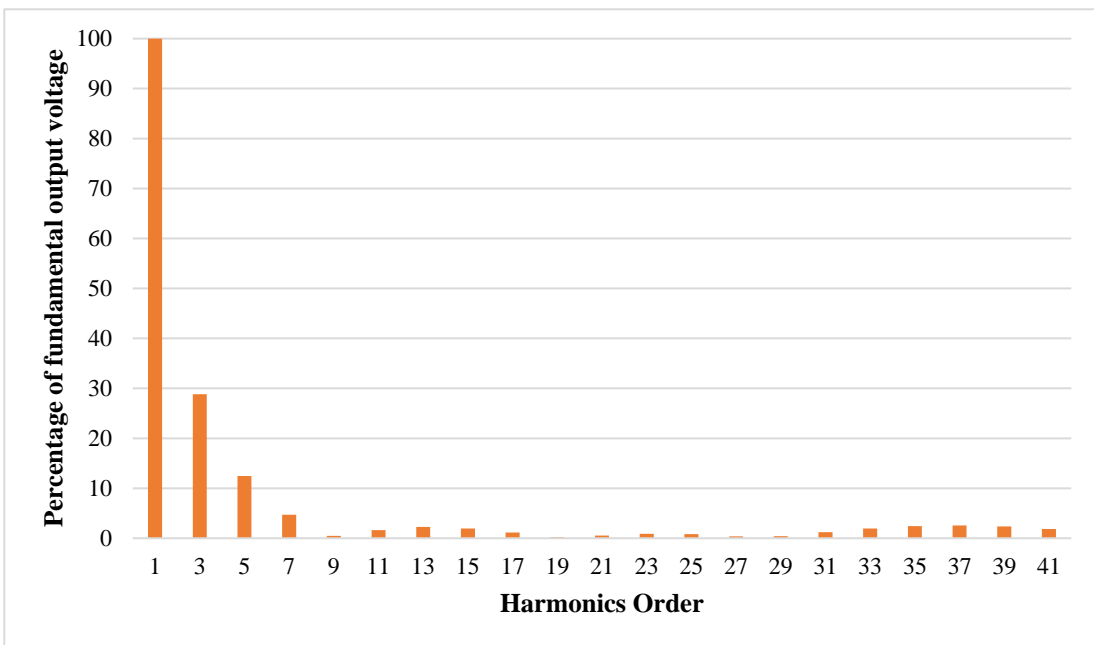


Figure 3.24 Harmonics spectrum of five-levels SCB-MLI output voltage

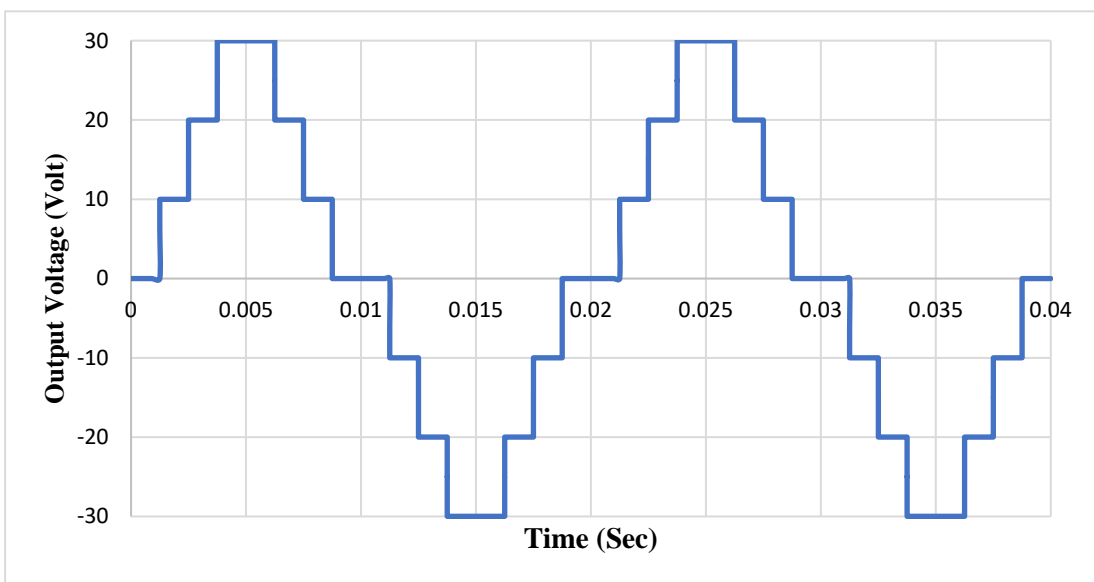


Figure 3.25 Seven-levels output voltage of the SCB-MLI circuit

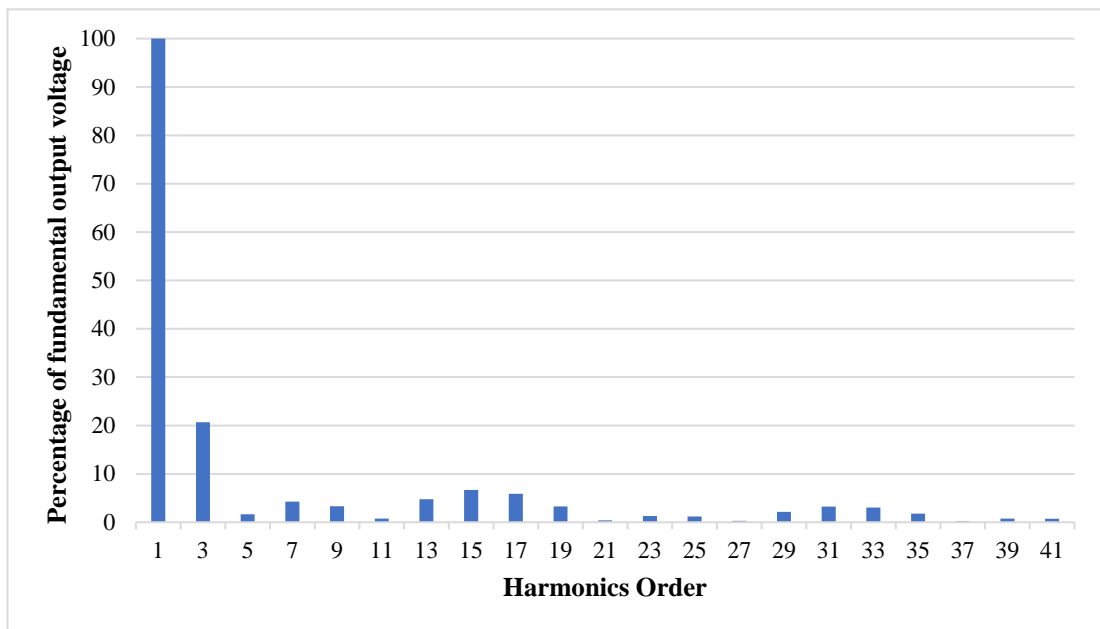


Figure 3.26 Harmonics spectrum of seven-levels SCB-MLI output voltage

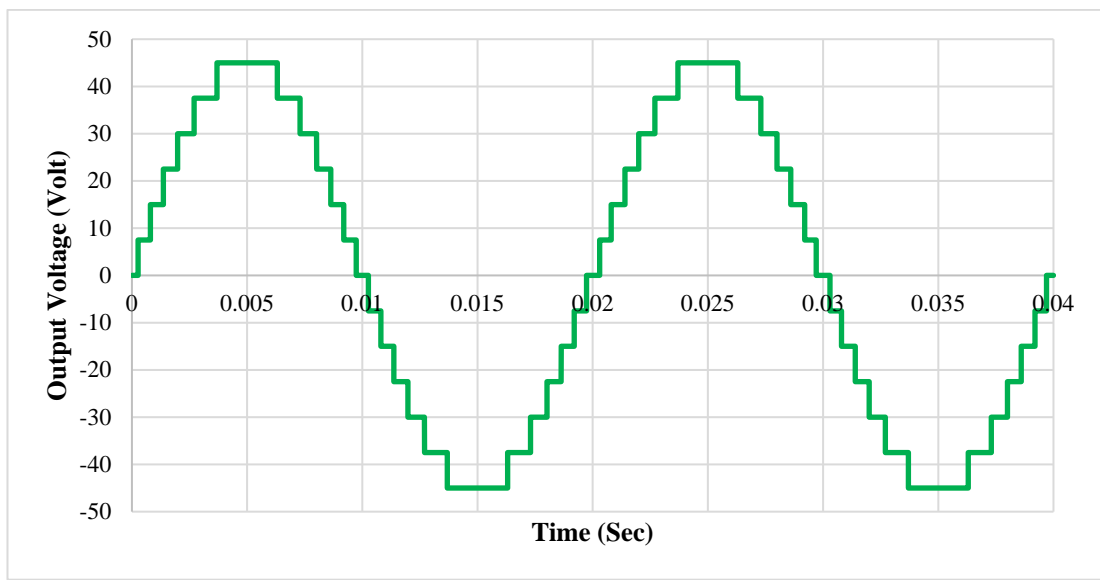


Figure 3.27 Thirteen-levels output voltage of the SCB-MLI circuit

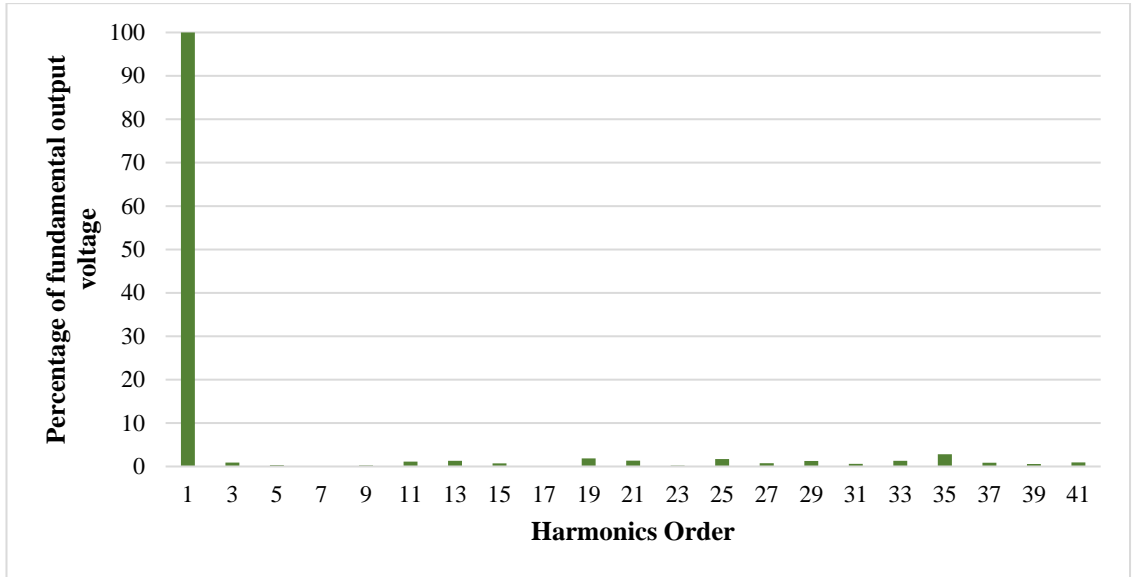


Figure 3.28 Harmonics spectrum of thirteen-levels SCB-MLI output voltage

### 3.7.3 Switched-Inductor Multi-Level Inverter

Switched-Inductor Multi-Level Inverter (SI-MLI) topology has been proposed by Luo and Ye (2013). Figure 3.29 shows the single-phase seven-levels SI-MLI circuit and Figure 3.30 and 3.31 shows staircase output voltage waveform and the frequency spectrum of output voltage respectively. It consists of two-stage circuits which are connected in cascade. The first stage is a combined conventional boost DC/DC converter and switched-capacitor (S-C) circuit and the second stage is an H-bridge circuit. The conventional boost DC/DC is used to boost the low input voltage and then charge the DC link capacitors of the switched-capacitor (S-C) circuit to certain DC bus voltage level. The switched-capacitor (S-C) circuit is controlled in such a way that DC bus voltage is divided by each voltage level per capacitor. For seven output voltage levels (multi-level), three voltage steps can be obtained across three series-connected capacitors during positive half cycle of the fundamental period. This multi-level voltage waveform is transformed into staircase/multi-level AC waveform  $V_o$  by H-

bridge circuit. The peak output voltage  $V_o$  (peak) depends on the duty cycle of the main switch ( $S_1$ ). SI-MLI topology is controlled by using hybrid modulation control operation where only power switch ( $S_1$ ) operates at high switching frequency while other power switches operate at fundamental or low switching frequency. This topology has the unique function of boosting up the input voltage to produce higher AC output voltage without requiring multiple several isolated DC sources (only single DC source at input) and transformers. This inverter circuit is ideal for use in renewable energy systems with low input resource and high power industrial applications.

However, to achieve low THD, the number of output voltage levels should be increased, thus demanding a large number of capacitors and power switches. These power switches are associated with complicated control operations and complex control gate circuits. The S-C circuit of m-level Switched-inductor multi-level inverter (SI-MLI) require  $n$  capacitors ( $n = (m-1)/2$ ) and  $S$  switches ( $S = (m-1)/2 + 2$ ). The output voltage level,  $m$  can be obtained by  $2n+1$ , where  $n$  is number of capacitor and  $S$  is number of power switches.

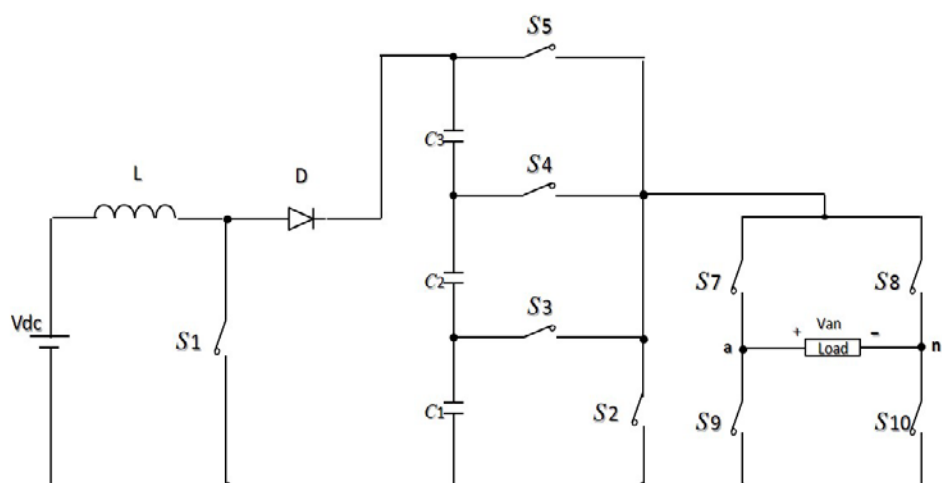


Figure 3.29 Seven-levels Switched-Inductor Multi-Level Inverter circuit topology

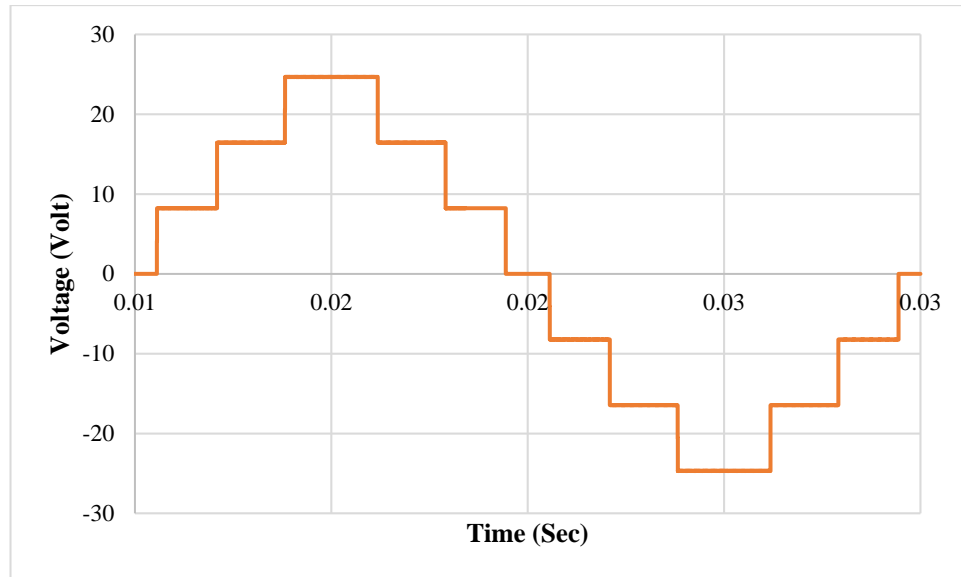


Figure 3.30 Seven-levels output voltage waveform of SI-MLI circuit

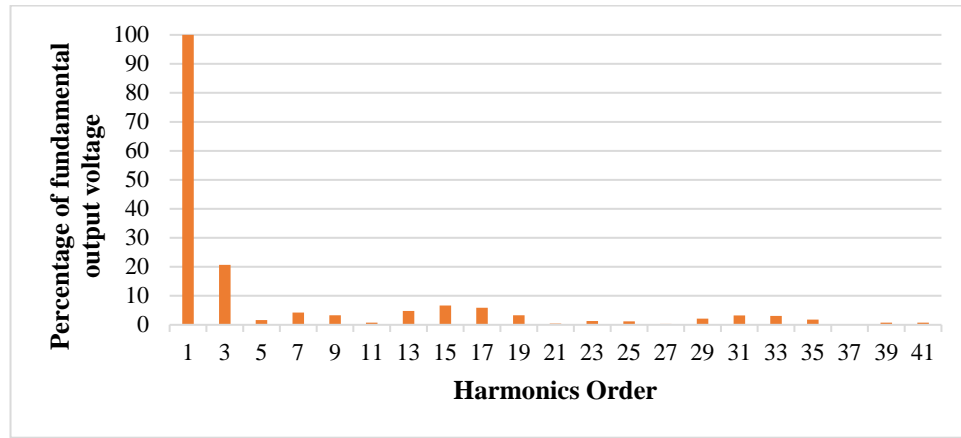


Figure 3.31 Frequency spectrum of output voltage of SI-MLI circuit

### 3.7.4 Switched-Capacitor Inverter using Series/Parallel Conversion

Figure 3.32 shows a single-phase switched-capacitor inverter using series/parallel conversion (SCI-S/P) (Hinago, Koizumi 2012). A capacitor-based SCC stage is used to generate three different voltage levels ( $V_{c1}$ ,  $V_{c2}$  and  $V_{c3}$ ) using series or parallel conversion of switches and capacitor connection. Seven-levels multi-level or staircase AC output voltage waveform can be generated if this SCC stage is

connected to the H-bridge circuit. By applying appropriate switching control, three different voltage levels can be obtained on DC bus voltage, Vbus during positive cycle of fundamental period of output voltage. Each voltage level could have equal step ( $V_{c1} = V_{c2} = V_{c3}$ ) or unequal step( $V_{c1} \neq V_{c2} \neq V_{c3}$ ). Multi-level voltage waveform during the positive cycle of the fundamental output voltage is achieved by controlling the DC voltage source and capacitor which are alternately connected in series-parallel connection through controlling power switches (Hinago,Koizumi 2012, Ye et al. 2014, Barzegarkhoo et al. 2016). Capacitors are charged when they are connected in parallel with a DC input voltage source through controlled power switches and discharged on load through power switches when capacitors are connected in series. The type of modulation is used to achieve staircase AC output voltage and is a high-frequency multicarrier PWM control method (Ye et al. 2014). The DC link capacitor voltage, also known as DC bus voltage, is added when all capacitors are connected in series. Multi-level bus voltage levels can be extended to higher levels by adding multiple stages of the power switch and capacitor components. H-bridge circuit transforms the waveform into staircase AC output voltage without a bulky transformer at the output. This topology does not have any bulky inductors which could make systems small. Output voltage can be larger than input voltage where the maximum output voltage is determined by the number of capacitors with its associated switches control. The harmonics content in output voltage can be reduced by increasing the number of output voltage levels (i.e. multi-level output voltage) (Ye et al. 2014).

However, large numbers of power switches and capacitor components are required, which causes the overall system to become more complicated. Small size low pass filter circuits, composed of an inductor (L) and capacitor (C), can be used to

achieve minimum harmonics of inverter output voltage. This inverter topology also could have capacitor voltage unbalancing problem (Barzegarkhoo et al. 2016).

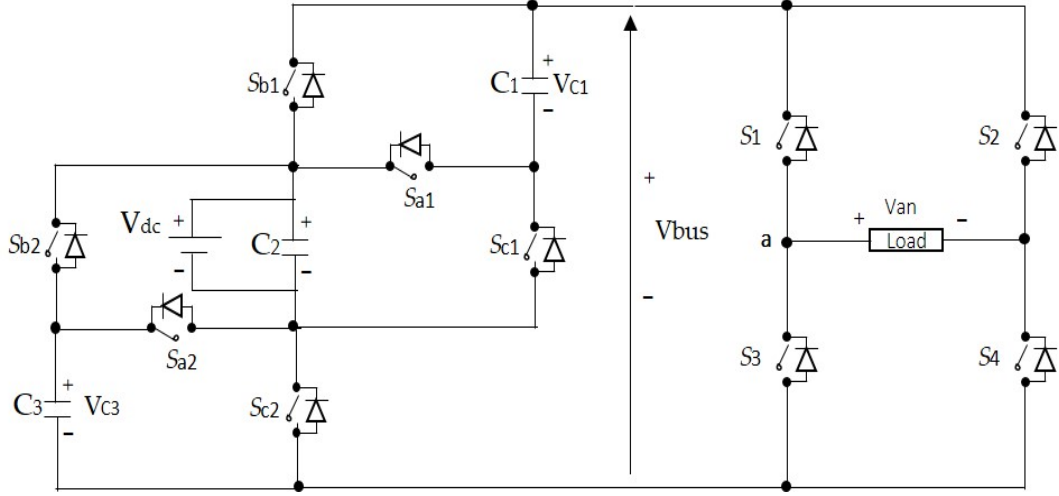


Figure 3.32 Seven-level switched-capacitor inverter using series/parallel conversion

### 3.7.5 Hybrid Multi-Level Inverter using Switched-Capacitor unit

Figure 3.33 shows the multi-level inverter circuit topology using switched-capacitor (S-C) circuit unit proposed for high power applications (Luo and Ye, 2013, Babaei, Gowgani 2014). This circuit topology is composed of multi-stage of switched-capacitor units and a conventional cascaded H-bridge inverter. Hybrid modulation control is used where the power switches in SCC unit are switched at high switching frequency while the power switches in H-bridge inverter are switched at low fundamental switching frequency. Each SCC unit is controlled in such a way all capacitors are charged in parallel with a DC input voltage source and discharged on load through power switches in series connection. The number of voltage levels of the multi-level waveform is determined by the number of switched-capacitor units is a cascade. Rectified multi-level voltage waveform can be shaped by applying appropriate switching pattern to the associated control switches. H-bridge inverter

circuit transformed the waveform into line frequency AC output voltage. The AC output voltage may be higher than input dc voltage source without using line frequency transformer at the output. The capacitor voltage is balanced by fundamental frequency switching without needing complicated switching pattern. Seventeen-levels of staircase sinusoidal voltage waveform at fundamental output frequency can be achieved in Luo and Ye, 2013, Babaei, Gowgani 2014 with Low THD (< 5%) and R-L output load. Due to low pass filter characteristic of the R-L load, the load current waveform is exhibited almost sinusoidal.

However, this technique requires multiple stages of switched-capacitor units to achieve a higher number of output voltage levels to obtain minimum output distortion.

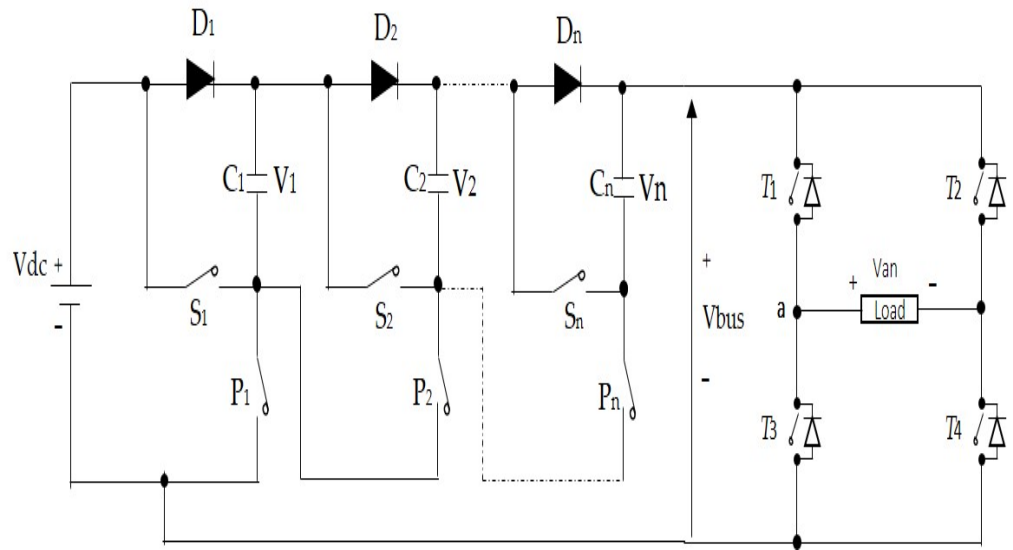


Figure 3.33 Hybrid Multi-Level Inverter using Switched-Capacitor Circuit unit

The following section summarize and compare each type of DC/AC inverter topologies surveyed in the literature. The advantages and disadvantages each of topologies were briefly discussed.

### 3.8 Comparison of Different DC/AC Inverter Topologies

The implementation of DC/AC inverter is highly dependent on the application for which it needs to be employed. The general selection requirement of DC/AC inverter is often based on an assessment of the merits.

1. Total harmonic distortion (THD);
2. Power losses;
3. Power semiconductor switch and other components (inductors, diodes and capacitors) count
4. Small component size.

Table 3.4 shows a general performance comparison of different multi-level DC/AC inverter topologies reviewed in the published literature survey. Meanwhile, Table 3.5 shows a comparison of different multi-level DC/AC inverter topologies reviewed in the literature survey in terms of the number of power switches, diodes, and capacitors used for generating thirteen-levels AC output voltage.

Different DC/AC inverter topologies which have been surveyed in literature are:

- Voltage Source Inverter Sinusoidal Pulse Width Modulation (VSI-SPWM)  
(Bai, Zhang & Zhang 2007)
- Current Source Inverter Sinusoidal Pulse Width Modulation (CSI-SPWM)  
(Takatsuka, Yamanaka & Hara 2013, Bai, Zhang & Zhang 2007)
- Impedance Source Inverter Sinusoidal Pulse Width Modulation (ISI-SPWM)  
(Anderson, Peng 2008)
- Diode-Clamped Multi-Level Inverter (DC-MLI) (De et al. 2011, Mecke 2011)

- Flying-Capacitor Multi-Level Inverter (FC-MLI) (Jing Huang, Corzine 2004, He, Cheng 2016)
- Cascaded H-Bridge Multi-Level Inverter (CHB-MLI) (Alamri, Darwish 2015, Beig, Dekka 2012)
- Cascaded Boost-Switched-Capacitor Multi-Level Inverter (CBSC – MLI) (Axelrod, Berkovich and Ioinovici 2005)
- Switched-Capacitor Boost Multi-level Inverter Using Partial Charging (SCM-MLI) (Chan and Chau 2007)
- Switched-Inductor Multi-level Inverter (SI-MLI) (Luo and Ye, 2013, Ye et al. 2014, S Salehahari, E Babaei 2016)
- Switched-capacitor inverter using series/parallel conversion (SCI-S/P) (Hinago,Koizumi 2012, Luo and Ye, 2013, Ye et al. 2014, (Barzegarkhoo et al. 2016)
- Hybrid Multi-Level Inverter using Switched-Capacitor unit (HMI-SC) (Babaei, Gowgani 2014).

The three-levels PWM inverters (VSI, CSI and ISI) and the classical multi-level DC/AC inverter topologies (DC-MLI, FC-MLI and CHB-MLI) were discussed and summarized in Chapter 2 under Section 2.3. Although classical multi-level DC/AC inverters are effective, however they suffer from the increasing number of components (power switches, diodes and DC link capacitors) and also isolated DC sources when to generate higher number of output voltage levels. This increases the overall inverter cost, volume, and control complexity. Another family of multi-level DC/AC inverter which is new evolved topology which is called switched-capacitor multi-level inverter

(SC-MLI) or also known as multi-level inverter based switched-capacitor circuit. This also can be represented as DC/AC inverter topology with reduce number of component count (Gupta, Ranjan, Bhatnagar, Sahu, & Jain, 2016).

An important common trend observed for many newer switched-capacitor multi-level inverter topologies in achieving lower output harmonics distortion is that they have been implemented with high switching frequency PWM control operation. In general, both capacitor-based and resonant-based types of the switched-capacitor multi-level inverter topologies have several advantages in common (Taghvaie, Adabi, & Rezanejad, 2016, Zamiri, N Vosoughi, Hosseini, Barzegarkhoo, & Sabahi, 2016, Sun et al., 2016, Barzegarkhoo et al. 2016) such as:

- High output voltage resolution can be achieved without requiring a large number of isolated DC sources at input.
- Effectively increase the number of voltage levels by using multiple stages of switched-capacitor circuit (SCC) unit with appropriate control technique.
- Boosting input voltage feature; the output voltage can be larger than the input voltage.
- Suitable for application where the output voltage needs to be boosted larger than the input voltage without a transformer, limited multiple input DC voltage sources, and constraints on the power semiconductor switches voltage stress.

Capacitor-based type of switched-capacitor multi-level inverter circuit topologies in SCI - S/P (Hinago,Koizumi 2012), SC-MLI (Luo and Ye, 2013), HMI-SC (Babaei, Gowgani 2014) have their advantages which can be summarized as: (Barzegarkhoo et al. 2016, Sun et al. 2016)

- Operate without inductors at input.

- Reduced number of power switches and minimum DC source used in comparison to classical CHB-MLI topology.
- Multiple stages of SCC cells can be operated at high switching frequency. Hence, small size of passive components (i.e. capacitors and inductor) can be used when operating at very high switching frequency.
- High-voltage gain / voltage multiplication ability.
- Suitable to generate high multi-level voltage for high power application by adding stage of SCC cells.
- Modular structure which can be integrated into various structure.

However, these circuit topologies also have their disadvantages which can be summarized as:

- Large number of components and bulky circuit size.
- High power loss (switching losses) due to a large number of power switches which are required.
- High transient current (spike current) in the capacitor can degrade system efficiency.
- Need special method for capacitor voltage regulation such redundant switching state (RSS) method

The advantages of the resonant-based type of switched-capacitor multi-level inverter circuit topologies (SI-MLI (Luo and Ye, 2013), CBSC-MLI (Axelrod, Berkovich and Ioinovici 2005), SCB-MLI (Chan and Chau 2007)) can be summarized as: (Rosas-Caro et al. 2015)

- Reduced number of power switches and capacitors used in comparison to capacitor-based type of switched-capacitor multi-level inverter circuit topologies.
- Can operate with an inductor at input circuit and utilize resonant characteristic for voltage boosting.
- Spike current can be limited by the internal resistance of an inductor.
- Power semiconductor switches in switched-capacitor boost circuit stage (multiple stages of SCC cells) are controlled at high switching frequency PWM operation. This allows smaller component size capacitors and inductors to be used. Also, a narrower pulse width of pulse voltage that is controlled by the power switch can smooth the output voltage. Hence, low THD can be achieved.

However, these circuit topologies also have their limitations such as: (Barzegarkhoo et al. 2016)

- High switching frequency PWM operation however can lead to high power dissipation (power losses) in power semiconductor switches.
- Need more numbers of stage of the switched-capacitor circuit cells to generate higher number of voltage levels so that minimum THD can be achieved.
- Require many clamping diodes used to block voltage.
- Complicated control circuit due to many power switches used to block/control capacitor voltage/ DC link voltage.
- High switches voltage stress due to high dv/dt which can result in high electromagnetic interference (EMI).
- High switching loss due to many power switches used.

Most of switched-capacitor multi-level inverters topologies have common limitations that is associated with (Rozlan, Darwish, Sallama, & Khodapanah, 2015):

- The requirement of multiple stages of switched-capacitor circuit (SCC) units or cells, which demand large numbers of power semiconductor switches and capacitors needed for increased number of output voltage levels in achieving lower harmonics.
- High switching losses in power semiconductor switches due to high switching frequency operation.
- High switch voltage stress due to high  $dv/dt$  which can result in high electromagnetic interference (EMI).

This can lead to increased overall inverter cost, volume or weight, and control complexity of the inverter control circuit. Each power switch (i.e. Power MOSFET gate terminal) requires each control driver unit (i.e. MOSFET driver chip), protection circuit (i.e. opto-isolator) and cooling unit (heat sink) (Gupta et al. 2016).

Table 3.4 General Performance comparison of different multi-level DC/AC inverter topologies

<b>Topologies</b>	<b>THD</b>	<b>Power losses</b>	<b>Efficiency</b>	<b>Total of component count</b>	<b>Single DC source</b>	<b>Cost</b>	<b>EMI</b>
VSI-SPWM	high	high	high	low	yes	Low	High
CSI-SPWM	high	high	less	low	yes	Low	High
ISI-SPWM	high	high	less	low	yes	Low	High
DC - MLI	high	low	high	high	yes	High	Low
FC - MLI	high	low	high	high	yes	High	Low
CHB - MLI	high	low	high	high	no	High	Low
CBSC - MLI	high	low	high	low	yes	Low	High
SCB - MLI	low	high	low	low	yes	Low	High
SCI - S/P	low	high	low	high	yes	High	Low
SI-MLI	low	high	high	high	yes	High	Low
HMI-SC	low	low	high	high	no	High	Low

Therefore, it is important to look for a new DC/AC inverter circuit topology that generates a near AC (multi-level/staircase) output voltage waveform with fewer harmonic without requiring increasing numbers of components (power switch, diodes and DC-link capacitor) and numbers of isolated DC input source. This can lead to have simple control operation and simple control circuit (gate driver units). This new proposed inverter can be used for low power applications, like aerospace, where size and weight are most critical requirements. To achieve low output voltage harmonics

without needing an increasing number of switch and capacitor, a DC/AC inverter topology with reduced component (switches and capacitor count) is introduced in this thesis.

Table 3.5 Comparison of different multi-level DC/AC inverter topologies to produce thirteen-levels output voltage

Topologies	Number of output voltage levels	Number of switches	Number of diodes	Number of inductors	Number of capacitors
VSI-SPWM	3	4	0	0	0
CSI-SPWM	(sine-modulated output waveform)	5	1	1	1
ISI-SPWM	(sine-modulated output waveform)	6	1	2	2
DC - MLI	13	24	132	0	12
FC - MLI	13	24	0	0	66
CHB - MLI	13	224	0	0	6
CBSC - MLI	13	10	12	1	6
SCB - MLI	13	11	3	1	2
SCI - S/P	13	15	15	0	6
SI-MLI	13	9	1	1	4
HMI-SC	25	12	2	0	2

### **3.9 Summary**

This chapter presents a critical review of the switched capacitor technique in addition to other voltage boosting techniques (magnetic coupling and multi-stage booster) surveyed in published literature. It contains the classification of techniques according to their circuit topology/configuration and connection. This chapter is important in identifying the weaknesses and strengths of each of the covered techniques and circuit topologies and/or configuration surveyed. These points are very useful in providing a comparative study of each technique and circuit topology and/or configuration surveyed in published literature. The comparative study shows that switched-capacitor circuit (SCC) technique should be given special attention due to its advantages in comparison with other techniques. Two types of comprehensive mathematical analyses are performed on the resonant-based SCC DSSC configuration with applied varying switch duty cycle control technique, showing its ability to behave like a variable capacitor. This also shows its ability to vary/regulate voltage like a voltage regulator. The relationship between effective capacitance and varying switch duty cycle is presented. In addition, the relationship between varying voltage and varying switch duty cycle is presented for this circuit configuration. Several performance criteria are set by the author as guidelines to decide the optimum SCC topology/technique to be integrated into the proposed inverter circuit. This provides a comparative analysis that shows each technique and circuit topology and/or configuration surveyed capable of satisfying the criteria assessed by the author. The result/outcome showed the resonant-based SCC DSSC configuration has a specific advantage over the others.

This chapter also presents a review of new evolved different DC/AC inverter topologies/techniques over the last few years surveyed in published literature. The weaknesses and strengths of each of the covered DC/AC inverter topologies are identified. These points are very useful in providing a comparative study of each technique and circuit topology and/or configuration surveyed in published literature. The comparative study shows that generating higher voltage levels using multi-level topologies/techniques (classical and new evolved) demands high component (power switches, diodes, and capacitors) usage. Efforts made to reduce the number of components in multi-level inverter topologies based switched-capacitor is given special attention in this thesis. Therefore, a new simple inverter topology capable of generating a high number of levels of near sinusoidal (multi-level/staircase) AC output voltage with reduced component count will be proposed. This new DC/AC inverter topology is introduced and discussed in detail in Chapter 4.

## **Chapter 4 Proposed DC/AC Inverter Circuit Topology and Control Technique**

### **4.1 Introduction**

Many existing multi-level inverters based switched-capacitor circuit (SCC) with H-bridge topologies require large number of power switches and capacitors to construct high numbers of voltage levels (DC multi-level bus voltage) in order to minimise harmonics distortion in AC output voltage (Rozlan, Darwish, Sallama, & Khodapanah, 2015) (Gupta, Ranjan, Bhatnagar, Sahu, & Jain, 2016) (Taghvaie, Adabi, & Rezanejad, 2016) (Barzegarkhoo, Kojabadi, Zamiry, Vosoughi, & Chang, 2016) (Zamiri, N Vosoughi, Hosseini, Barzegarkhoo, & Sabahi, 2016). This can increase the complexity of the control circuit where each power switch is associated with a gate drive unit (opto-isolator), MOSFET drive, and cooling unit (heat-sink). Hence, the overall system is bulky and costly. In this chapter, the proposed inverter circuit with a reduced component (power semiconductor switches, diodes, and capacitors) count is introduced. The principle operation, design and analysis, and control technique of the proposed inverter system are elaborated on in detail. The main idea is to utilise the ability of the resonant-based DSSC SCC circuit that varies the DC input voltage by variable switch duty cycle control technique as investigated in Chapter 3.

## 4.2 Proposed Inverter System

The proposed inverter system comprises a single-phase inverter circuit and an open-loop control circuit. Figure 4.1 shows the block diagram of the proposed inverter system. The proposed inverter circuit evolves from a single-phase current source (CSI) circuit topology. It consists of two stages of power conversion. The resonant-based DSSC SCC is introduced in the first stage. This is controlled in such a way that a rectified sine wave appears across a fixed capacitor ( $C_1$ ) of this circuit. The H-Bridge circuit is connected in the second stage to convert the waveform into a line-frequency AC output. Both stages are connected in cascade.

The decision to accept resonant-based DSSC SCC configuration circuit is based on the relationship between effective capacitance and variable switch duty cycle control, as well as the relationship between voltage and duty cycle results obtained in Chapter 3. This is illustrated in Figure 3.6 and 3.10 (in Chapter 3). The results show that this circuit may exhibit voltage varying voltage behaviour by applying variable switch duty cycle control technique. This led to adopting the resonant-based DSSC SCC configuration to be inserted in the first stage of the new proposed inverter system. The adoption of this circuit configuration is also due to its ability to comply with sets of criteria as explained in Chapter 3, which justify its adoption into the new proposed DC/AC inverter. Figure 4.2 shows the circuit diagram of the proposed inverter.

The resonant-based DSSC SCC is formed by a current source and a DSSC SCC configuration. Where a current source contains a DC input voltage is connected in series with an inductor ( $L$ ) and internal resistance of inductor, ( $R_1$ ) is connected to the input of the proposed inverter. DSSC circuit is formed by one capacitor ( $C_1$ ), two switches ( $S_1$ ) and ( $S_2$ ). This circuit aims to generate a rectified near sine (multi-

level/staircase) voltage waveform by applying suitable control technique (variable switch duty cycle control in appropriate switching timing).

It should be noted that this two-unidirectional semiconductor switch operates in anti-parallel operation so that when ( $S_1$ ) is switched on, ( $S_2$ ) is off and vice versa over one switching cycle,  $T_s$ . These two switches operate at relatively high switching frequency i.e.  $< 50$  kHz (high enough to smooth and narrow the capacitor ripple voltages but not too high to limit switching losses). This switching frequency is assigned as  $F_s$ . A diode (D) and a smoothing capacitor ( $C_2$ ) are also included into the proposed inverter. These are mainly for voltage filtering purposes. A diode is placed in between a two-stage circuit, which is used to clamp the voltage (maintain at positive levels and prevent from reverse current), while a smoothing capacitor connected in parallel to the output load is used to smooth the output ripple voltage. An H-bridge circuit is formed by switches ( $S_3$ ,  $S_4$ ,  $S_5$  and  $S_6$ ) which are used to transform a rectified voltage waveform across a capacitor of the DSSC Circuit (terminal point X-Y) into a multi-level/staircase AC waveform, where the switches ( $S_3 - S_6$ ) operate at a fundamental line frequency of (50 Hz).

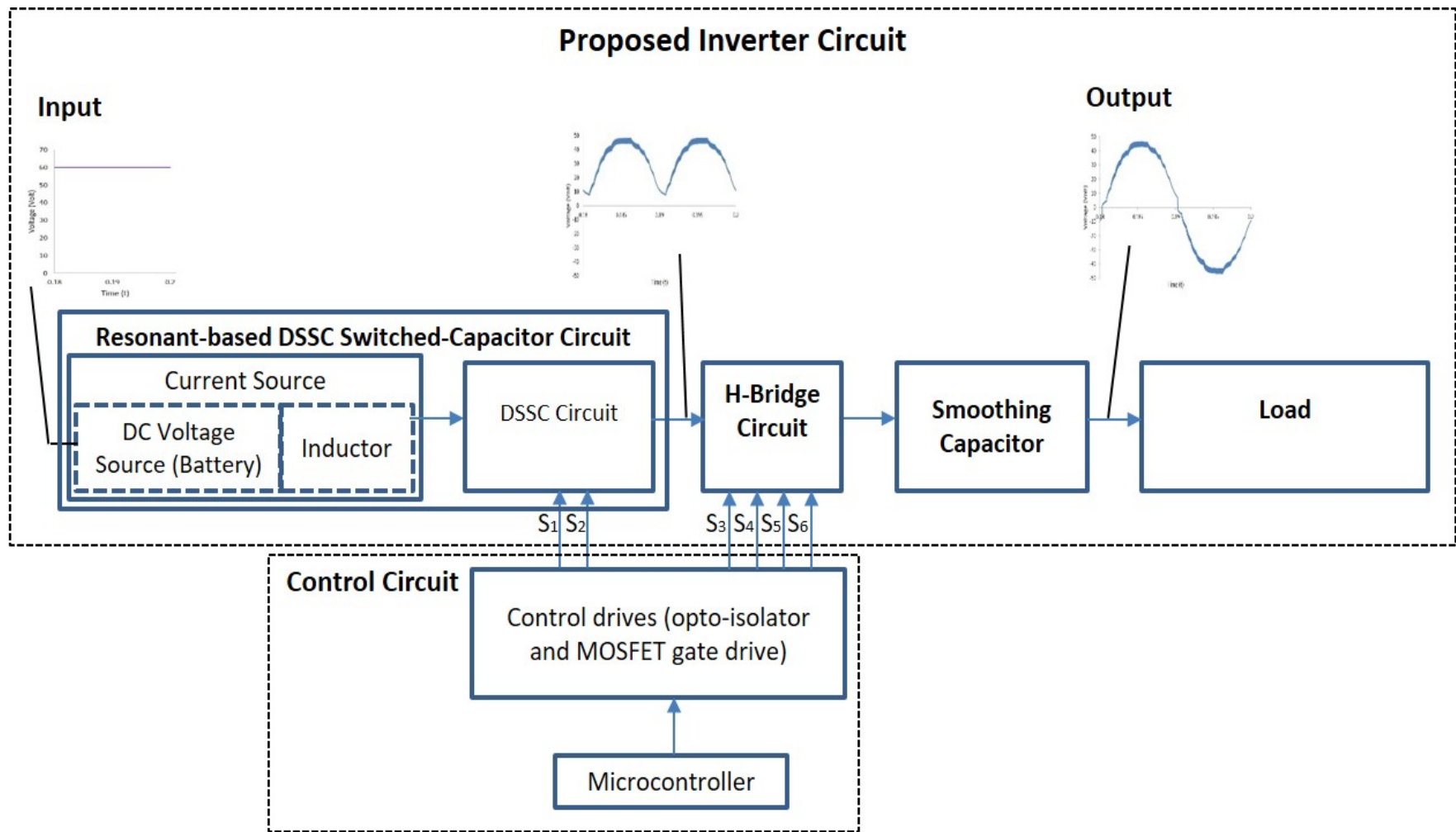


Figure 4.1 Circuit Block Diagram of Proposed Inverter System

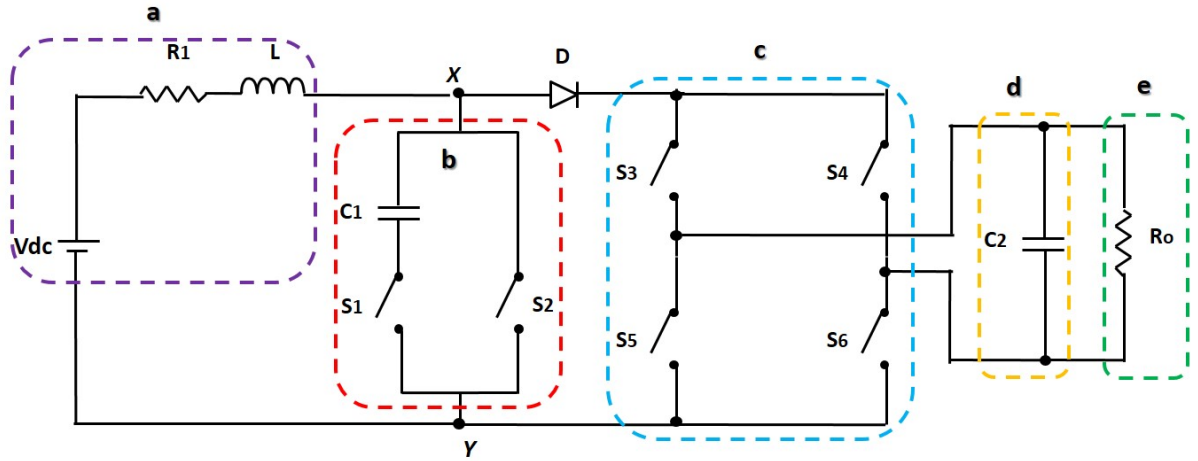


Figure 4.2 Circuit diagram of the proposed inverter:

- a) Current Source (DC voltage in series with Inductor L and inductor resistance  $R_1$ )
- b) DSSC SCC configuration circuit (terminal point X-Y)
- c) H-Bridge Circuit
- d) Smoothing Capacitor
- e) Load

The following section discusses the operating modes of the proposed inverter system.

### 4.3 Operating Modes of the Proposed Inverter System

The proposed inverter is designed to produce multi-level/staircase AC output voltage at fundamental line frequency. The inverter operation has two types of operating frequency; the high switching period and the fundamental switching period. In achieving AC output voltage, the proposed inverter circuit needs to operate in three different modes. A rectified multi-level waveform needs to be first generated during the first half cycle of the fundamental switching period. This process involves two switching modes; Mode 1 and Mode 2. This rectified waveform will then be transformed to sinusoidal AC waveform by H-bridge during Mode 3.

The proposed inverter is required to produce multi-level/staircase AC output voltage at fundamental frequency  $f_o$ . The fundamental switching period is

$$T_o = \frac{1}{f_o} \quad (4.1)$$

The switching control of the power semiconductor switches in DSSC circuit has constant chopping high-frequency operation, (i.e.  $f_s > 10$  kHz) and varying on-time,  $t_k$ . The high switching period is

$$T_s = \frac{1}{f_s} \quad (4.2)$$

The duty cycle  $D_k$  of the switch  $S_1$  is defined as the ratio of on-time switch  $t_k$  over entire high switching period,  $T_s$ .

$$D_k = \frac{t_k}{T_s} \quad (4.3)$$

with  $n$  times repeating high switching period  $T_s$ , the capacitor is charged (voltage exponentially rise) during  $t_k = D_k n T_s$  (on-time switch subinterval) and capacitor store charges (voltage constant) during  $t_b = (1 - D_k) n T_s$  (off-time switch subinterval). Therefore, the high switching period can also be expressed as

$$T_s = t_k + t_b = D_k n T_s + (1 - D_k) n T_s = \frac{1}{F_s} \quad (4.4)$$

where the number of repeating switching cycle,

$$n = \frac{t_k}{D_k T_s} \quad (4.5)$$

and time point  $t_k = D_k n T_s$

The proposed inverter is designed to operate in three circuit operating modes. The process of generating a rectified multi-level waveform involves two switching circuit modes, Mode 1 and Mode 2. Each circuit mode is operated in the transient state. The piecewise-linear derivation DC transient analysis method (Mellitt & Rashid, 1974) is used for analysing the proposed inverter circuit behaviour in terms of voltage and current in the cycle by cycle basis. Sets of the piecewise-linear equation are established for each circuit operating mode within the repetitive cycle of operation. The piecewise-linear DC transient derivation analysis for circuit operating Mode 1 and 2 is presented in the following equation:

The first mode (Mode 1) takes place during the first half cycle of the high switching period( $0 \leq t_k \leq D_k n T_s$ ). Figure 4.3 shows the equivalent circuit for Mode 1. When switch ( $S_1, S_3$  and  $S_6$ ) are turned on and ( $S_2, S_4$  and  $S_5$ ) are off, the diode (D) is conducting (in forward biased). Both capacitors ( $C_1$ ) and ( $C_2$ ) are connected in parallel and both are charged through inductor (L). The capacitor ( $C_1$ ) is desired to have small capacitance ( $1\mu F$ ) in order to achieve high voltage ripple across it. The output capacitor ( $C_2$ ) would have large capacitance (i.e.  $> 80\mu F$ ) which can be used as a smoothing filter used to limit the ripple output voltage. These parallel-connected capacitors form a total capacitance of ( $C_T$ ) which is the summation of ( $C_1$ ) and ( $C_2$ ). The equivalent circuit can be simplified as shown in Figure 4.4. The connection forms a switched parallel resonant-topology where inductor (L) and inductor series resistance

$(R_1)$  are connected in parallel to capacitors ( $C_T$ ) and load ( $R_o$ ).

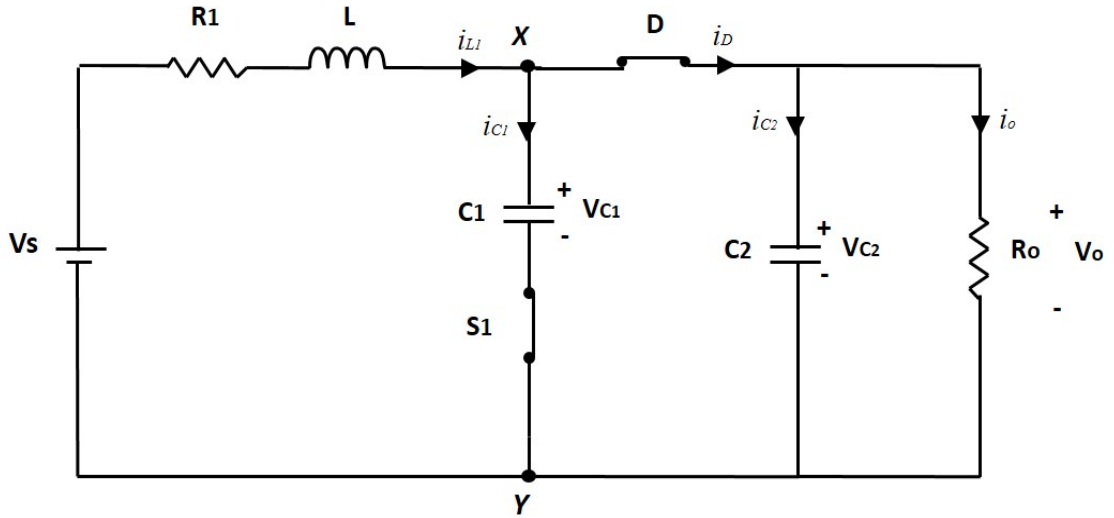


Figure 4.3 Equivalent Circuit for Mode 1

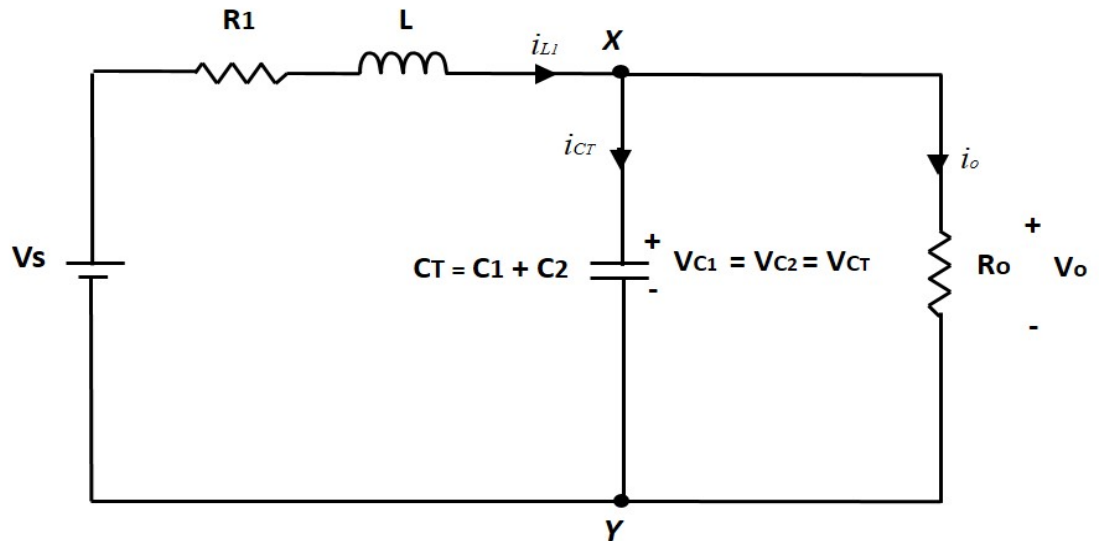


Figure 4.4 Simplified Equivalent Circuit for Mode 1

The instantaneous voltage for this Mode 1 is described by following equation :

$$V_s = i_{L1}(t)R_1 + L \frac{di_{L1}(t)}{dt} + v_{CT_1}(t) \quad (4.6)$$

$$V_s = i_{L1}(t)R_1 + L \frac{di_{L1}(t)}{dt} + \left[ \frac{1}{C_T} \int i_{CT} dt + v_{CT_1}(t=0) \right] \quad (4.7)$$

where initial condition  $i_{L_1}(t = 0) = I_{L_1}$  and  $v_{CT}(t = 0) = V_{c_1}$

The inductor current  $i_{L_1}(t)$  can be expressed as

$$i_{L_1}(t) = I_0 + e^{-(\frac{R_1}{L})t} \left[ (I_{L_1} - I_0) \cos(\omega_r t) + \frac{(2V_s - V_{c_1}) - R(I_{L_1} + I_0)}{2\omega_r L} \sin(\omega_r t) \right] \quad (4.8)$$

The capacitor voltage  $v_{CT_1}(t)$  can be expressed as

$$v_{CT_1}(t) = V_s - I_0 R_1 + e^{-(\frac{R_1}{L})t} \left[ \left( (V_{c_1} - V_s) + \frac{R_1(I_0 - I_{L_1})}{2} \right) \cos(\omega_r t) + \left\{ \frac{R_1}{2\omega_r L} \left[ (V_{c_1} - V_s) + \frac{R_1(I_0 - I_{L_1})}{2} \right] + \omega_r (I_0 - I_{L_1}) \right\} \sin(\omega_r t) \right] \quad (4.9)$$

At the end of this mode

$$i_{L_1}(t_k = D_k n T_s) = I_{L_2} \quad (4.10)$$

$$v_{CT_1}(t_k = D_k n T_s) = V_{c_2}$$

The second mode (Mode 2) takes place during the second half cycle of the high switching period ( $D_k n T_s \leq t_b \leq (1 - D_k) n T_s$ ). It should be noted that both Mode 1 and 2 are operated during the first half cycle of fundamental switching period ( $0 \leq t \leq \frac{T_o}{2}$ ). Figure 4.5 shows the equivalent circuit for Mode 2 which forms an (R-L) circuit. When switches ( $S_2, S_3$  and  $S_6$ ) are turned on and ( $S_1, S_4$  and  $S_5$ ) are off, the diode (D) is in reverse biased, disconnecting the load from input. The capacitor ( $C_1$ ) is disconnected and voltage across it will remain constant (in this particular condition mode, the capacitor charge is stored for the duration  $t_b$ ). The capacitor ( $C_2$ ) is

connected in series with load ( $R_o$ ). It should be noted that, both Mode 1 and 2 are operated during the first half cycle of fundamental switching period ( $0 \leq t \leq \frac{T_o}{2}$ ).

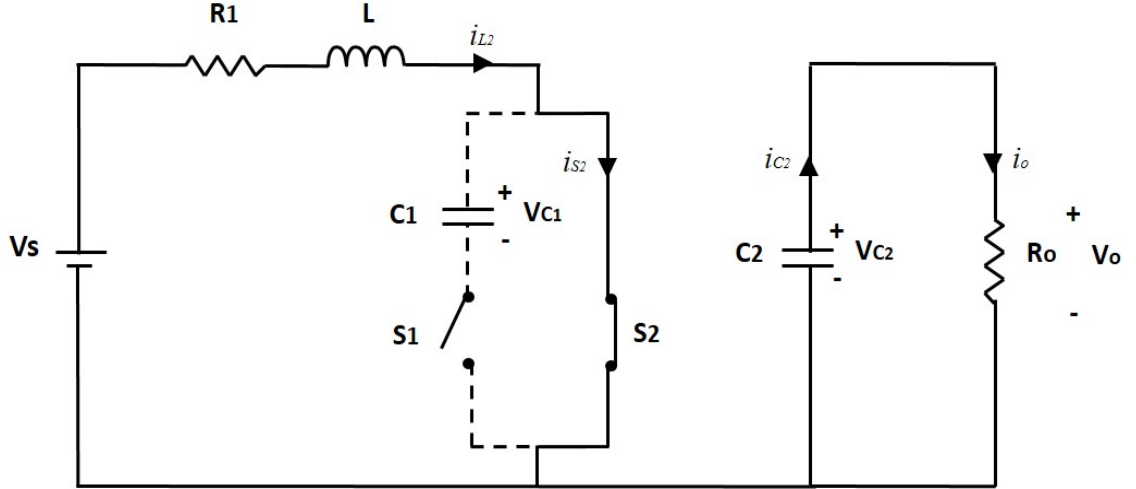


Figure 4.5 Equivalent Circuit for Mode 2

The instantaneous voltage for this Mode 2 is described by the following equation:

$$V_s = i_{L_2}(t)R_1 + L \frac{di_{L_2}(t)}{dt} \quad (4.11)$$

Redefine the time origin,  $t = 0$ , the initial condition  $i_{L_2}(t = 0) = I_{L_2}$  and  $v_{c_2}(t = 0) = V_{c_2}$

The inductor current  $i_{L_2}(t)$  can be expressed as

$$i_{L_2}(t) = \frac{V_s}{R_1} \left( 1 - e^{-\left(\frac{R_1}{L}\right)t} \right) + I_{L_2} e^{-\left(\frac{R_1}{L}\right)t} \quad (4.12)$$

The capacitor voltage  $v_{c_2}(t)$  can be expressed as

$$v_{c_2}(t) = V_{c_2} e^{-\left(\frac{1}{R_o C_2}\right)t} \quad (4.13)$$

The capacitor ( $C_2$ ) discharge its initial energy stored to load ( $R_o$ ) while the initial energy remains stored in Capacitor ( $C_1$ )

At the end of this mode

$$i_{L_2}(t_b = (1 - D_k)nT_s) = I_{L_3} \quad (4.14)$$

$$v_{c_2}(t_b = (1 - D_k)nT_s) = V_{c_3}$$

The switch operation is repeated for  $n$  times switching cycle in previous equation (4.5) where time point,  $t_k$  will be determined later. This will be discussed in detail during the determination of switching time in next Switching Control section. The duration of the square pulse signal to be applied to the switch ( $S_1$ ) (switch duty cycle) in DSSC circuit can be controlled which is valid for specific time intervals (control the amount of charge to be stored in the fixed capacitor ( $C_1$ ) i.e. controlling the capacitor charging). Applying different duty cycle control values to the associated switch, different transient capacitor voltage levels (multi-level voltage waveform) can be obtained across capacitor ( $C_1$ ). The repeating switching action between circuit modes can create ripple voltage across DSSC circuit (terminal X-Y). The peak-to-peak voltage across point terminal X-Y can become larger when the duration of the square pulse signals is increased with time point,  $t_k$ . At the output of this circuit, this ripple voltage can be filtered by smoothing capacitor ( $C_2$ ) which is connected in parallel to the load. Therefore, a rectified multi-level voltage waveform can be shaped by applying different duty cycle values which valid in specific timing control. Different duty cycle mode values can be achieved by comparing different DC levels ( $V_{dc_k}$ ) (as references signal) with a high-frequency triangular carrier signal ( $V_{tri}$ ). This creates a switching control pattern (or gating signals), and this proposed control technique is called variable switch duty cycle control. The gating signals are to be fed to the switches in the DSSC SCC circuit. This is elaborated on in detail in the following control technique section. A multi-level/staircase waveform can be generated by using

variable switch duty cycle control technique (variable duty cycle control in specific switching timing).

The third mode (Mode 3) taking place during the second half cycle of the fundamental switching period ( $\frac{T_o}{2} \leq t \leq T_o$ ). The H-bridge switches ( $S_3$  and  $S_6$ ) transform a rectified multi-level voltage waveform into a sinusoidal AC output voltage waveform.

#### 4.4 Design & Analysis

The resonant-based DSSC SCC circuit with variable switch duty cycle control technique demonstrated the ability to vary the DC input voltage, as investigated in Chapter 3. This behaves like a voltage regulator. By using variable switch duty cycle control in specific switching timing, the voltage across resonant-based DSSC SCC circuit can be varied/regulated in such a way that rectified near sine (multi-level/staircase) voltage waveform can be generated/shaped across a fixed capacitor ( $C_1$ ) of this circuit. Assuming ideal staircase shape of the capacitor voltage steps (neglect the transient in capacitor voltage). The design procedure and example is shown in the following section, showing the formation of rectified multi-level/staircase voltage waveform across ( $C_1$ ) of the DSSC circuit (terminal X-Y) and eventually multi-level/staircase AC voltage waveform across the load.

#### 4.4.1 Design Procedure of the Proposed Inverter

A new proposed DC/AC inverter output voltage waveform is desired to have output waveform as close to sinusoidal waveform as possible, so that minimum harmonics distortion can be achieved. In theory, the sinusoidal voltage is given by

$$V_o(t_k) = V_i \sin(\omega t_k) \quad (4.15)$$

where,

$V_o(t)$  is the output voltage

$V_i$  is the peak amplitude of the output voltage

$\omega$  is the angular frequency in radians per second (rad/seconds)

$t_k$  is the time

In order to trace the sine waveform, the output voltage of the new proposed DC/AC inverter can be divided into  $m$  voltage levels with respect to  $k$ -th switching time which can be expressed as

$$V_o(t_k) = \begin{cases} \frac{V_{2k}}{N}, & k \leq N \\ \frac{V_{2N-k}}{3}, & N < k \leq 2N \end{cases} \quad (4.16)$$

where

$t_k = \{t_1, t_2, \dots, \dots, t_{2N}\}$  is the switching time (or time point)

$$k = 1, 2, \dots, N \text{ and } N = \frac{m-1}{2}$$

$m$  is number of voltage levels (include zero level).

Hence, for  $m$ -level staircase/multi-level AC output voltage, there are  $N$ -main voltage steps of a staircase rectified voltage waveform.

Using equation (4.16). The output voltage is given by

$$V_o(t_k) = \left\{ V_{\frac{2k}{N}}, \dots, V_2, \dots, V_{\frac{2k}{N}} \right\} \quad (4.17)$$

and the switching time (or time point) for positive half cycle of the fundamental switching period  $T_o$  is denote as

$$t_k = \{t_k, \dots, t_N, \dots, t_{2N}\} \quad (4.18)$$

Or in another form the output voltage is given by

$$V_o(t_k) = \begin{cases} V_{\frac{2k}{N}}, & t_k \leq t \leq t_{k+1} \\ \vdots \\ V_2, & t_N < t \leq t_{N+1} \\ \vdots \\ V_{\frac{2k}{N}}, & t_{2N-1} < t \leq t_{2N} \end{cases} \quad (4.19)$$

The first  $N$ -main voltage steps can be described by the piece-wise expression:

$$V_{o(peak)} = \sum_{k=1}^N V_k(t_k) = V_{\frac{2k}{N}}(t_1) + \dots + V_2(t_N) \quad (4.20)$$

which can also be expressed as

$$\begin{aligned} V(0) &= 0 \\ V_{\frac{2k}{N}}(t_1) &= v_{c_1}(t_1) + V(0) \\ &\quad \ddots \\ V_2(t_N) &= v_{c_N}(t_N) + V_{\frac{2(N-1)}{N}}(t_{N-1}) \end{aligned} \quad (4.21)$$

where

$v_{c_1}(t_1)$  to  $v_{c_N}(t_N)$  are the capacitor voltages level which can also be represented as voltage increment as shown in equation (3.37).

m is number of voltage levels (include zero level).

$V_2(t_N)$  represent the peak maximum voltage level of the output phase voltage.

A near AC (staircase/multi-level) output voltage  $V_o(t_k)$  waveform needs to be shaped close to sinusoidal waveform. To obtain low total harmonic distortion in output voltage  $V_{THD}$ , the switching time or angle is determined by using the Half-Height method (Luo and Ye, 2013). This method can arrange the main switching angle in simple way according to the sine function. For known  $k$ -th staircase steps/levels of sine wave output voltage, the corresponding switching time at that particular intersection voltage levels can be set. The switching time during the positive cycle of the output voltage waveform,  $t_k = \frac{T_o}{2}$  (or 10 ms) is defined as the main switching time (or time point)

$t_k = \{t_1, \dots, t_N\}$  which can be determined by the formula,

$$t_k \text{ (in milisecond)} = \sin^{-1} \left( \frac{2k - 1}{m - 1} \right) \times \frac{10ms}{180^\circ} = D_k n T_s \quad (4.22)$$

where  $k = 1, 2, \dots, N$  and  $N = \frac{m-1}{2}$  and m is peak-to-peak output voltage level (include zero)

During the negative cycle of the output voltage waveform,  $\frac{T_o}{2} < t_k < T_o$  (10ms to 20ms), the switching time (or time point)  $t_k = \{t_{k+1}, \dots, t_{2N}\}$  can be determined by using the following formula

$$t_{k+1} \text{ (in milisecond ms)} = \pi - t_k = 10ms - t_k \quad (4.23)$$

$$t_7 \text{ (in milisecond ms)} = \pi - t_6 = 10ms - t_6$$

$$t_8 \text{ (in milisecond ms)} = \pi - t_5 = 10ms - t_5$$

. (4.24)

$$t_{11} \text{ (in milisecond ms)} = \pi - t_2 = 10ms - t_2$$

$$t_{2N} \text{ (in milisecond ms)} = \pi - t_1 = 10ms - t_1$$

#### 4.4.2 Fourier Analysis

The harmonics content of the output voltage can be determined by using Fourier series:

$$V_0(t) = a_0 + \sum_{n=1}^{\infty} (a_n \cos n(\omega t) + b_n \sin n(\omega t)) \quad (4.25)$$

The output voltage  $V_0(t)$  is an odd function,  $a_n = 0$  and

$$b_n = \frac{2}{T} \int_0^T V_0(t) \sin n(\omega t) dt \quad (4.26)$$

Substituting equation (4.16) into equation (4.26),  $b_n$  can be expressed as

$$b_n = \sum_{x=1}^N V_{\frac{2k}{N}} (\cos n(\omega t_x) - \cos n(\omega t_{x+1}))$$

$$+ \sum_{y=N+1}^{2N} \left( V_{\frac{2N-k}{3}} \right) (\cos n(\omega t_y) - \cos n(\omega t_{y+1})) \quad (4.27)$$

To assess the harmonics spectrum of inverter output, the total harmonic distortion (THD) is a parameter index used to assess harmonics distortion. The THD of a voltage waveform is defined as

$$THD = \sqrt{\frac{\sum_{n=2}^{\infty} b_n^2}{b_1^2}} \quad (4.28)$$

where  $b_1$  and  $b_n$  are the fundamental voltage and nth harmonics voltage components.

#### 4.4.3 Design Example and Calculation of the Proposed Inverter

For the proposed/designed thirteen-levels inverter, the thirteen-levels ( $m = 13$ ) staircase/multi-level AC output voltage over half cycle of fundamental period can be generated by using equations (4.16) and (4.17), the output voltage is given by

$$V_o(t_k) = \left\{ V_{\frac{1}{3}}, V_{\frac{2}{3}}, V_1, V_{\frac{4}{3}}, V_{\frac{5}{3}}, V_2, V_{\frac{5}{3}}, V_{\frac{4}{3}}, V_1, V_{\frac{2}{3}}, V_{\frac{1}{3}} \right\} \quad (4.29)$$

and the switching time (or time point) for half cycle of fundamental period,  $T_o$  are denote as

$$t_k = \{t_1, t_2, t_3, t_4, t_5, t_6, t_7, t_8, t_9, t_{10}, t_{11}, t_{12}\} \quad (4.30)$$

Using equation (4.20), the six-main voltage steps of the staircase/multi-level output voltage over half cycle of fundamental period,  $T_o$  can be represent as

$$V_o(t_k) = \begin{cases} V_{\frac{1}{3}}, & t_1 \leq t_k \leq t_2 \\ V_{\frac{2}{3}}, & t_2 \leq t_k \leq t_3 \\ V_1, & t_3 \leq t_k \leq t_4 \\ V_{\frac{4}{3}}, & t_4 \leq t_k \leq t_5 \\ V_{\frac{5}{3}}, & t_5 < t_k \leq t_6 \\ V_2, & t_6 < t_k \leq t_7 \\ V_{\frac{5}{3}}, & t_7 < t_k \leq t_8 \\ V_{\frac{4}{3}}, & t_8 < t_k \leq t_9 \\ V_1, & t_9 < t_k \leq t_{10} \\ V_{\frac{2}{3}}, & t_{10} \leq t_k \leq t_{11} \\ V_{\frac{1}{3}}, & t_{11} < t_k \leq t_{12} \end{cases} \quad (4.31)$$

where  $V_2(t_6)$  represent the peak/maximum voltage step of the multi-level output voltage. The six-voltage increment (or capacitor voltage level) ( $v_{c_1}(t_1)$  to  $v_{c_N}(t_N)$ ) can be obtained as follows:

$$\begin{aligned}
 V(0) &= 0 \\
 V_{\frac{1}{3}}(t_1) &= v_{c_1}(t_1) + V(0) \\
 V_{\frac{2}{3}}(t_2) &= v_{c_2}(t_2) + V_{\frac{1}{3}}(t_1) \\
 V_{\frac{1}{3}}(t_3) &= v_{c_3}(t_3) + V_{\frac{2}{3}}(t_2) \\
 V_{\frac{4}{3}}(t_4) &= v_{c_4}(t_4) + V_{\frac{1}{3}}(t_3) \\
 V_{\frac{5}{3}}(t_5) &= v_{c_5}(t_5) + V_{\frac{4}{3}}(t_4) \\
 V_{\frac{2}{3}}(t_6) &= v_{c_6}(t_6) + V_{\frac{5}{3}}(t_5)
 \end{aligned} \tag{4.32}$$

It should be noted that the first six different voltage levels could have unequal voltage steps due to different voltages increment. Using equation (4.32), the capacitor voltage level  $v_{c_1}(t_1)$  to  $v_{c_6}(t_6)$ (can also be represented as voltage increment) is obtained as illustrated in Table 4.1.

Table 4.1 Relationship between capacitor voltage level and duty cycle (Theoretical Calculation)

k	Duty cycle Value $D_k$	Capacitor Voltage level $v_{c_k}(t_k)$ (Volt)
1	0.95	6.8
2	0.85	18.3
3	0.75	27.8
4	0.65	34.9
5	0.55	40.0
6	0.4	44.8

Using equation (4.22) to (4.24), the pre-calculated offline main switching angles / times for thirteen-levels AC output voltage ( $m = 13$ ) is obtained as illustrated in Table 4.2.

Table 4.2 Main switching angle or time (Theoretical Calculation)

	$\theta_1$	$\theta_2$	$\theta_3$	$\theta_4$	$\theta_5$	$\theta_6$
Switching Angle (in degree)	4.78	14.48	24.62	35.69	48.59	66.44
	$t_1$	$t_2$	$t_3$	$t_4$	$t_5$	$t_6$
Switching Time (in millisecond)	0.266	0.804	1.368	1.983	2.699	3.691
	$\theta_7$	$\theta_8$	$\theta_9$	$\theta_{10}$	$\theta_{11}$	$\theta_{12}$
Switching Angle (in degree)	113.56	131.41	144.31	155.38	165.52	175.22
	$t_1$	$t_2$	$t_3$	$t_4$	$t_5$	$t_6$
Switching Time (in millisecond)	6.309	7.301	8.017	8.632	9.196	6.309

The switching angles/time shown in Table 4.2 represents the optimum angles/time that can reduce the harmonics content resulting in minimum total harmonics distortion. It also represents the switching timing for the control signals which is programmed in the microcontroller to generate the control signals (CS1 to CS6) as shown in Figure 4.9.

The selection of the components value ( $R$ ,  $L$  and  $C$ ) is based on the assumption that the circuit is underdamped ( $\alpha < \omega_0$  or  $R^2 < \frac{L}{C}$ ) where  $\alpha$  and  $\omega_0$  as the damping factor and resonant frequency respectively. In this research work, the value of damping factor is set as 50K rad/s and the low equivalent series resistance of the inductor and wire resistance  $R$  is set as  $1\Omega$  to give small damping factor so that higher transient voltage overshoot can be achieved. Also, three different resonant frequencies of 100K, 316K and 1000K rad/s were set to yield different sets of component parameter values

range of options (Case 1,2 and 3) which can obtain low THD output. By substituting the damping ratio, resonant frequency, the capacitor voltage levels and switching time obtained (as illustrated in Table 4.1 and 4.2) into equation (3.32), three different cases of parameter components values of  $L$ ,  $C_1$  and  $C_2$  can be determined as follows:

Case 1:  $R_1=1\Omega$ ,  $L=10\mu H$ ,  $C_1=10\mu F$ ,  $C_2=100\mu F$ ,  $R_o=10\Omega$

Case 2:  $R_1=1\Omega$ ,  $L=10 \mu H$ ,  $C_1=1\mu F$ ,  $C_2=100\mu F$ ,  $R_o=10\Omega$

Case 3:  $R_1=1\Omega$ ,  $L=10\mu H$ ,  $C_1=0.1\mu F$ ,  $C_2=100\mu F$ ,  $R_o=10\Omega$

Using equation (4.28), the voltage THD for designed thirteen-levels inverter is obtained. The relationship between voltage THD and high switching frequency (DSSC SCC circuit) for three different cases is plotted in Figure 4.6.

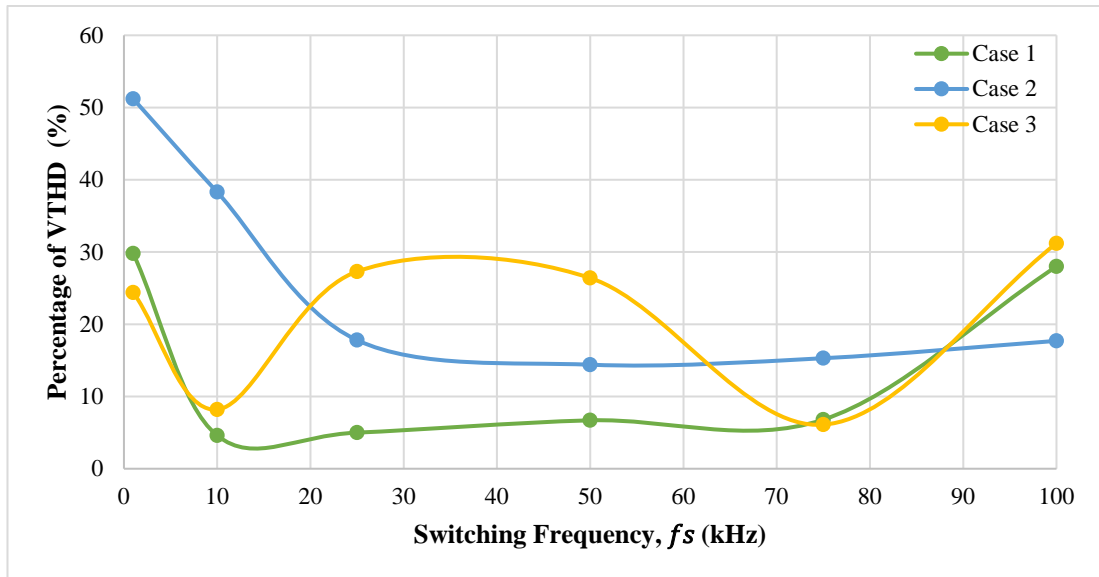


Figure 4.6 Percentage of THD of output voltage  $V_{THD}$  in terms of high switching frequency

For a thirteen-levels proposed inverter, the component parameter Case 1 is chosen that can consistently provide low THD performance for wide switching frequency operation ( $10 \text{ kHz} \leq f_s \leq 70 \text{ kHz}$ ) of the DSSC circuit. Under pure resistive load ( $R_o = 10 \Omega$ ), the lowest  $V_{THD}$  can be obtained when DSSC circuit operating at 10

kHz switching frequency  $f_s$ . The estimated calculation THD output voltage ( $V_{THD}$ ) is 4.6 % as shown in Figure 4.6 (Case 1 (Green)). Therefore, Case 1 is chosen to be used in design simulation of the proposed DC/AC inverter in Chapter 5.

## 4.5 Proposed Control Technique

This section explains the control technique used for the proposed DC/AC inverter. The formation of a near AC (staircase/multi-level) voltage involves two processes:

- 1) To generate full rectified multi-level waveform during the positive cycle of the AC output.
- 2) To transform generated rectified multi-level waveform into complete near multi-level AC voltage waveform.

Different transient capacitor voltage levels (multi-level voltage) can be obtained by suitably charging a fixed capacitor ( $C_1$ ) in the resonant-based DSSC SCC circuit (in Figure 4.2). This charging capacitor can be controlled by the proposed open-loop control circuit shown in Figure 4.1 and Figure 4.7. The control logic circuit outputs two PWM signals labelled as  $S_1$  and  $S_2$  which are responsible for controlling the charging capacitor ( $C_1$ ) through switches ( $S_1$ ) and ( $S_2$ ). These switches have anti-parallel operation i.e. when ( $S_1$ ) is turned on, ( $S_2$ ) is off and vice versa. The variable switch duty cycle control PWM technique is proposed to generate control signals for switches ( $S_1$ ) and ( $S_2$ ). The variable switch duty cycle control PWM technique is variable switch duty cycle control in specific switching timing. This technique is used to obtain a variable switch duty cycle PWM control signal. This is achieved by comparing fundamental frequency multi-level DC waveform (reference signal) to the

high-frequency triangular waveform (carrier signal). Each step of the multi-level DC waveform (reference signal) is controlled in specific switching timing. Figure 4.8 shows the control logic circuit used to generate the variable switch duty cycle PWM control signal. This control signal will be applied to the control switches of the resonant-based DSSC circuit so that six transient voltage steps/levels of the rectified staircase/multi-level waveform (thirteen-levels peak-to-peak output voltage) can be generated during the positive cycle of the fundamental period (0 to 10 ms).

The circuit comprises six AND gates, six comparators (Op-Amp), single OR gate, and single NOT (inverter) gate to produce pulse train signals at six different duty cycle modes. These pulse train signals can be divided into two control signals. The first control signal  $S_1$  will be applied to switch ( $S_1$ ) of the resonant-based DSSC circuit. The second control signal  $S_2$  will be applied to switch ( $S_2$ ) via a NOT (inverter) gate. The input signals ( $V_{dc1}$  to  $V_{dc6}$ ) (signals at six different DC voltage levels) and control signals (CS1 to CS6) are the input signals to be fed to the control circuit. (CS1 to CS6) are pre-programmed in microcontroller according to the main switching time calculated above. These microcontroller output signals are then multiplied by ( $V_{dc1}$  to  $V_{dc6}$ ) through AND gates so that reference signals (RS1-RS6) can be generated. PWM gating signals (with different duty cycle modes (D1 to D6)) can be generated by comparing reference signal (RS1-RS6) with triangular carrier signal ( $10 \text{ kHz} \leq f_s \leq 70 \text{ kHz}$ ) using comparator (Op Amp) as shown in Figure 4.8.

The PWM signal (D1 to D3) is applied to the switch  $S_1$  to step-up capacitor voltage in three transient voltage steps/levels during the first quarter cycle of AC output waveform (0 to 5ms). The maximum voltages can be reached during duty cycle when mode 3 (D3) is applied (where the determination of capacitance ( $C_1$ ) is based on this maximum voltage). During the second quarter cycle of the fundamental period

(5ms to 10ms), the PWM signal (D3 to D6) is applied to the switch S<sub>1</sub> step-down capacitor voltage in three transient voltage steps/levels. OR gate is used to combine each PWM signal (D1 to D6).

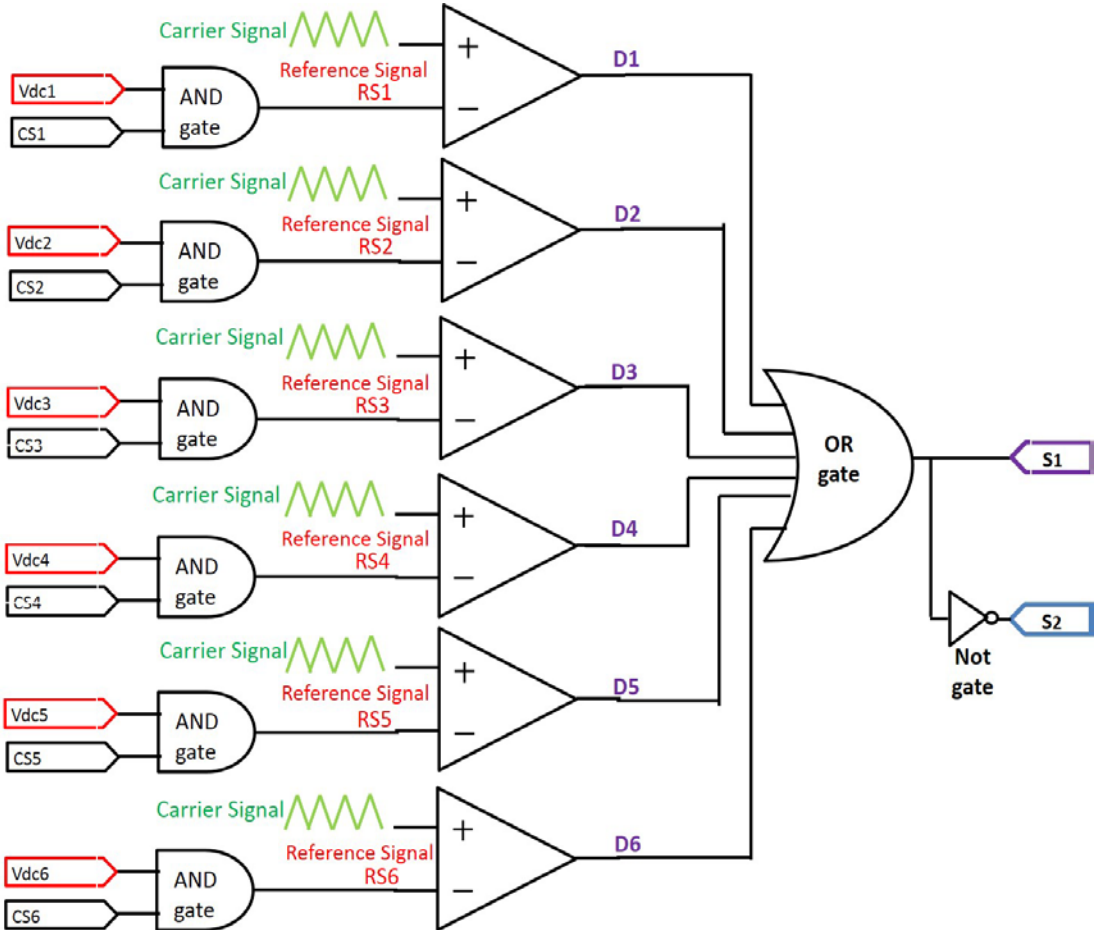


Figure 4.7 Control logic circuit for DSSC circuit

This PWM signal is called variable switch duty cycle PWM control signal (S<sub>1</sub>). The signal (S<sub>2</sub>) is the inverted signal of (S<sub>1</sub>) via inverter gate. A hard-limiter is used to obtain a square wave gating pulse. The variable switch duty cycle PWM control signal is applied to switch (S<sub>1</sub>) and (S<sub>2</sub>) through isolating circuit (opto-isolator).

Figures 4.9 and 4.10 shows the example of 2 kHz control signals. The pulse train signal S<sub>2</sub> represents the inverted signal of S<sub>1</sub>. Figures 4.9 and 4.10 show the

theoretical timing diagram of the variable switch duty cycle PWM control signals S<sub>1</sub> and S<sub>2</sub> with variable amplitude modulation  $m_{a_k}$  is shown in Table 4.3 and the frequency modulation  $m_f$  of 200. These output signals are generated from control circuit in Figure 4.8 to be fed to switches (S<sub>1</sub>) and (S<sub>2</sub>) in the resonant-based DSSC circuit. The switch duty cycle, which is also called amplitude modulation ratio  $m_a$  can be calculated using formula (4.33).  $m_{a_k}$  is the ratio of the different DC levels in multi-level DC waveform (amplitude of reference signal) to the amplitude of a triangular waveform (amplitude of carrier signal). The frequency modulation ratio  $m_f$  is the ratio of the frequency of triangular waveform (frequency of the carrier signal) to the frequency of multi-level DC waveform (frequency of the reference signal). This can be calculated using equation (4.34).

$$\text{Amplitude Modulation, } m_{a_k} = \frac{V_{\text{ref}}}{V_{\text{tri}}} = \frac{V_{\text{dc}_k}}{V_{\text{tri}}} \quad (4.33)$$

$$\text{Frequency Modulation, } m_f = \frac{F_{\text{tri}}}{F_{\text{ref}}} \quad (4.34)$$

where,

The gating pulse S<sub>1</sub> = 1, when V<sub>dc<sub>k</sub></sub> > V<sub>tri</sub>(carrier)

The gating pulse S<sub>1</sub> = 0, when V<sub>dc<sub>k</sub></sub> < V<sub>tri</sub>(carrier)

V<sub>tri</sub> is the amplitude of the carrier signal (10 Volts)

V<sub>dc<sub>k</sub></sub> is the different DC levels (multi-level DC voltage) reference signal

F<sub>tri</sub> is the carrier signal frequency

F<sub>ref</sub> is reference signal frequency (multi-level DC waveform)

Table 4.3 Variable amplitude modulation (or variable duty cycle) (Theoretical Calculation)

k	Different DC levels, $V_{dc_k}$ (in Volts)	Amplitude Modulation $m_{a_k}$ or Duty cycle value, $D_k$
1	9.5	0.95
2	8.5	0.85
3	7.5	0.75
4	6.5	0.65
5	5.5	0.55
6	4	0.4

In the first power conversion stage of the of the designed inverter system, a full rectified multi-level/staircase waveform can be generated across a fixed capacitor ( $C_1$ ) of the DSSC SCC circuit. This can be achieved by applying variable switch duty cycle control PWM technique (variable duty cycle control in specific switching timing) to the associated switches. In the second power conversion stage, a multi-level AC output voltage waveform can be generated at output by a H-Bridge circuit. The resonant-based DSSC SCC with variable switch duty cycle control PWM technique can generate multi-step/multi-level voltages without the need of multiple stages of switched-capacitor cells (which contains several number of switches and capacitor). This technique could help to reduce the need of multiple stage of SCC cells such required in many recent switched-capacitor multi-level inverter topologies.

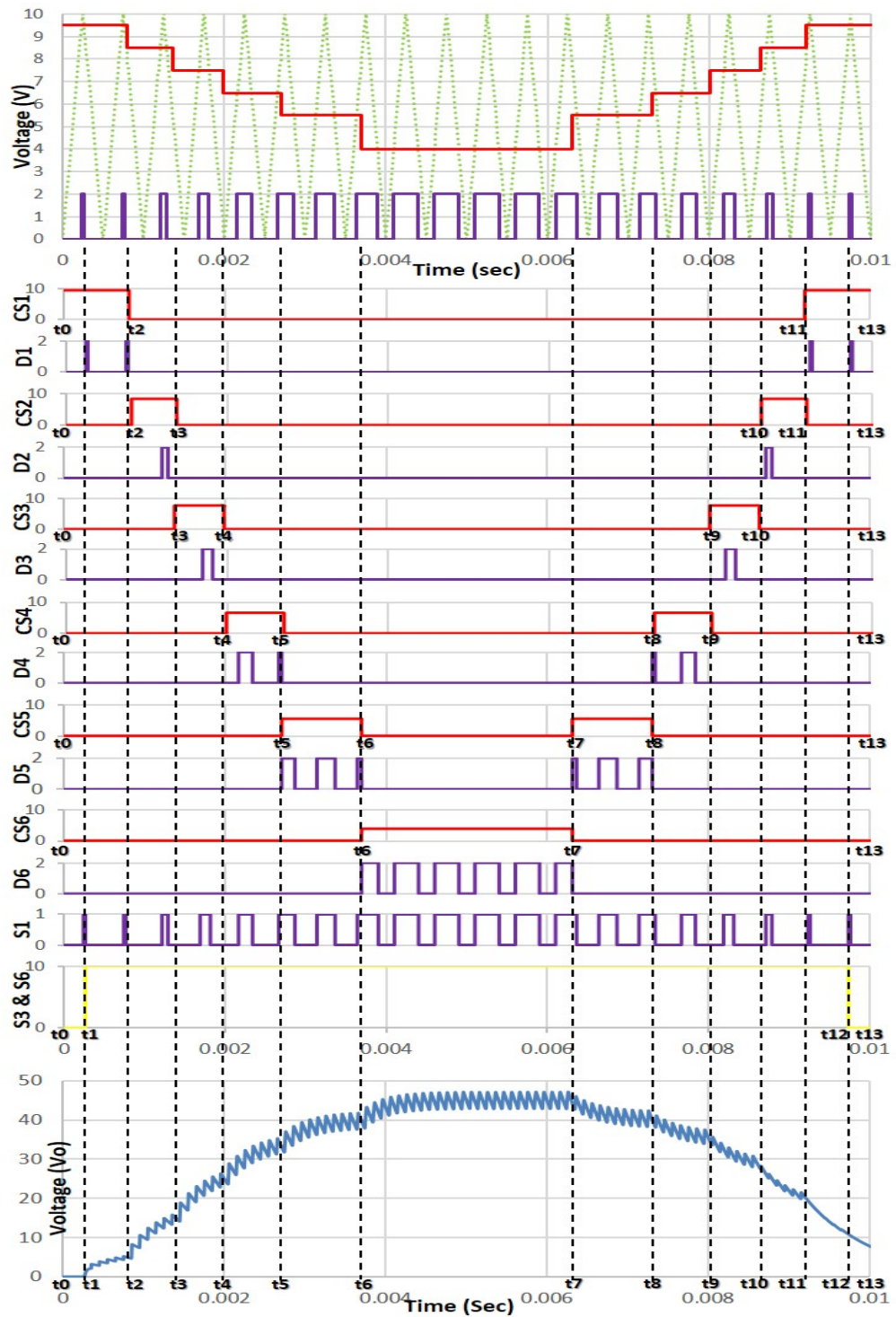


Figure 4.8 Timing diagram of the control signal for a rectified staircase/multi-level waveform during period (0 to 10ms) (Theoretical)

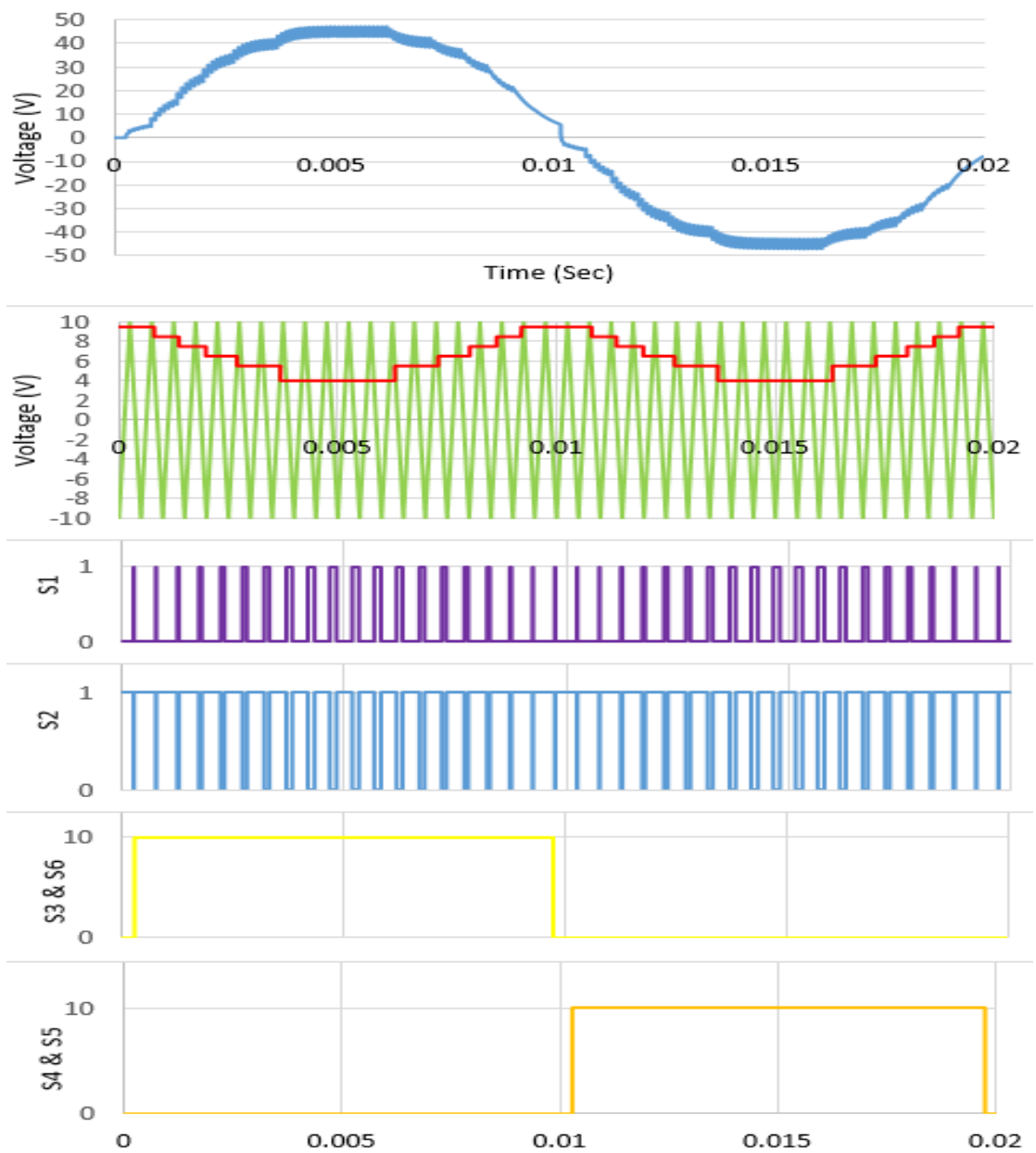


Figure 4.9 Timing diagram of the control signal for one cycle near AC output voltage waveform (0 to 20ms) (Theoretical)

## 4.6 Summary

In this chapter, a single-phase DC/AC inverter based switched-capacitor circuit with reduced component count and its control technique were designed and proposed. The principle operation, design, and analysis were presented. The theoretical estimation analysis through a comprehensive mathematical derivation that provides the relation between output voltage THD and switching frequency of the resonant-based DSSC SCC circuit is presented. This relationship led to adopting circuit parameter values and optimum switching to be used in simulation as well as practical implementation so that near AC output voltage with low THD ( $V_{THD}$ ) can be obtained.

In Chapter 5, the proposed inverter is discussed by showing near AC output voltage and current waveform through simulation results, and the practical experimental result of this circuit is proved. In addition, the designed proposed inverter is compared with the well-known PWM VSI inverter topology, classical Cascaded H-Bridge multi-level inverter topology and also the recent switched-capacitor multi-level inverter topology in terms of output voltage THD and components count.

# **Chapter 5 Simulation and Practical Implementation of the Proposed Inverter System**

## **5.1 Introduction**

Reviews of the published literature on the traditional three-levels PWM inverter topologies and multi-level inverter topologies (classical and newly evolved) are presented in both Chapter 2 and Chapter 3. A review of the newly evolved inverters focused on switched-capacitor multi-level inverter topologies (or also known as multi-level inverter based switched-capacitor circuit topologies) due to their advantages (generating a high number of output voltage levels with less component count and single DC source usages in comparison to the classical topology). The drawbacks each of the covered inverter topologies were presented and discussed. These limitations have led the author to propose a new DC/AC inverter circuit topology with a reduced component count for use in low power applications. The available voltage boosting/varying techniques were reviewed in Chapter 3.

A resonant-based DSSC configuration circuit with varying switch duty cycle controlled technique was found to be suitable for boosting/varying the DC input voltage. This topology and technique was adopted (due to its superiority over other topologies/techniques). This adopted circuit was applied to the first power conversion stage of the designed/proposed inverter circuit system, and the control technique (variable switch duty cycle control PWM technique) was proposed to generate rectified multi-level/staircase waveform as presented and discussed in Chapter 4.

In this chapter, the proposed inverter circuit is simulated and practically implemented. The choice of simulation software to design the proposed inverter is reviewed and simulation results of the designed/proposed inverter are presented,

showing the THD measurement of the output voltage and current. The experimental result is also presented, showing the THD measurement of the output voltage and current to prove the correct operation of the designed/proposed inverter circuit. The proposed inverter is compared with 13-levels Cascaded H-bridge Multi-level Inverter (CHB-MLI) circuit topology and Switched-Capacitor-Boost Multi-level Inverter (SCB-MLI) in terms of harmonics distortion (THD) and number of components used.

## 5.2 Choice of Simulation Modelling Package

The simulation package is essential in examining the concept of many power electronics circuit design and operation. It is a computer simulation program that allows users to simulate circuit design and to observe output results in either tabular format or in plotted out graphics using its measurement tools. Many packages are available, such Matlab/SIMULINK, PSim, and OrCAD PSPICE. Matlab/SIMULINK is a system level simulation. It is a graphical user tool which allows the user to simulate by connecting blocks. This can act as an interface for embedded system electronics devices, such as microcontroller and Digital Signal Processing. PSim has integrated C-compiler, allowing the user to enter C-programming code without compiling it. Both PSim and Matlab have the ability to interact with C language. The choice of simulation package mainly depends upon the area of work and application. PSPICE stand for Simulation Program for Integrated Circuits Emphasis and is an analogue circuit simulator that allows multiple result plots (voltage, current, and power) to be observed simultaneously. As far as design at component level simulation is concerned, OrCAD PSPICE is superior in providing accurate modelling for inverter circuit design. PSPICE comprises of libraries of components according to manufacturer's

specification which can lead to obtaining realistic simulation results. It also contains an extensive library of commercial electric components. Hence, OrCAD PSPICE was adopted for the design and simulation of the proposed inverter circuit in this research.

### **5.3 Simulation of the Proposed Inverter Circuit using OrCAD PSPICE**

The proposed inverter circuit is designed and simulated using OrCAD PSPICE software in order to verify design topology and its operation. The proposed inverter performances are also assessed through this (measuring the quality of output waveform ( $V_{THD}$ ) and power losses). PSPICE software has the ability to perform a mathematical simulation of the circuit's behaviour, which enables computing the average value and root mean square (RMS) value of the voltage and current, and graphically displaying the output results faster. The transient analysis is conducted for viewing voltage and current with respect to time for this purpose. The Fourier analysis function is performed to measure THD performance of the proposed inverter. The only limitation observed in using PSPICE is the convergence problem. When giving some parameter component values and running the simulation for a specific time, the computation in PSPICE can have convergence problem.

### **5.4 Parameter of the Proposed Inverter Circuit**

The circuit parameter values and optimum switching frequency operation were adopted based on the relationship between output voltage THD and switching

frequency, derived from a comprehensive mathematical analysis (theoretical estimation) as conducted in Chapter 3. Tables 5-1 and 5-2 illustrate the calculated parameter values that can yield low-voltage THD ( $V_{THD}$ ). These values are used in proposed inverter circuit model in PSPICE simulation. The parameter components used in this simulation are modelling and components parts taken from the library in PSPICE software.

Table 5.1 Proposed inverter parameter for highly resistive load

Parameter	Symbol	Value
Input voltage	$V_{dc}$	60 volts
Inductor	$L$	$10 \mu H$
Inductor resistance	$R_1$	$1 \Omega$
Capacitor (in DSSC circuit)	$C_1$	$10 \mu F$
Smoothing Capacitor	$C_2$	$100 \mu F$
Resistive Load	$R_o$	$10 \Omega$

The passive components such as resistor, inductor, and inductor, as well as active components such as Power MOSFETs IRFZ34 switches and a diode, are placed into the proposed system schematic model from PSPICE software part list library.

Table 5.2 Proposed inverter parameter for highly inductive load

Parameter	Symbol	Value
Input voltage	Vdc	82 volts
Inductor	L	10 mH
Inductor resistance	R <sub>1</sub>	0.1 Ω
Capacitor (in DSSC circuit)	C <sub>1</sub>	10 μF
Smoothing Capacitor	C <sub>2</sub>	130 μF
Resistive Load	R <sub>o</sub>	0.932 Ω
Inductive Load	L <sub>o</sub>	84 mH

## 5.5 Simulation of the Designed Inverter System

The simulation of the proposed inverter system includes the single-phase inverter circuit and its control circuit as shown in Figures 5.1 and 5.2. This proposed inverter system has the ability to generate staircase/multi-level AC output voltage at fundamental line frequency (50 Hz). The designed inverter circuit is composed of switched-capacitor circuit (SCC) stage (resonant-based DSSC circuit) and inverting stage (H-bridge circuit). The modulation control for the proposed inverter system has hybrid switching operation (combined high and low switching frequency). Two power MOSFETs switches (S<sub>1</sub>) and (S<sub>2</sub>) of the resonant-based DSSC SCC are switched at a high switching frequency of 10 kHz. Meanwhile, the other four power MOSFETs switches (S<sub>3</sub> - S<sub>6</sub>) of the H-bridge circuit are switched at a fundamental line frequency of 50 Hz.

Figure 5.1 shows the control circuit used to obtain the switching control signals to be applied to each power MOSFETs switches in the proposed inverter. Figure 5.2 shows that the PSPICE simulation result; control signal derived from the control circuit

includes; (a) carrier signals and the multi-level DC reference signal & (b) to (e) control signals ( $S_1$  to  $S_6$ ). The variable switch duty cycle PWM control technique is used to generate the switching pattern of the control signals ( $S_1$  and  $S_2$ ). These are obtained by comparing multi-level DC reference signal ( $V_{ref}$ ) with a high-frequency triangular carrier signal ( $V_{tri}$ ). Two control signals ( $S_1$  and  $S_2$ ) are generated by the control circuit and applied to the two power MOSFETs switches ( $S_1$ ) and ( $S_2$ ) in the resonant-based DSSC switched-capacitor circuit. Control signals ( $S_3$  to  $S_6$ ) are used to control the MOSFETs switches in the H-bridge circuit.

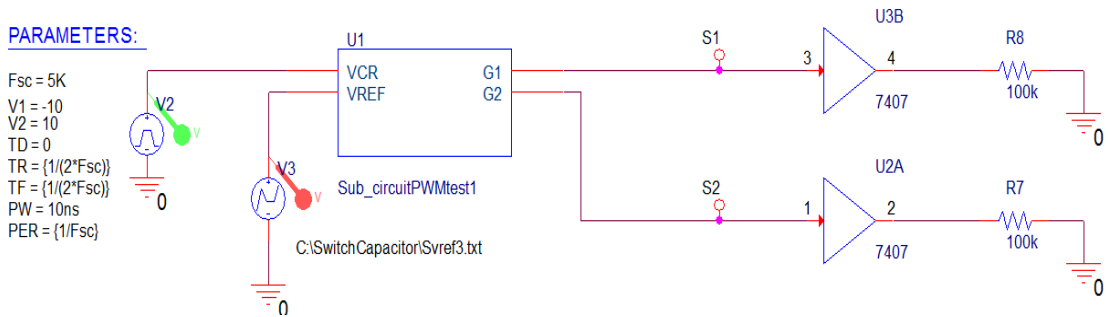


Figure 5.1 Control Circuit

The following subsection shows that the simulation of the proposed inverter system is conducted under two different output loads: pure resistive load and highly inductive load. The simulation result of the proposed inverter system includes the rectified multi-level/staircase voltage waveform, output voltage and current waveform, and frequency spectrum of the output waveform (using Fourier fast transform (FFT) function in PSPICE).

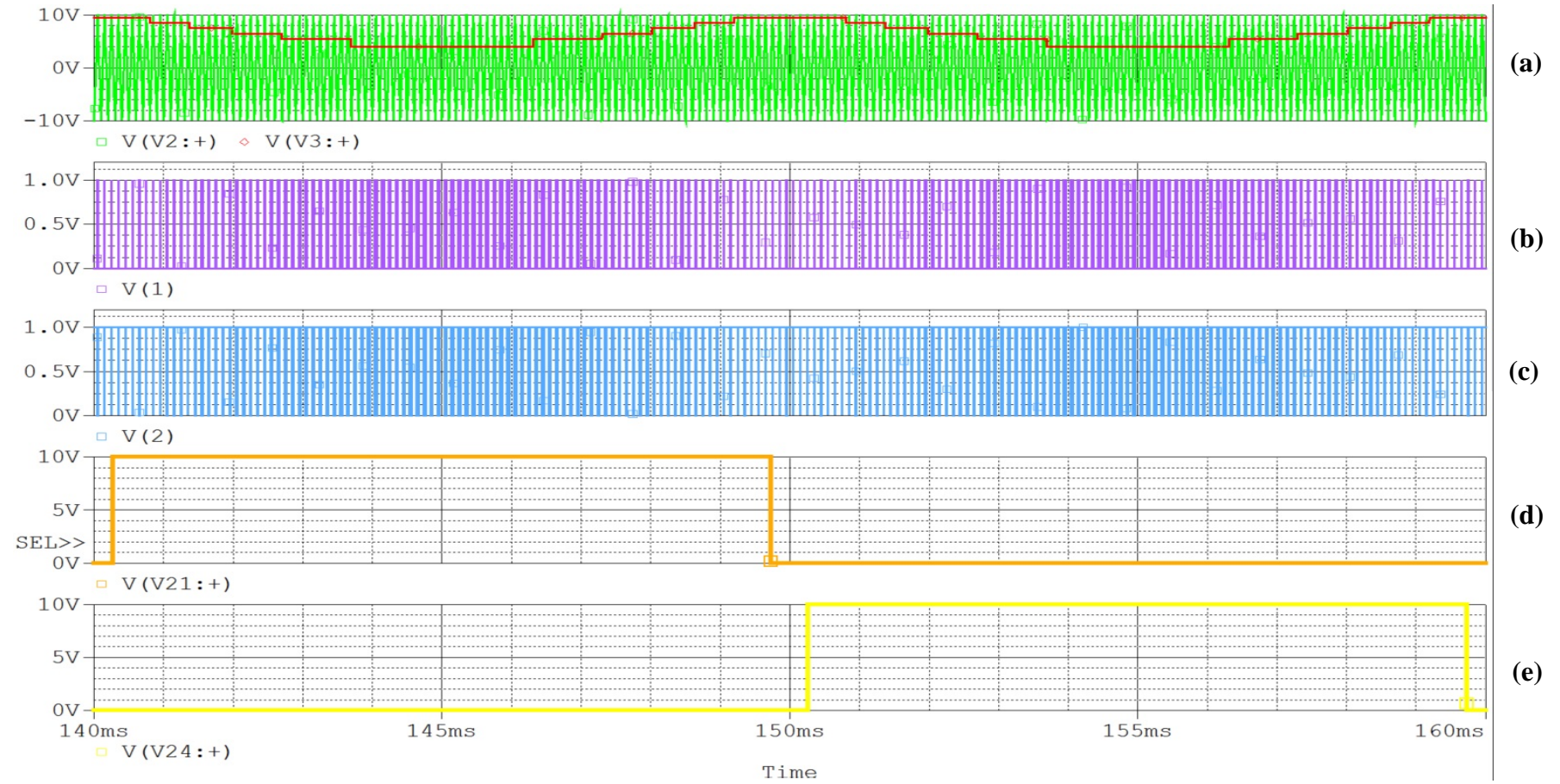


Figure 5.2 PSPICE switching pattern result: (a) carrier and reference signals & (b) to (e) control signals

### 5.5.1 Pure Resistive Load

The proposed inverter circuit with pure resistive load simulated in PSPICE is shown in Figure 5.3.

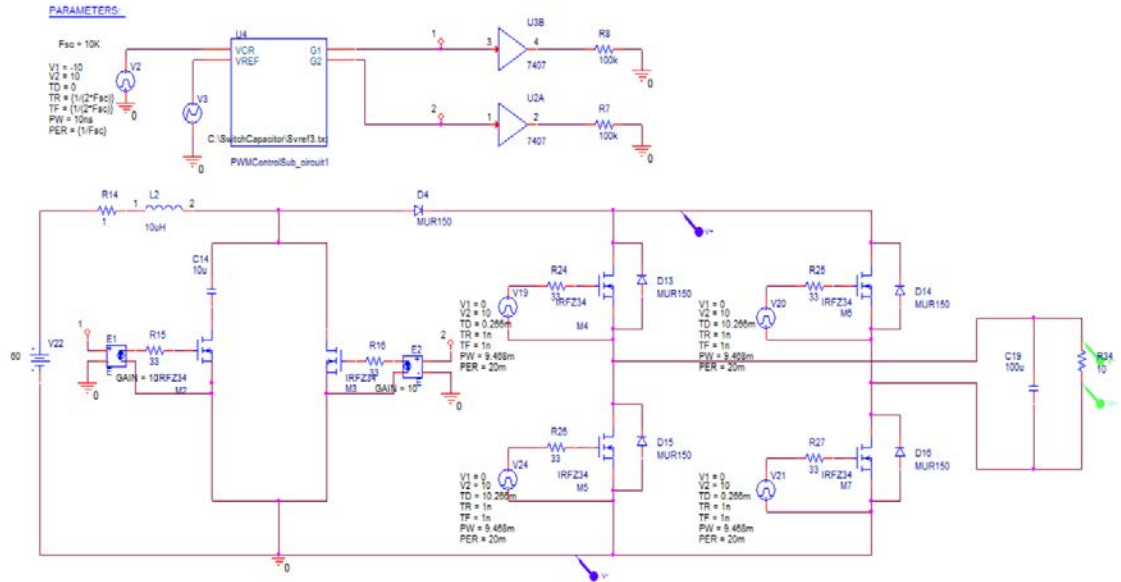


Figure 5.3 Proposed inverter circuit with pure resistive load  $R_o = 10 \Omega$

Figure 5.4 shows the simulation result; the rectified voltage across H-Bridge, output voltage, and current for a purely resistive load. The output voltage is sine wave modulated with an amplitude of 33.8 V RMS at 50 Hz output frequency. The RMS output current is 3.38 A. The output power is 114 Watt and in this case the proposed inverter has efficiency of 70 %.

Figure 5.5 shows the output voltage and current and the Fourier Fast Transform (FFT) of the output voltage and current. The magnitude distortion in both voltage and current in terms of harmonics order in harmonics spectrum are almost equaled. The THD of the output voltage  $V_{THD} = 4.6\%$  and current harmonics  $I_{THD} = 4.5\%$ . There are two bands of frequency are identified in the output voltage at chosen R, L and C value. A lower-order harmonic near the fundamental and a high-order harmonic appears around

switching frequency and its multiple. The amplitude of fundamental output voltage is 46.9 Volt. The lower-order harmonics are less than 8 % of the amplitude of fundamental output voltage,  $V_o$ . The amplitude of the 3<sup>rd</sup> harmonic is 2.19 Volts, which is 5 % of the fundamental output voltage respectively. The amplitude of 200<sup>th</sup> of the high-order harmonics are about 3 % and 2 % of the fundamental output voltage, as shown in Figure 5.6 and 5.7.

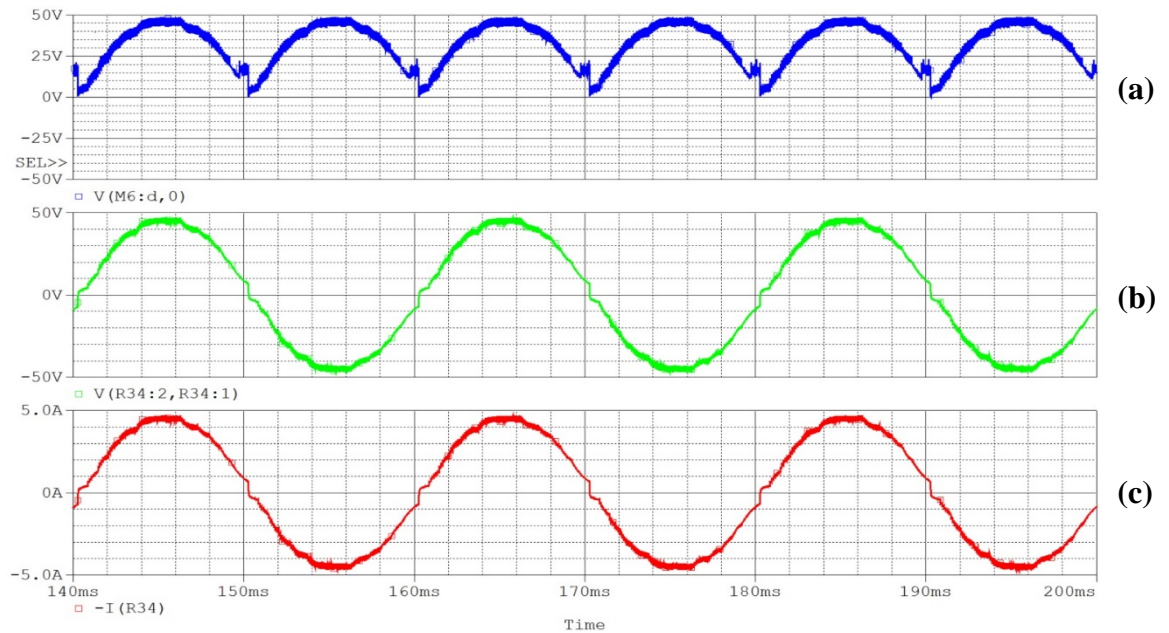


Figure 5.4 Proposed inverter simulation result (for resistive load): (a) rectified voltage across H-Bridge, (b) output voltage and (a) output current

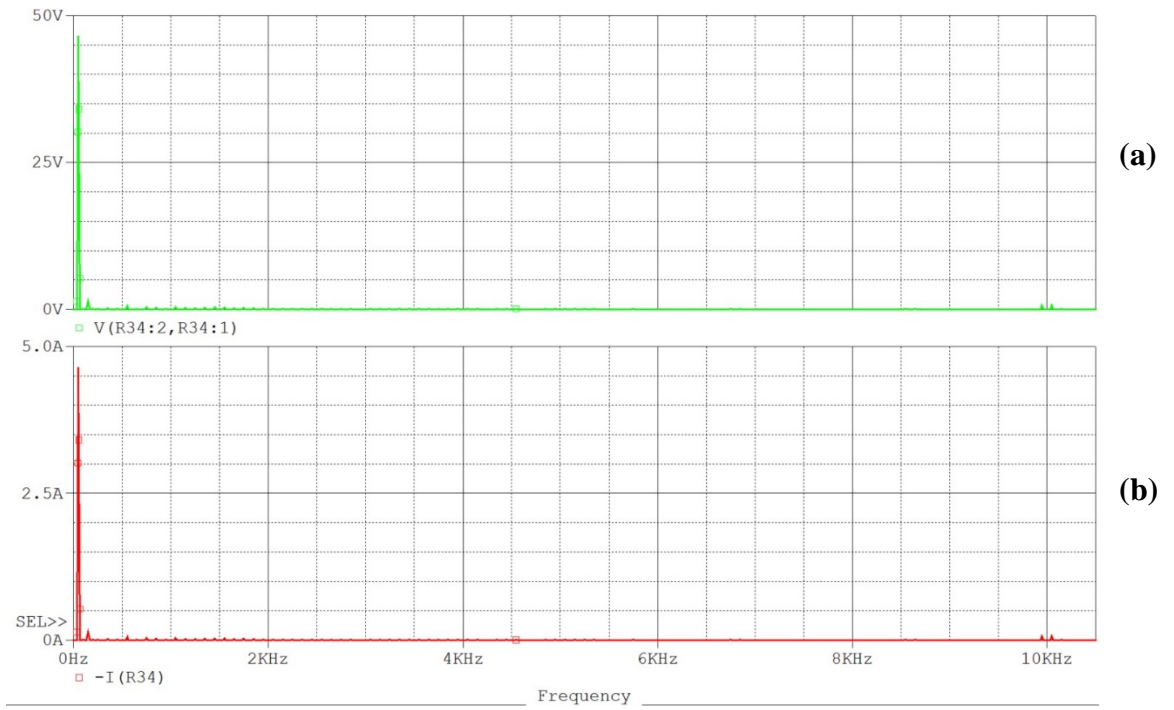


Figure 5.5 FFT analysis of the (a) output voltage and (b) output current spectrum (for resistive load)

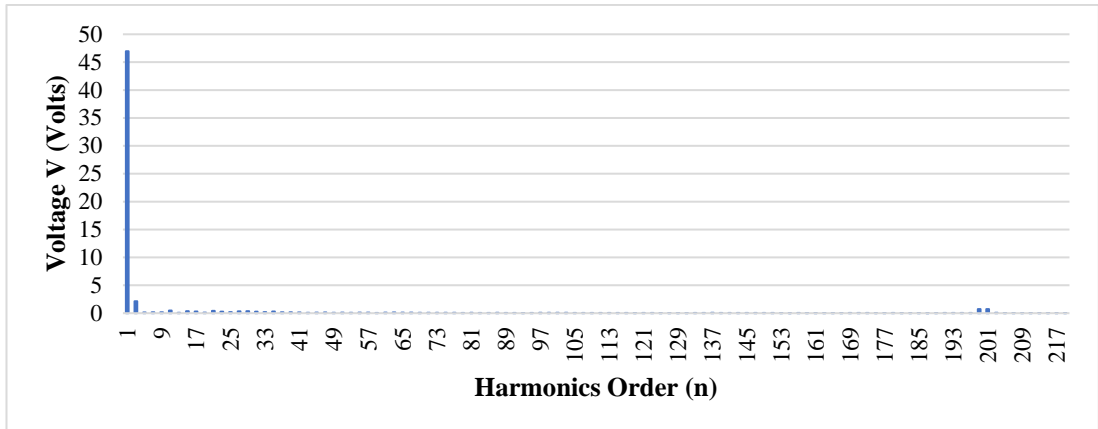


Figure 5.6 FFT of the output voltage of the proposed inverter for purely resistive load (Simulation)

The reasons for the lower-order harmonics presented in the output voltage spectrum in case for pure resistive load are mainly due to non-zero value of the voltage across the capacitor when the H-Bridge swaps output polarity and non-unity load power factor (Georgakas, Vovos & Vovos 2014) and (Marouchos et al. 2015).

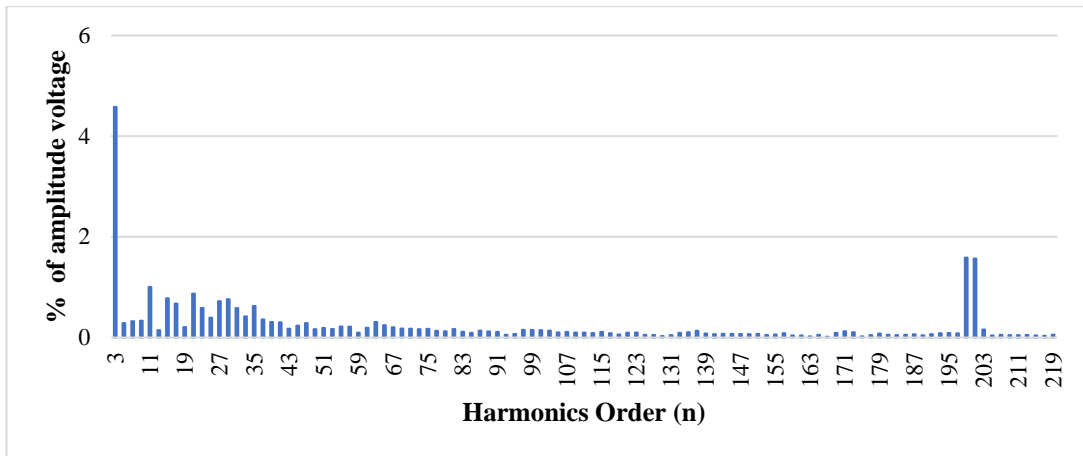


Figure 5.7 FFT of the output voltage of the proposed inverter for purely resistive load (Simulation)

The low-order harmonics can be minimised by optimising the switching control pattern. The higher-order harmonics can be further reduced by increasing the switching frequency but the switching losses must be compromised. The following subsection shows the losses in the proposed inverter under pure resistive load

#### **5.5.1.1 Losses in the proposed inverter circuit for purely resistive load.**

The Power MOSFETs IRZ34 switches and fast recovery diode MUR150 are used in this simulation. Only two MOSFETs switches ( $S_1$  and  $S_2$ ) are switched at a high switching frequency of 10 kHz and other four MOSFETs switches ( $S_3$  to  $S_6$ ) are switched at fundamental line frequency of 50 Hz. The power losses are computed using the following equation.

Power dissipated in  $R_1$

$$P_{d(R1)} = I_{in(\text{avg})}^2 \times R_1 \quad (5.1)$$

Switching losses in MOSFETs switch  $S_1$

$$P_{sw(S1)} = \frac{1}{2} \times V_{ds(\text{RMS})} \times I_{ds(\text{RMS})} \times (t_{on(ns)} + t_{off(ns)}) \times F_{sw} \quad (5.2)$$

Conduction losses in MOSFETs switch  $S_1$

$$P_{cond(S1)} = I_{ds(\text{RMS})}^2 \times R_{ds\text{on}} \quad (5.3)$$

Conduction losses in a Diode

$$P_{cond(D)} = I_{d(\text{RMS})}^2 \times R_d \quad (5.4)$$

Total inverter losses

$$P_{totlosses} = P_{d(R1)} + P_{totsw(S1 \text{ to } S6)} + P_{totcond(S1 \text{ to } S6)} + P_{cond(D)} \quad (5.5)$$

The total power loss of the proposed inverter under pure resistive load is 551.4 Watt which 32 % of the total power delivered to load. More than 50 % of the power losses are the power dissipated in input resistance ( $R_1$ ). About 35 % and 7 % of the losses come from conduction losses in power MOSFETs switches and a diode, as shown in

Figures 5.8 and 5.9. The comparison of losses in each power MOSFETs switch in the proposed inverter is presented in Figure 5.10. The conduction loss is higher than switching loss, which is mainly due to anti-parallel PWM switching control. Every time ( $S_2$ ) is switched ON for certain switch conduction time, the (R-L) circuit is formed and the inductor is charged to the input DC voltage. High conduction loss in switch ( $S_2$ ) is due to high inductor current and high conduction period. The proposed inverter has efficiency of nearly 70 %.

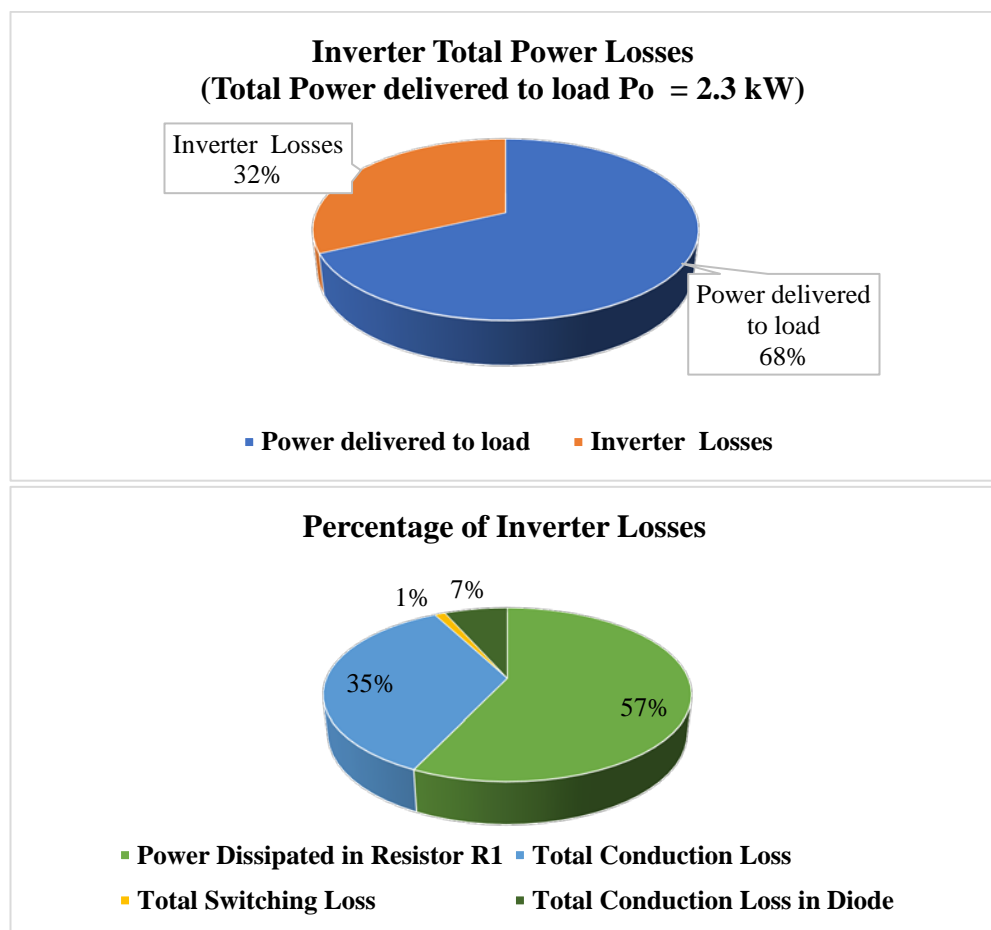


Figure 5.8 Total power losses in the proposed inverter

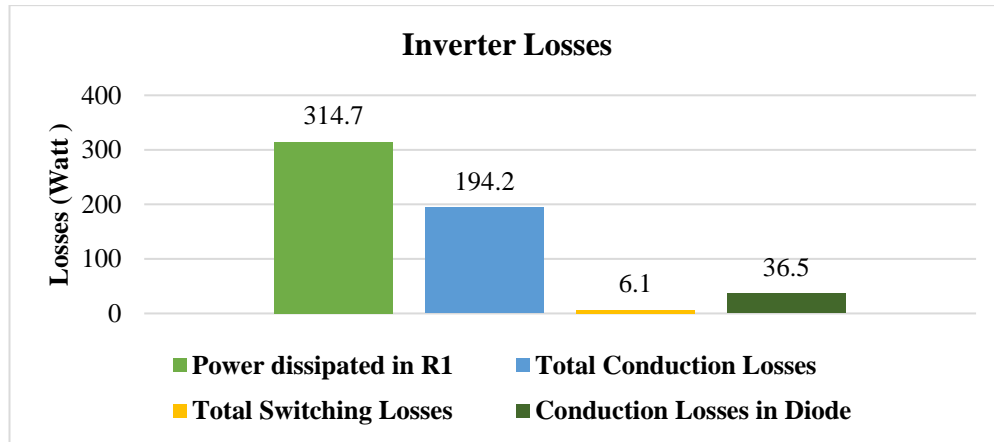


Figure 5.9 losses in the proposed inverter system

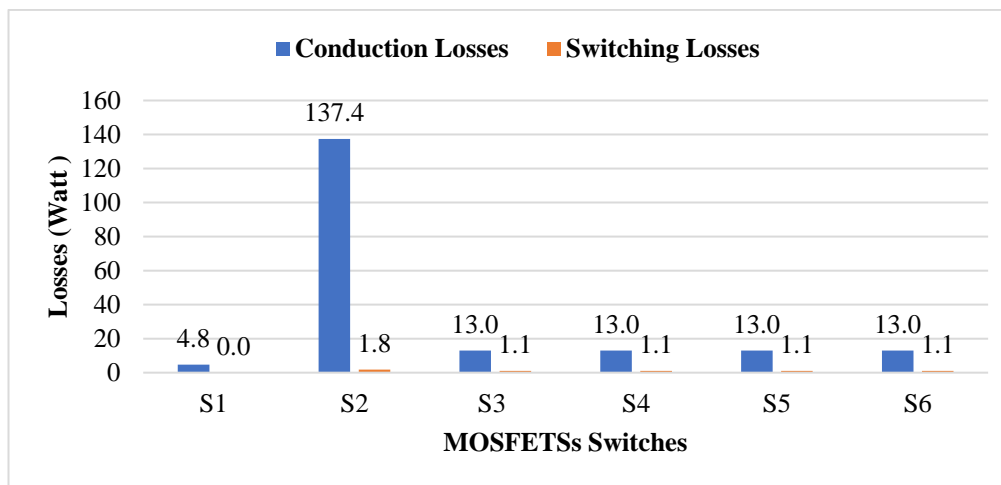


Figure 5.10 Losses in MOSFETs Switches

### 5.5.2 High Inductive Load

The proposed inverter circuit with highly inductive load ( $R-L$  load  $R_o = 0.932 \Omega$  and  $L_o = 84 \text{ mH}$ ) is simulated in PSPICE is shown in Figure 5.11. The parameter value of  $R_1 = 0.1 \Omega$ ,  $L = 10 \text{ mH}$ ,  $C_1 = 10 \mu\text{F}$ ,  $C_2 = 130 \mu\text{F}$  and  $R-L$  load = ( $R_o = 0.932 \Omega$  and  $L_o = 84 \text{ mH}$ ). The output voltage and frequency are 250 Volt and 50 Hz.

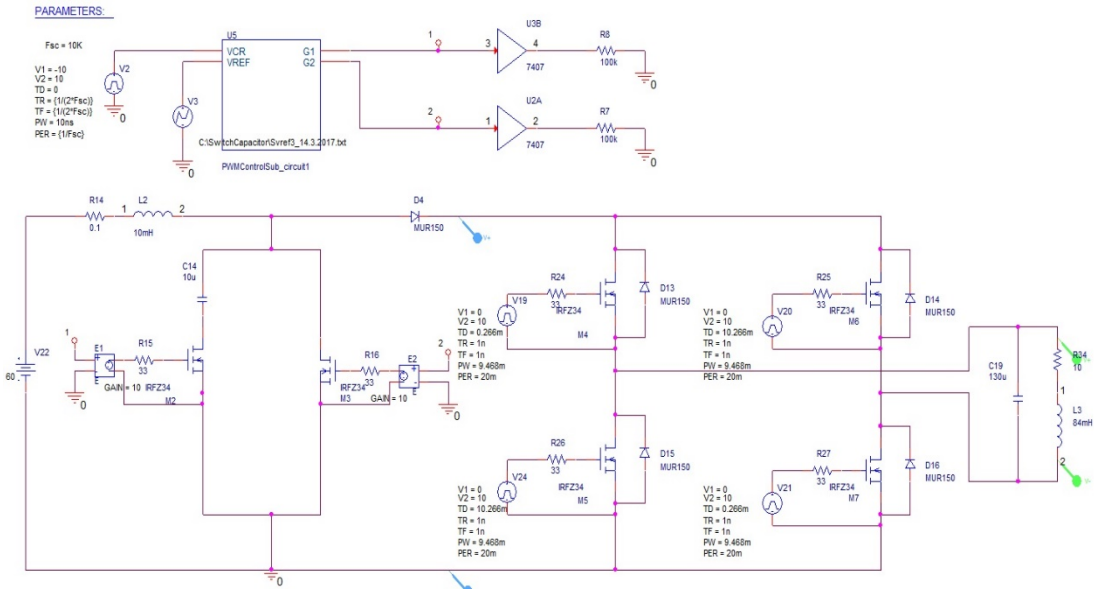


Figure 5.11 The proposed inverter circuit with highly inductive load.

Figures 5.12 and 5.13 show the simulation result; the rectified sine voltage across H-Bridge, output voltage and current for a highly inductive load. The output voltage is nearly a sine wave with an amplitude of 269 V RMS at 50 Hz output frequency. The RMS output current is 9.3 A. The output power is 2.3 kW.

Figure 5.14 shows the output voltage and current and the Fourier Fast Transform (FFT) of the output voltage and current. The magnitude distortion in both voltage and current in terms of harmonics order in harmonics spectrum are almost equal. The THD of the output voltage  $V_{THD} = 1.8\%$  and current harmonics  $I_{THD} = 1.6\%$ . The amplitude of fundamental output voltage is 381 Volt. The lower-order harmonics near the fundamental are less than 3 % of the amplitude of fundamental output voltage,  $V_o$ .

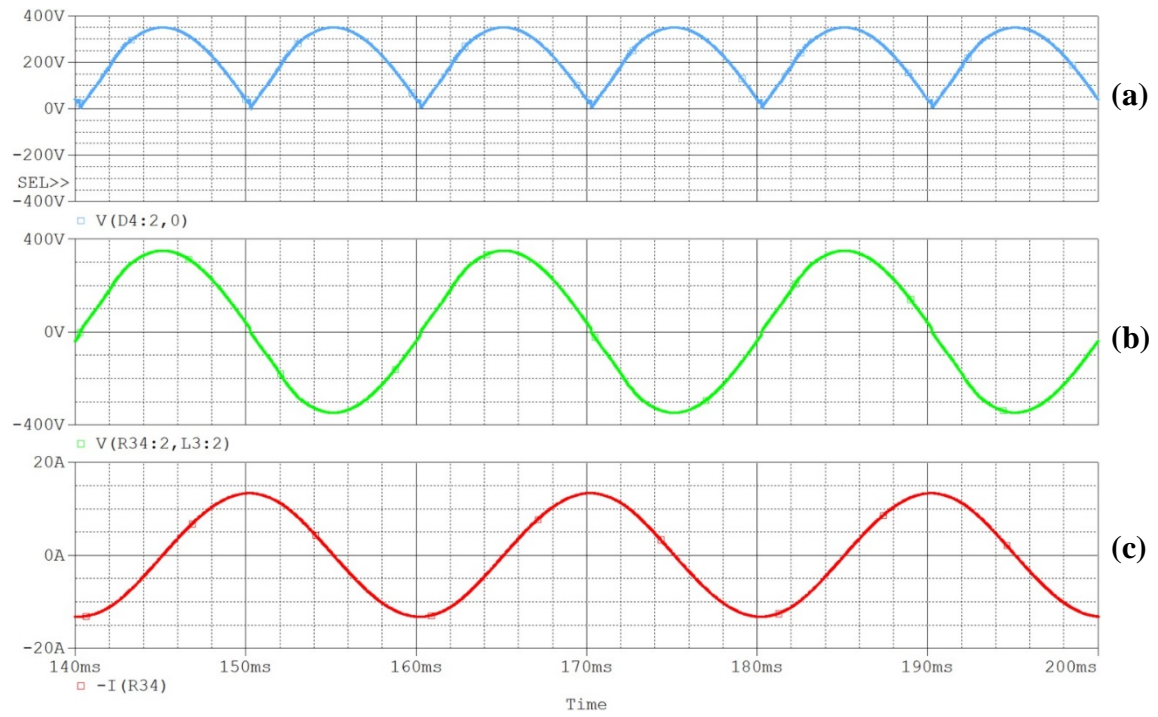


Figure 5.12 Proposed inverter simulation result (for inductive load): (a) rectified voltage across H-Bridge, (b) output voltage and (a) output current

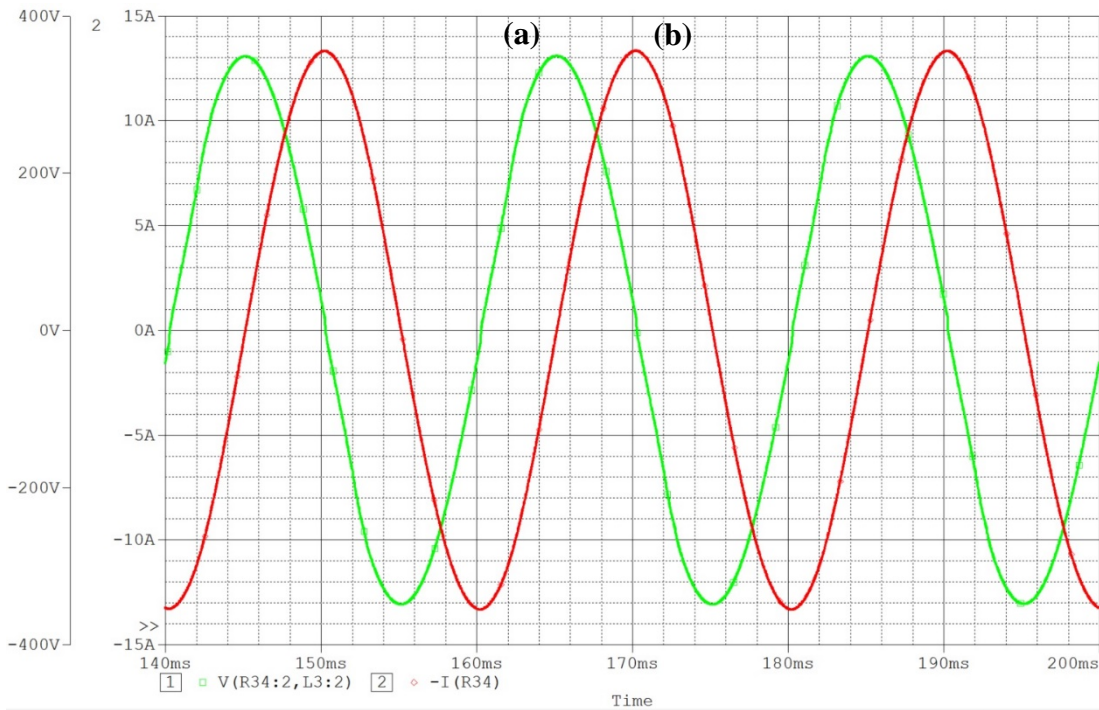


Figure 5.13 Proposed inverter simulation result (for inductive load): (a) output voltage and (b) output current

The amplitude of 3<sup>rd</sup> and 5<sup>th</sup> harmonics are 10 Volt and 9 Volt which 2.63 % and 0.1 % of the fundamental output voltage respectively. The amplitudes of the high-order harmonics are less than 1 % of the fundamental output voltage as shown in Figure 5.14. This means the highly inductive load acts as a passive filter at the output of the proposed circuit.

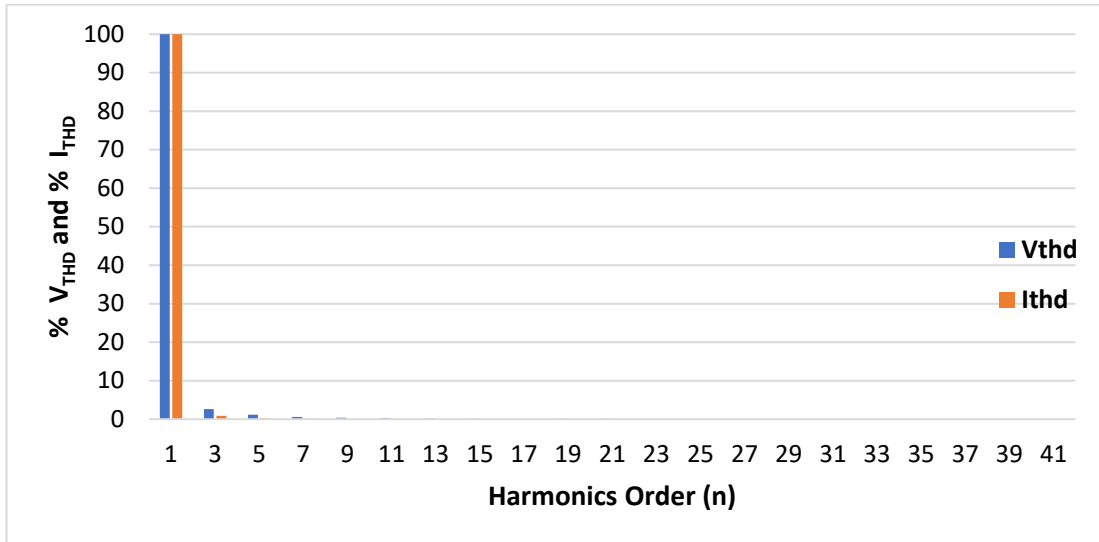


Figure 5.14 FFT of the output voltage of the proposed inverter for highly inductive load (Simulation)

## 5.6 Practical Implementation of the Proposed Inverter

The practical experiment has been implemented for the proposed inverter circuit. Figure 5.15 shows the overall experimental set up of the proposed system on the working bench, including Digital Oscilloscope and DC Power supplies. The proposed inverter circuit topology is constructed in the laboratory to prove the correct operation according to the theoretical relation and simulation conducted previously. The practical results i.e. output voltage waveform and its harmonics spectrum were obtained for two different load conditions using different component parameter value as shown in Table 5.3. The experiment setup of the proposed inverter circuit has been

implemented in the laboratory which is based on the design the PSPICE design simulation. This is to verify its performance in terms of harmonics distortion in output voltage and current. The detailed experiment setup of the proposed inverter, shown in Figure 5.16 illustrates the control signal and inverter circuit. The proposed inverter is prototyped using power MOSFET switches (IRFZ34). Each power switch is fed by switching pattern signal through a driver circuit (which contains an opto-isolator (6N137) and a MOSFETs driver circuit (ICL7667)). Microcontroller Arduino Uno is used to output the switching pattern signals to a driver circuit via Arduino Uno output port.

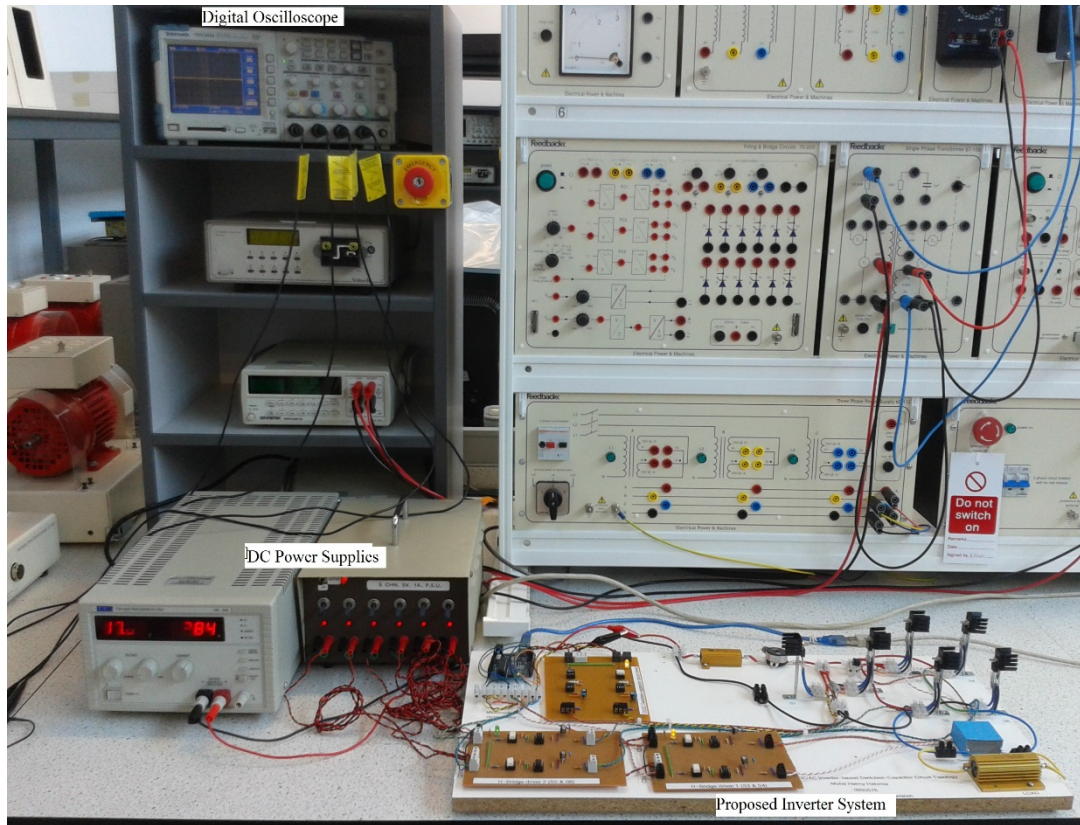


Figure 5.15 The experimental setup showing the proposed inverter system and its associated equipment.

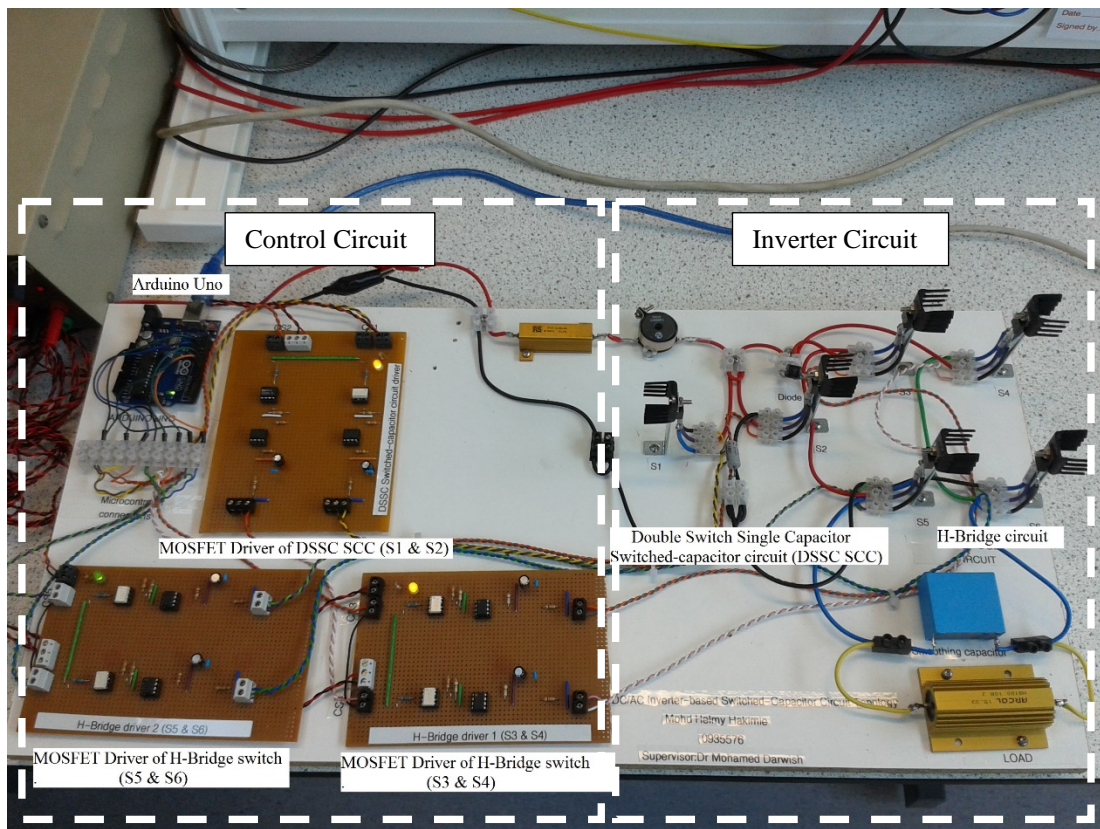


Figure 5.16 The proposed system showing control circuit (left) and inverter circuit (right)

Microcontroller Arduino UNO is used as a controller which is programmed using Arduino Software. A simple C language program has been written to generate the desired control signal pattern as shown in Appendix A. The voltage and current are measured using voltage and current probes which are connected to Textronix TPS2024 Digital Oscilloscope. The output voltage and current waveforms and its harmonics spectrum are monitored on Digital Oscilloscope and the screen shots results are captured.

The experimental circuit is built based on the design in simulation. However, due to practical laboratory limitations:

- The output load power was downscaled to smaller power so as to illustrate the concept of the proposed inverter operation.
- It was not possible to use the exact component value of R, L, and C used in the simulation due to a limited range of component values available in the lab. Hence, for practical set-up purposes, different parameter component values were used as shown in Table 5.3.

The following figure 5.19 to 5.22 show the images of the experimental results of the proposed inverter, which includes the control signals waveform, output voltage, and output current waveform with its output frequency spectrum

Table 5.3 Parameter component values (Experimental)

No.	Component	Value
1.	DC Voltage	20 Volts
2.	Microcontroller (Arduino)	UNO
3.	Two MOSFETs switch in DSSC circuit	MOSFETs IRFZ34
4.	H-Bridge Circuit (four MOSFETs switch and four drivers)	MOSFETs IRFZ34
5.	Ultrafast-Recovery Diodes	MUR150
6.	Inductor	42 uH
7.	Capacitor	10 uF
8.	Load Resistance	10 Ω

Figure 5.19 shows two switching pattern signals in anti-parallel waveform used to feed to the gate terminal of the two power MOSFETs IRFZ34 switches (labelled as S<sub>1</sub> and S<sub>2</sub> in circuit diagram Figure 4.2) of the DSSC SCC circuit.

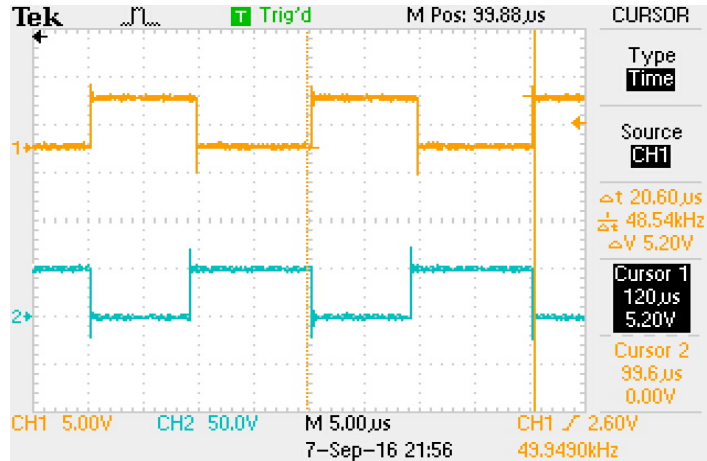


Figure 5.15 Switching pattern control signals

The experiment is conducted to measure the harmonics distortion in proposed inverter output for operating under two different load conditions. The first case is when a purely resistive element is applied at output load and the second case is when a highly inductive element is applied. The following figures show the images of the experimental results of the voltage and current waveform captured from the oscilloscope. Figure 5.18 and 5.19 show the output voltage and current waveforms measured across a purely resistive load of  $10 \Omega$  measured result from oscilloscope. The output voltage is stepped sinusoidal waveform with 15.9 Volts peak-to-peak output voltage. The measured RMS output voltage  $V_o$  is 11.3 Volts. The output voltage frequency is 50 Hz and the output load power is 12.77 Watt.

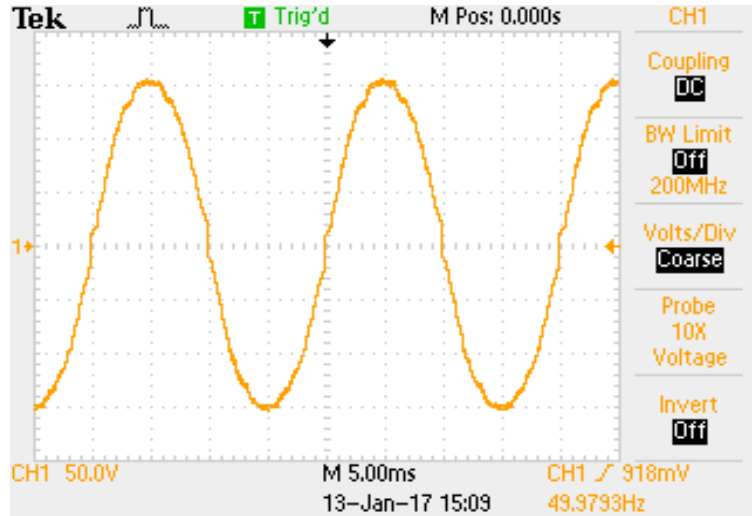


Figure 5.16 Measured output voltage waveform (resistive load)

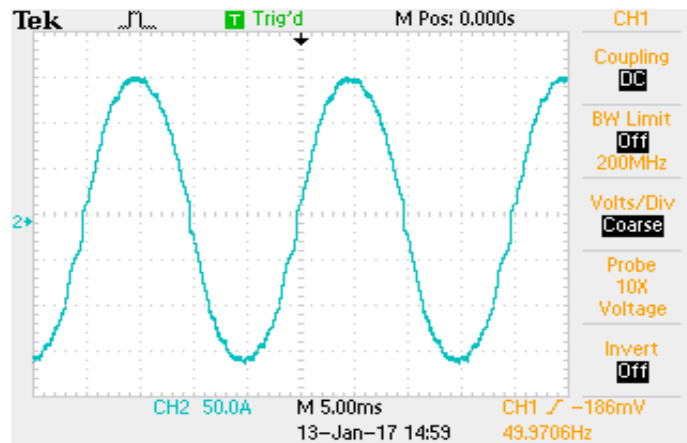


Figure 5.17 Measured output current waveform (resistive load)

Figure 5.20 shows the output voltage harmonics spectrum of the proposed inverter measured using FFT function in the oscilloscope. With only single smoothing capacitor  $C_2$  connected in parallel with the output pure resistive load, the measured total harmonic distortion of output voltage  $V_{THD}$  waveform is 5.65 %. The value of fundamental magnitude  $V_{o1}$  is 11.13 Volt. In this case, the amplitude value of lower-order harmonics is quite high. The percentage of harmonic magnitude for 3<sup>rd</sup>

harmonics order is 4.6 % of the fundamental magnitude and other low-order harmonics are small, less than 1 % of the fundamental magnitude.

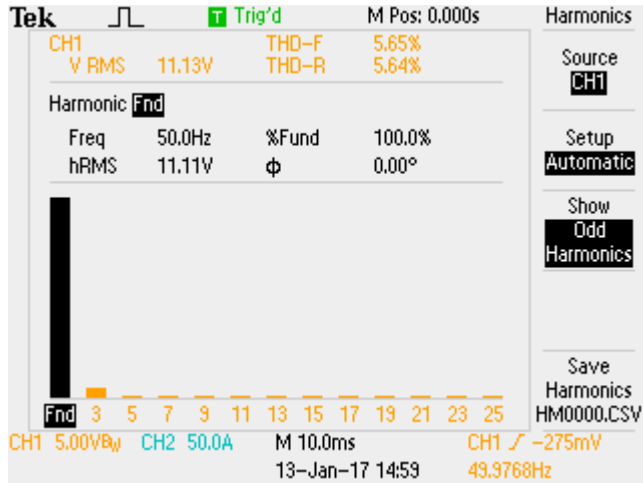


Figure 5.18 Measured output voltage harmonics spectrum (resistive load)

Table 5.4 Amplitude of output harmonics (purely resistive load)

Harmonics Order	Harmonics magnitude (in %)
3	4.6
5	0.3
7	0.3
9	0.3
11	1.0
13	0.2

Figure 5.21 shows the output voltage waveform across a highly inductive load,  $Z = 20 + j 62.8\Omega$  measured result from oscilloscope. The output voltage is a sinusoidal waveform with 15.9 Volts peak-to-peak output voltage. The measured RMS output voltage  $V_o$  is 11.2 Volts. The output voltage frequency is 50 Hz. The apparent power is 5 VA.

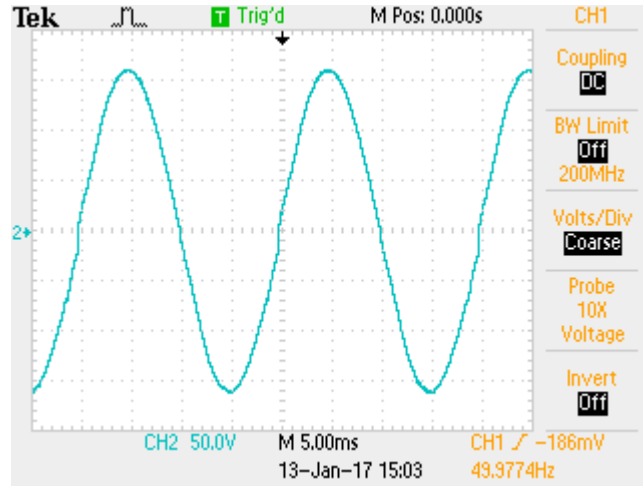


Figure 5.19 Measured output voltage waveform (highly inductive load)

Figure 5.22 shows the output voltage harmonics spectrum of the proposed inverter measured using FFT function in oscilloscope. The total harmonic distortion of output voltage  $V_{THD}$  waveform is 3.4 %. The value of fundamental magnitude  $V_{o1}$  is 11.15 Volt. In this case, the amplitude value of lower-order harmonics is quite high. The percentage of low-order harmonics is small, less than 2 % of the fundamental magnitude.

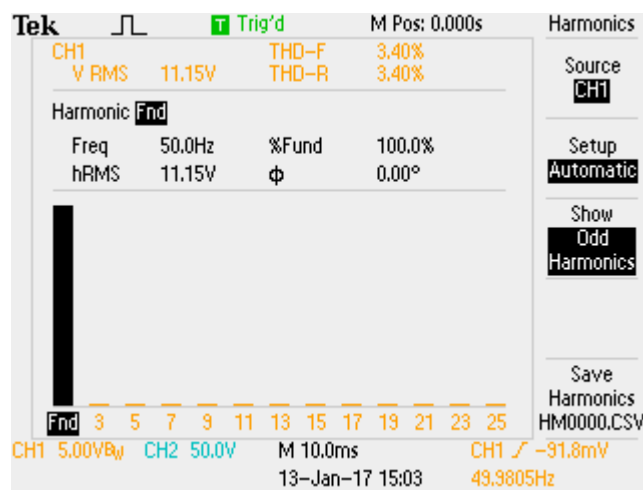


Figure 5.20 Measured output voltage harmonics spectrum (highly inductive load)

Table 5.5 Amplitude of output harmonics (highly inductive load)

Harmonics Order	Harmonics magnitude (in %)
3	1.9
5	0.3
7	0.6
9	0.6
11	0.4
13	0.2

Figures 5.18 and 5.20 show the proposed inverter output voltage and its output frequency spectrum which represents the experimental results for operating resistive load. Only a single smoothing capacitor is used which is connected in parallel to the load, and the measured THD of the output voltage ( $V_{THD}$ ) across pure resistive load was found to be 5.65 %, which slightly deviated from both the theoretical estimated results and the simulation results, which are 4.6 % as shown in Figure 5.20. The slight deviation of experiment result is due to different parameter component value was used for practical set-up. In addition, the deviation is also due to the assumption to neglect the inductor resistance, the ohmic resistance of the wires and the bleeder resistance in capacitor of the proposed/designed inverter circuit. Figure 5.21 and 5.22 shows the proposed inverter output voltage and its output frequency spectrum which represents the experimental results for operating highly inductive load. The output voltage and current waveform is smooth sinusoidal which the measured  $V_{THD}$  was found to be 3.4 % as shown in Figure 5.20. This is because the inductor acts as passive filter. Therefore, this proposed inverter is ideal to operate with an inductive load. However,

it can be seen from the experimental results that the measured THD of the output voltage waveforms ( $V_{THD}$ ) of the proposed inverter shows agreement and validation with the theoretical concept and estimation calculation results in terms of the THD performance and operation as presented in Chapter 4, as well as the simulated result.

## 5.7 Practical Comparison amongst DC/AC Inverter Topologies

Table 5.6 shows the comparison amongst different types of DC/AC Inverter circuit; the traditional three-levels PWM inverter, classical Cascaded H-Bridge Multi-level inverter (CHB-MLI) circuit topology (Alamri, Darwish 2015), Switched-Capacitor Boost Multi-Level Inverter (SCB-MLI) circuit topology (Chan and Chau 2007) and the proposed inverter (A DC/AC Inverter based Switched-Capacitor topology with reduced number of component). The performance each of topologies are compared in terms of Total Harmonic Distortion (THD), rating output power and Efficiency as shown in Table 5.6. These inverter circuit topologies were also compared in terms of the number of component used for generating thirteen-levels of output voltage. These circuits are compared in almost same condition for producing a thirteen-levels of output voltage, rating output power and without use of filter at output.

Table 5.6 Experimental comparison between proposed inverter circuit topology and other inverter topologies performance for thirteen-levels output voltage

Topology	Number of voltage levels m	Vdc V	Output Power Watt	Efficiency	THD %
PWM Inverter (VSI)	3	60	40	93 %	76
CHB-MLI	13	60	40	93 %	2.01
SCB-MLI	13	60	40	72%	6.3
Proposed Inverter	13	60	40	70%	5.64

Table 5.7 Comparison between proposed inverter and other multi-level inverter topologies in term of components count for thirteen-levels output voltage

Topology	DC sources	Inductor	Capacitor	Diode	Power Switch	Total number of Component
PWM Inverter (VSI)	1	0	0	0	4	4
CHB-MLI	6	0	6	24	24	54
SCB-MLI	1	1	2	3	11	17
Proposed Inverter	1	1	2	1	6	13

## 5.8 Discussion

The classical CHB-MLI inverter topology and the recent SCB-MLI inverter topology can obtain low THD and perform at high efficiency performance as illustrated in Table 5.6. However, most of these circuit topologies require large number of components i.e. power switches, diodes and capacitors, and/or isolated DC sources as illustrated in Table 5.7. The proposed inverter can achieve low THD with less number of component used in comparison to the CHB-MLI and SCB-MLI topology. The output voltage shape is highly depending on the component parameter value, type of semiconductor device used and type of output load. The output voltage is also sensitive to the parasitic resistance in passive (capacitor and inductor) and active (Power semiconductor switch) components. The efficiency of the practical experimentation of the proposed inverter circuit is 70 %. This proposed circuit also can operate with highly inductive load which can results in smoother output waveform and lower THD in output voltage and current waveform.

## 5.9 Summary

This chapter presents the simulation and practical hardware implementation of the proposed inverter circuit. The proposed inverter circuit was designed using the OrCAD PSPICE simulation package. The simulation shows the ability of the proposed inverter to generate staircase/multi-level AC output with low THD that can be achieved without increasing the number of components. The results from the practical, simulation, and theoretical estimations are consistent. This verified that the proposed inverter circuit has the ability to generate near AC output voltage waveform with low

harmonics distortion using fewer components (power switches and capacitors). The comparison has been made between the proposed inverter topology and the classical multi-level inverter topology (Cascaded H-Bridge MLI) in terms of THD performance and component count. In the final chapter, the conclusions and suggestions of future works are presented.

# **Chapter 6 Conclusions and Future Work**

## **6.1 Conclusions**

In this thesis, a new optimum DC/AC inverter based switched-capacitor circuit with reduced component count was proposed. The following objectives have been conducted to achieve the research aim where the contribution of knowledge in the field of DC/AC inverters is described:

1. A critical literature review of DC/AC inverters, conventional PWM, classical, and newly-evolved multi-level topologies was presented, showing the advantages and disadvantages of each topology. In addition, the review on the available voltage boosting technique was presented.
2. The weaknesses of each well-known classical PWM and multi-level DC/AC inverter topologies covered in the literature were identified. The classical PWM inverter topologies' limitations are associated with high total harmonics distortion and high power losses. Meanwhile, classical multi-level DC/AC inverter topologies are associated with a large number of power semiconductor switches, diodes, capacitors, and isolated DC sources. This is to achieve high output voltage and also to increase the number of levels (high-voltage resolution) so that low output voltage THD can be obtained. Due to many advantages, multi-level topology is preferred than traditional three-levels PWM topology.

3. A review on the available voltage boosting technique was conducted. Many efforts have made to integrate switched-capacitor circuit (SCC) techniques for boosting voltage. The advantages of this technique can boost voltage and/or varying voltage with a reduced number of multiple isolated DC input sources. The decision was made to select SCC as the preferred boosting technique. The SCC is a cell-based structure which is easy to integrate into other circuit structures and provides high voltage gain/step-up ability.
4. Switched-capacitor circuit topologies have been examined and other voltage boosting techniques have been reviewed for voltage gain and varying voltage ability. Two types of mathematical analysis of the resonant-based DSSC SCC were carried out. The theoretical relationship between effective capacitance and duty-cycle, and the relationship between voltage across capacitor and duty cycle were estimated. It was concluded that with varying duty-cycle the DSSC circuit varies the capacitance value. It was also found that the voltage across capacitor varies with varying duty-cycle. By appropriate duty cycle switch control applied to the associated power switches, this configuration exhibits voltage gain and regulating voltage abilities. This characteristic lead to the formation of rectified staircase/multi-level voltage waveform. This configuration has fewer power switches and capacitors components which may have less power loss results in an improvement of the efficiency of the system.
5. Other voltage boosting techniques (magnetic couple and multi-stage booster) were not discussed in detail and selected due to their bulky and inefficient system. However, they have high-voltage boost voltage ability. The SCC was found to be suitable as part of a proposed inverter system due to high-voltage

gain and varying voltage ability. The other resonant-based SCC configurations were not discussed in detail due to them being unsuitable for producing multi-level voltage waveform with duty-cycle controlled applied. The DSDC configuration does not have varying voltage ability. In SCCC configuration, short-circuit problems represent a major drawback. It can occur when a switch is closed while voltage across capacitor has not reached zero. Triplen configuration may have varying voltage ability. However, it is composed of many power switches which added to the power losses. Also, high power dissipation in branch auxiliary resistors may degrade the overall system efficiency. This represents a major drawback of this configuration.

6. DC/AC inverter-based switched-capacitor circuit topology with reduced number of components was designed/introduced. The circuit configuration and modulation control technique were designed, showing the integration of a DSSC configuration type of SCC with variable duty-cycle control technique into a single-phase current source inverter (CSI) topology. The principle operation, design procedure, and analysis were presented.
7. A mathematical derivation was developed for the designed inverter circuit showing the design procedure leading to the formation of the staircase/multi-level AC output voltage waveform. During the positive cycle of output waveform, a rectified near sine (staircase/multi-level) can be first formed/shaped by controlling the DSSC SCC with variable duty-cycle control technique in specific switching time pattern. This rectified staircase/multi-level is then transformed into sinusoidal AC waveform during the negative cycle. To

obtain low THD of AC output voltage waveform, the best switching time or angle is determined by using the Half-Height method. This method is selected due to simple way to arrange switching angle according to the sine function. The formation of this rectified waveform is well-accorded to the estimated relationship (between capacitor voltage and duty-cycle) which was conducted earlier. Smoother waveform of rectified staircase/multi-level is obtained by narrowing the pulse width signal applied to control switches. This is achieved by operating switches of the selected switched-capacitor circuit (resonant-based DSSC circuit) at high switching frequency. Smooth rectified staircase waveform can lead to obtaining low THD of AC output voltage of the designed inverter. Also, only single smoothing capacitor is used at output which act as output filters. For these reasons, the decision was made for the selected switched-capacitor circuit with variable duty-cycle controlled to operate at high switching frequency.

8. The theoretical relationship between voltage THD and switching frequency of the selected switched-capacitor circuit (resonant-based DSSC circuit) was estimated. The optimum switching frequency that can yield was identified from this theoretical estimation. However, switching losses can increase in direct proportion with switching frequency. The decision of optimum switching frequency was made by taking into consideration harmonics distortion and switching losses where both of them must promise. To realise the variable duty-cycle control technique, the open-loop control logic circuit, which provides the switching timing control pattern, is presented.

9. An investigation has been conducted on commonly used power electronics simulation software packages for designing and simulating electronics circuits. OrCAD PSPICE and Psim software packages were identified as two best alternatives to use. OrCAD PSPICE was found to be superior in providing accurate modelling for inverter circuit design. PSPICE comprises of libraries of components according to manufacturer's specification which can lead to obtaining realistic simulation result. It also includes an extensive library of commercial electric components. Hence, OrCAD PSPICE was adopted for simulating the proposed inverter circuit in this research.
  
10. The proposed inverter operating under different loads (pure resistive load and highly inductive load) were verified experimentally. The measured THD of output voltage across pure resistive load was consistent with the theoretical estimated results and the simulation results. Meanwhile, the measured THD of output voltage across highly inductive load was consistent with the simulation results.
  
11. The proposed inverter was simulated, showing the full wave rectified near sine (multi-level) voltage across H-bridge circuit is generated by applying the control signals (proposed variable duty cycle control technique) fed to the associated power switch. Also, showing its performance producing near AC output voltage waveform. The simulation result proved that the new designed inverter able to generate near sinusoidal AC output voltage with low total harmonics distortion. It showed an effective way of generating multi-level/staircase voltage waveform using a reduced number of components

(power switches and capacitors) and single DC sources. This was proved experimentally showing its feasibility in the reduction in the number of components used compared to VSI PWM inverter and multi-level inverters i.e. Cascaded H-Bridge Multi-Level Inverter and Switched-Capacitor Boost Multi-Level Inverter.

12. The simulation result of the new DC/AC inverter topology was discussed from different views, which is considered as a major contribution to knowledge in this thesis as follows:

- Contribution of a different way of generating staircase/multi-level voltage waveform using a DSSC switched-capacitor circuit with variable duty cycle control technique;
- Contribution to present the new DC/AC inverter-based switched-capacitor circuit topology with reduced number of components showing its merits compared to existing multi-level inverter based switched-capacitor circuit topology.

The system testing and practical implementation were conducted. The simulation and experimental results are compared which shows good agreement between practical and simulation results of the new proposed inverter. This will allow researchers to appreciate the performance of this developed DSSC switched-capacitor circuit with variable duty cycle control technique by modifying other DC/AC inverter topologies (multi-stage) for component reduction in future, as well as appreciating the new designed inverter for use in low power applications.

## 6.2 Future Works

The following suggestions for future works are to improve the implementation of the proposed inverter system.

- An investigation is required to assess the proposed inverter suitability to work in three-phase AC system high power applications.
- More investigation on Triplen switch configurations of switched-capacitor circuit with appropriate control technique can be conducted to prove its suitability to work as a voltage regulator (to the DC input voltage to different voltage levels). The current rating flow through auxiliary resistor should be controlled in order to have minimum power dissipation leading to high efficiency of the overall system.
- More investigation should be done in improving power losses and efficiency performance of the proposed inverter by adding lossless snubber circuit. The snubber circuit can be used to limit switch voltage stress  $dv/dt$  and reduce switching losses in switch device. It also provides protection for power switch devices.
- A closed-loop control system can be implemented to suitably control the charging capacitor in switched capacitor circuit to achieve more number of voltage levels in order to improve output voltage resolution.
- An accurate cost analysis of the proposed inverter system at manufacturing stage can be carried out.

## References

- A. Rahim, K. Chaniago & J. Selvaraj 2011, "Single-Phase Seven-Level Grid-Connected Inverter for Photovoltaic System", *IEEE Transactions on Industrial Electronics*, vol. 58, no. 6, pp. 2435-2443.
- A. Silva 2013, "Advanced DC/AC Inverters: Applications in Renewable Energy (Luo, F.L. and Ye, H.; 2013) [Book News]", *IEEE Industrial Electronics Magazine*, vol. 7, no. 4, pp. 68-69.
- Alamri, B. & Darwish, M. 2014, "Precise modelling of switching and conduction losses in cascaded h-bridge multilevel inverters", *Power Engineering Conference (UPEC), 2014 49th International Universities*, pp. 1.
- Alepuz, S., Busquets-Monge, S., Bordonau, J., Gago, J., Gonzalez, D. & Balcells, J. 2006, "Interfacing Renewable Energy Sources to the Utility Grid Using a Three-Level Inverter", *Industrial Electronics, IEEE Transactions on*, vol. 53, no. 5, pp. 1504-1511.
- Amini & M. Moallem 2017, "A Fault-Diagnosis and Fault-Tolerant Control Scheme for Flying Capacitor Multilevel Inverters", *IEEE Transactions on Industrial Electronics*, vol. 64, no. 3, pp. 1818-1826.
- Anderson & F. Z. Peng 2008, "Four quasi-Z-Source inverters", *2008 IEEE Power Electronics Specialists Conference*, pp. 2743.
- Arman, M.F. & Darwish, M.K. 2009, "Critical Review of Cascaded H-Bridge Multilevel Inverter Topologies", *International Review of Electrical Engineering*, vol. 4, no. 5, pp. 703-743.
- Axelrod, Y. Berkovich & A. Ioinovici 2005, "A cascade boost-switched-capacitor-converter - two level inverter with an optimized multilevel output waveform", *IEEE Transactions on Circuits and Systems I: Regular Papers*, vol. 52, no. 12, pp. 2763-2770.
- Babaei & S. S. Gowgani 2014, "Hybrid Multilevel Inverter Using Switched Capacitor Units", *IEEE Transactions on Industrial Electronics*, vol. 61, no. 9, pp. 4614-4621.
- Bailu Xiao, Filho, F. & Tolbert, L.M. 2011, "Single-phase cascaded H-bridge multilevel inverter with nonactive power compensation for grid-connected photovoltaic generators", *Energy Conversion Congress and Exposition (ECCE), 2011 IEEE*, pp. 2733.
- Barbosa, P.G., Braga, H.A.C., Rodrigues, M.C.B. & Teixeira, E.C. 2006, "Boost current multilevel inverter and its application on single-phase grid-connected

photovoltaic systems", *Power Electronics, IEEE Transactions on*, vol. 21, no. 4, pp. 1116-1124.

Barzegarkhoo, E. Zamiri, N. Vosoughi, H. M. Kojabadi & L. Chang 2016, "Cascaded multilevel inverter using series connection of novel capacitor-based units with minimum switch count", *IET Power Electronics*, vol. 9, no. 10, pp. 2060-2075.

Barzegarkhoo, H. M. Kojabadi, E. Zamiry, N. Vosoughi & L. Chang 2016, "Generalized Structure for a Single Phase Switched-Capacitor Multilevel Inverter Using a New Multiple DC Link Producer With Reduced Number of Switches", *IEEE Transactions on Power Electronics*, vol. 31, no. 8, pp. 5604-5617.

Beig, A.R. & Dekka, A. 2012, "Experimental verification of multilevel inverter-based standalone power supply for low-voltage and low-power applications", *Power Electronics, IET*, vol. 5, no. 6, pp. 635-643.

Bellar, M.D., Wu, T., Tchamdjou, A., Mahdavi, J. & Ehsani, M. 1998, "A review of soft-switched DC-AC converters", *Industry Applications, IEEE Transactions on*, vol. 34, no. 4, pp. 847-860.

Bragard, M., Soltau, N., Thomas, S. & De Doncker, R.W. 2010, "The Balance of Renewable Sources and User Demands in Grids: Power Electronics for Modular Battery Energy Storage Systems", *Power Electronics, IEEE Transactions on*, vol. 25, no. 12, pp. 3049-3056.

C. Marouchos, D. Xenofontos, M. Darwish, M. S. Moghadam & C. Armefti 2014, "The switched capacitor inverter as a MPPT in a photovoltaic application", *2014 49th International Universities Power Engineering Conference (UPEC)*, pp. 1.

Caceres, R.O. & Barbi, I. 1999, "A boost DC-AC converter: analysis, design, and experimentation", *Power Electronics, IEEE Transactions on*, vol. 14, no. 1, pp. 134-141.

Calais, M. & Agelidis, V.G. 1998, "Multilevel converters for single-phase grid connected photovoltaic systems-an overview", *Industrial Electronics, 1998. Proceedings. ISIE '98. IEEE International Symposium on*, pp. 224.

Carrasco, J.M., Franquelo, L.G., Bialasiewicz, J.T., Galvan, E., Guisado, R.C.P., Prats, M.A.M., Leon, J.I. & Moreno-Alfonso, N. 2006, "Power-Electronic Systems for the Grid Integration of Renewable Energy Sources: A Survey", *Industrial Electronics, IEEE Transactions on*, vol. 53, no. 4, pp. 1002-1016.

Chakraborty and S. Dalapati "A new voltage source inverter realized by controlled capacitor charging", *Conf.Rec.International Power Electronic Conference (IPEC 2005)*, , pp. 2023-2029.

Chan, M.S. & Chau, K. 2007, "A new switched-capacitor boost-multilevel inverter using partial charging", *Circuits and Systems II: Express Briefs, IEEE Transactions on*, vol. 54, no. 12, pp. 1145-1149.

Chellammal, N., Dash, S.S., Velmurugan, V. & Gurram, R. 2012, "Power quality improvement using multilevel inverter as series active filter", *Emerging Trends in Science, Engineering and Technology (INCOSET), 2012 International Conference on*, pp. 450.

D. Mahale & R. J. Patil 2016, "Comparative analysis of various impedance source inverters", *2016 International Conference on Automatic Control and Dynamic Optimization Techniques (ICACDOT)*, pp. 207.

Daher, S., Schmid, J. & Antunes, F.L.M. 2008, "Multilevel Inverter Topologies for Stand-Alone PV Systems", *Industrial Electronics, IEEE Transactions on*, vol. 55, no. 7, pp. 2703-2712.

Darwish, B. R. Alamri & C. Marouchos 2015, "OrCAD vs Matlab Simulink in teaching power electronics", *2015 50th International Universities Power Engineering Conference (UPEC)*, pp. 1.

De, S., Banerjee, D., Gopakumar, K., Ramchand, R. & Patel, C. 2011, "Multilevel inverters for low-power application", *IET Power Electronics*, vol. 4, no. 4, pp. 384-392.

Ertl, H., Kolar, J.W. & Zach, F.C. 2002, "A novel multicell DC-AC converter for applications in renewable energy systems", *Industrial Electronics, IEEE Transactions on*, vol. 49, no. 5, pp. 1048-1057.

Fang Zheng Peng, Jih-Sheng Lai, McKeever, J. & VanCoevering, J. 1995, "A multilevel voltage-source inverter with separate DC sources for static VAr generation", *Industry Applications Conference, 1995. Thirtieth IAS Annual Meeting, IAS '95., Conference Record of the 1995 IEEE*, pp. 2541.

Floricau & L. Kreindler 2015, "Generalized multilevel inverter topology with stacked coupled inductors", *2015 17th European Conference on Power Electronics and Applications (EPE'15 ECCE-Europe)*, pp. 1.

Fri, A., El Bachtiri, R. & El Ghzizal, A. 2013, "Comparative study of H-bridge multilevel inverters dedicated to PV", *Renewable and Sustainable Energy Conference (IRSEC), 2013 International*, pp. 67.

G. Georgakas, P. N. Vovos & N. A. Vovos 2014, "Harmonic Reduction Method for a Single-Phase DC-AC Converter Without an Output Filter", *IEEE Transactions on Power Electronics*, vol. 29, no. 9, pp. 4624-4632.

Georgakas, K.G., Vovos, P.N. & Vovos, N.A. 2014, "Harmonic Reduction Method for a Single-Phase DC-AC Converter Without an Output Filter", *Power Electronics, IEEE Transactions on*, vol. 29, no. 9, pp. 4624-4632.

Ghasemi, N., Zare, F., Boora, A.A., Ghosh, A., Langton, C. & Blaabjerg, F. 2012, "Harmonic elimination technique for a single-phase multilevel converter with unequal DC link voltage levels", *Power Electronics, IET*, vol. 5, no. 8, pp. 1418-1429.

He & C. Cheng 2016, "A Flying-Capacitor-Clamped Five-Level Inverter Based on Bridge Modular Switched-Capacitor Topology", *IEEE Transactions on Industrial Electronics*, vol. 63, no. 12, pp. 7814-7822.

Heldwein, M.L. & Kolar, J.W. 2009, "Impact of EMC filters on the power density of modern three-phase PWM converters", *Power Electronics, IEEE Transactions on*, vol. 24, no. 6, pp. 1577-1588.

*IEEE Recommended Practice and Requirements for Harmonic Control in Electric Power Systems* 2014, .

J. C. Rosas-Caro, J. C. Mayo-Maldonado, F. Mancilla-David, A. Valderrabano-Gonzalez & F. Beltran Carbajal 2015, "Single-inductor resonant switched capacitor voltage multiplier with safe commutation", *IET Power Electronics*, vol. 8, no. 4, pp. 507-516.

J. C. Rosas-Caro, J. M. Ramirez, F. Z. Peng & A. Valderrabano 2010, "A DC-DC multilevel boost converter", *IET Power Electronics*, vol. 3, no. 1, pp. 129-137.

J. Liu, K. W. E. Cheng & Y. Ye 2014, "A Cascaded Multilevel Inverter Based on Switched-Capacitor for High-Frequency AC Power Distribution System", *IEEE Transactions on Power Electronics*, vol. 29, no. 8, pp. 4219-4230.

J. Zeng, J. Wu, J. Liu & H. Guo 2017, *A Quasi-Resonant Switched-Capacitor Multilevel Inverter With Self-Voltage Balancing for Single-Phase High-Frequency AC Microgrids*.

Jiang & T. A. Lipo 1998, "Switching angles and DC link voltages optimization for multilevel cascade inverters", *1998 International Conference on Power Electronic Drives and Energy Systems for Industrial Growth, 1998. Proceedings.*, pp. 56.

Jih-Sheng Lai & Fang Zheng Peng 1995, "Multilevel converters-a new breed of power converters", *Industry Applications Conference, 1995. Thirtieth IAS Annual Meeting, IAS '95., Conference Record of the 1995 IEEE*, pp. 2348.

Jing Huang & K. Corzine 2004, "Extended operation of flying capacitor multilevel inverters", *Conference Record of the 2004 IEEE Industry Applications Conference, 2004. 39th IAS Annual Meeting.*, pp. 813.

K. K. Gupta, A. Ranjan, P. Bhatnagar, L. K. Sahu & S. Jain 2016, "Multilevel Inverter Topologies With Reduced Device Count: A Review", *IEEE Transactions on Power Electronics*, vol. 31, no. 1, pp. 135-151.

K. Peter & V. Agarwal 2017, "Photovoltaic Module-Integrated Stand-alone Single-Stage Switched Capacitor Inverter with Maximum Power Point Tracking", *IEEE Transactions on Power Electronics*, vol. 32, no. 5, pp. 3571-3584.

K. Sano & H. Fujita 2008, "Voltage-Balancing Circuit Based on a Resonant Switched-Capacitor Converter for Multilevel Inverters", *IEEE Transactions on Industry Applications*, vol. 44, no. 6, pp. 1768-1776.

Lin, B.-. & Hung, T.-. 2002, "Analysis and implementation of a single-phase multilevel inverter for power quality improvement", *Industrial Electronics, 2002. ISIE 2002. Proceedings of the 2002 IEEE International Symposium on*, pp. 1235.

M. Darwish & C. Marouchos 2014, "Modular OrCAD simulation approach in teaching power electronics", *2014 49th International Universities Power Engineering Conference (UPEC)*, pp. 1.

M. Darwish & P. Mehta 1990, "Switched-capacitor technique for power electronic applications", *21st Annual IEEE Conference on Power Electronics Specialists*, pp. 698.

M. Darwish, P. Mehta & T. Thomson 1988, "Variable characteristic filters", *Third International Conference on Power Electronics and Variable-Speed Drives*, pp. 424.

M. F. Arman, C. C. Marouchos & M. K. Darwish 2012, "Self-tuning output passive-filter for low power DC/AC inverters", *2012 47th International Universities Power Engineering Conference (UPEC)*, pp. 1.

M. Forouzesh, Y. P. Siwakoti, S. A. Gorji, F. Blaabjerg & B. Lehman 2017, *Step-Up DC-DC Converters: A Comprehensive Review of Voltage Boosting Techniques, Topologies, and Applications*.

M. H. H. Rozlan, M. K. Darwish, A. Sallama & M. Khodapanah 2015, "Low loss inverter circuit based on buck and boost topology", *2015 50th International Universities Power Engineering Conference (UPEC)*, pp. 1.

Machado Martins, J. Antenor Pomilio & S. Buso 2001, "A single-phase low-frequency commutation inverter for renewables", *Industrial Electronics Society, 2001. IECON '01. The 27th Annual Conference of the IEEE*, pp. 1976.

Madouh, J., Ahmed, N.A. & Al-Kandari, A.M. 2012, "Advanced power conditioner using sinewave modulated buck-boost converter cascaded polarity

changing inverter", *International Journal of Electrical Power & Energy Systems*, vol. 43, no. 1, pp. 280-289.

Malad, C.P. & Rao, K.U. 2012, "Simulation of a buck-boost single phase voltage source inverter for distribution generation systems", *Int.J.Modern Eng.Res*, vol. 2, no. 5, pp. 3628-3632.

Malathy, S., Ramaprabha, R. & Mathur, B.L. 2013, "Asymmetrical multilevel inverters for partially shaded PV systems", *Circuits, Power and Computing Technologies (ICCPCT), 2013 International Conference on*, pp. 579.

Marchesoni, M., Mazzucchelli, M. & Tenconi, S. 1990, "A nonconventional power converter for plasma stabilization", *Power Electronics, IEEE Transactions on*, vol. 5, no. 2, pp. 212-219.

Marouchos, M. Darwish, M. S. Moghadam & M. Georgiou 2015, "A new switched capacitor inverter for stand alone photovoltaic applications", *2015 50th International Universities Power Engineering Conference (UPEC)*, pp. 1.

Martins, G.M., Pomilio, J.A. & Buso, S. 2001, "A single-phase low-frequency commutation inverter for renewables", *Industrial Electronics Society, 2001. IECON '01. The 27th Annual Conference of the IEEE*, pp. 1976.

Mecke, R. 2011, "Multilevel NPC inverter for low-voltage applications", *Power Electronics and Applications (EPE 2011), Proceedings of the 2011-14th European Conference on*, pp. 1.

Mellitt & M. H. Rashid 1974, "Analysis of d.c. chopper circuits by computer-based piecewise-linear technique", *Electrical Engineers, Proceedings of the Institution of*, vol. 121, no. 3, pp. 173-178.

Moghadam, M., Darwish, M. & Marouchos, C. 2013, "A simple drive induction motor based on buck/boost inverter topology", *Power Engineering Conference (UPEC), 2013 48th International Universities'IEEE*, , pp. 1.

Moghadam, M.S. & Darwish, M. 2012, "A buck/boost based Multilevel inverter topology for UPEC2012 conference proceeding", *Universities Power Engineering Conference (UPEC), 2012 47th International*, pp. 1.

Moir 1999, "More-electric aircraft-system considerations", *IEE Colloquium on Electrical Machines and Systems for the More Electric Aircraft (Ref. No. 1999/180)*, pp. 10/1.

Mosazadeh, S.Y., Fathi, S.H. & Radmanesh, H. 2012, "New high frequency switching method of cascaded multilevel inverters in PV application", *Power Engineering and Renewable Energy (ICPERE), 2012 International Conference on*, pp. 1.

Nabae, I. Takahashi & H. Akagi 1981, "A New Neutral-Point-Clamped PWM Inverter", *IEEE Transactions on Industry Applications*, vol. IA-17, no. 5, pp. 518-523.

Panagis, P., Stergiopoulos, F., Marabeas, P. & Manias, S. 2008, "Comparison of state of the art multilevel inverters", *Power Electronics Specialists Conference, 2008. PESC 2008. IEEE*, pp. 4296.

Pereda, J. & Dixon, J. 2013, "Cascaded Multilevel Converters: Optimal Asymmetries and Floating Capacitor Control", *Industrial Electronics, IEEE Transactions on*, vol. 60, no. 11, pp. 4784-4793.

R. Beig & A. Dekka 2012, "Experimental verification of multilevel inverter-based standalone power supply for low-voltage and low-power applications", *IET Power Electronics*, vol. 5, no. 6, pp. 635-643.

R. de Souza Santos, T. B. Lazzarin & I. Barbi 2015, "A new half-bridge Hybrid Switched-Capacitor inverter", *2015 IEEE 13th Brazilian Power Electronics Conference and 1st Southern Power Electronics Conference (COBEP/SPEC)*, pp. 1.

R. Lai, F. Wang, R. Burgos, Y. Pei, D. Boroyevich, B. Wang, T. A. Lipo, V. D. Immanuel & K. J. Karimi 2008, "A Systematic Topology Evaluation Methodology for High-Density Three-Phase PWM AC-AC Converters", *IEEE Transactions on Power Electronics*, vol. 23, no. 6, pp. 2665-2680.

Rodriguez, J., Jih-Sheng Lai & Fang Zheng Peng 2002, "Multilevel inverters: a survey of topologies, controls, and applications", *Industrial Electronics, IEEE Transactions on*, vol. 49, no. 4, pp. 724-738.

S. De, D. Banerjee, K. S. Kumar, K. Gopakumar, R. Ramchand & C. Patel 2011, "Multilevel inverters for low-power application", *IET Power Electronics*, vol. 4, no. 4, pp. 384-392.

Sabahi, M., Marami Iranaq, A.R.M., Bahrami, K.M., Bahrami, K.M. & Sharifian, M.B.B. 2011, "Harmonics elimination in a multilevel inverter with unequal DC sources using genetic algorithm", *Electrical Machines and Systems (ICEMS), 2011 International Conference on*, pp. 1.

Sanjeev, P. & Jain, S. 2013, "Analysis of conduction and switching losses in two level inverter for low power applications", *India Conference (INDICON), 2013 Annual IEEE*, pp. 1.

Shamil, M., Darwish, M. & Marouchos, C. 2012, "Single phase Multi level inverter with desire harmonics", *Universities Power Engineering Conference (UPEC), 2012 47th International*, pp. 1.

Shinohara, H., Kimoto, K., Itami, T., Ambou, T., Okado, C., Nakajima, K., Hojo, S., Owada, K., Kuniyoshi, M. & Sato, Y. 1994, "Development of a residential use, utility interactive PV inverter with isolation transformer-less circuit-development aspects", *Photovoltaic Energy Conversion, 1994.*, Conference Record of the Twenty Fourth. IEEE Photovoltaic Specialists Conference - 1994, 1994 IEEE First World Conference on, pp. 1216.

Shukla, A., Ghosh, A. & Joshi, A. 2012, "Control of dc capacitor voltages in diode-clamped multilevel inverter using bidirectional buck-boost choppers", *Power Electronics, IET*, vol. 5, no. 9, pp. 1723-1732.

Silva, F. 2013, "Advanced DC/AC Inverters: Applications in Renewable Energy (Luo, F.L. and Ye, H.; 2013) [Book News]", *Industrial Electronics Magazine, IEEE*, vol. 7, no. 4, pp. 68-69.

Taghvaei, J. Adabi & M. Rezanejad 2016, "Circuit Topology and Operation of a Step-Up Multilevel Inverter With a Single DC Source", *IEEE Transactions on Industrial Electronics*, vol. 63, no. 11, pp. 6643-6652.

Tolbert, L.M. & Peng, F.Z. 2000, "Multilevel converters as a utility interface for renewable energy systems", *Power Engineering Society Summer Meeting, 2000. IEEE*, pp. 1271.

Tsunoda, Y. Hinago & H. Koizumi 2012, "A grid connected inverter with switched capacitor inverter using series/parallel conversion", *2012 15th International Power Electronics and Motion Control Conference (EPE/PEMC)*, pp. LS7c.4-1.

Van der Broeck, H. & Miller, M. 1995, "Harmonics in DC to AC converters of single phase uninterruptible power supplies", *Telecommunications Energy Conference, 1995. INTELEC '95., 17th International*, pp. 653.

Velmurugan, V., Chellammal, N. & Abirami, R. 2013, "Power quality conditioning using Hybrid multilevel inverter as UPQC", *Circuits, Power and Computing Technologies (ICCPCT), 2013 International Conference on*, pp. 43.

X. Sun, B. Wang, Y. Zhou, W. Wang, H. Du & Z. Lu 2016, "A Single DC Source Cascaded Seven-Level Inverter Integrating Switched-Capacitor Techniques", *IEEE Transactions on Industrial Electronics*, vol. 63, no. 11, pp. 7184-7194.

Xue, Y., Chang, L., Kjaer, S.B., Bordonau, J. & Shimizu, T. 2004, "Topologies of single-phase inverters for small distributed power generators: an overview", *Power Electronics, IEEE Transactions on*, vol. 19, no. 5, pp. 1305-1314.

Y. Hinago & H. Koizumi 2012, "A Switched-Capacitor Inverter Using Series/Parallel Conversion With Inductive Load", *IEEE Transactions on Industrial Electronics*, vol. 59, no. 2, pp. 878-887.

Y. Ye, K. W. E. Cheng, J. Liu & K. Ding 2014, "A Step-Up Switched-Capacitor Multilevel Inverter With Self-Voltage Balancing", *IEEE Transactions on Industrial Electronics*, vol. 61, no. 12, pp. 6672-6680.

Z. Bai, Z. Zhang & Y. Zhang 2007, "A Generalized Three-Phase Multilevel Current Source Inverter with Carrier Phase-Shifted SPWM", *2007 IEEE Power Electronics Specialists Conference*, pp. 2055.

Zamiri, N. Vosoughi, S. H. Hosseini, R. Barzegarkhoo & M. Sabahi 2016, "A New Cascaded Switched-Capacitor Multilevel Inverter Based on Improved Series-Parallel Conversion With Less Number of Components", *IEEE Transactions on Industrial Electronics*, vol. 63, no. 6, pp. 3582-3594.

Zhong Du, Ozpineci, B., Tolbert, L.M. & Chiasson, J.N. 2009, "DC-AC Cascaded H-Bridge Multilevel Boost Inverter With No Inductors for Electric/Hybrid Electric Vehicle Applications", *Industry Applications, IEEE Transactions on*, vol. 45, no. 3, pp. 963-970.

## **Appendix A**

## **Arduino C-language Program Code: Switching Control Pattern Generation**

The following Arduino C-language Program Code shows the generation of the switching pattern pulses signals ( $S_1$  and  $S_2$ ) applied to the two power MOSFETs switches ( $S_1$ ) and ( $S_2$ ) in Double Switches Single Capacitor (DSSC) circuit. Each of power semiconductor MOSFETs used in the proposed circuit are controlled by the microcontroller (Arduino Uno). The control signals ( $S_1$  and  $S_2$ ) are in anti-parallel operation ( $S_1$  is HIGH(ON) and  $S_2$  is LOW(OFF)).

```
const int OutPin1 = 11; // control signals(S1)
const int OutPin2 = 10; // control signal (S2)

void setup()
{
    pinMode(OutPin1,OUTPUT);
    pinMode(OutPin2,OUTPUT);
}

void loop()
{
    digitalWrite(11, HIGH); //
    digitalWrite(10, LOW); //
    delayMicroseconds(10000); // On for 10ms

    digitalWrite(11, LOW); //
    digitalWrite(10, HIGH); //
    delayMicroseconds(10000); // On for 10ms
```

```

while(digitalRead(OutPin1) == HIGH)//while pin 11 high, perform looping
{
    for (int i = 1; i <= 4; i++) //repeat 4 cycles
    {
        // DutyCycle(D)=95% or D=0.95
        digitalWrite(13, LOW); //
        digitalWrite(12, HIGH); //
        delayMicroseconds(19); // On for 19us

        digitalWrite(13, HIGH); //
        digitalWrite(12, LOW); //
        delayMicroseconds(1); // Off for 1 microseconds
    }

    for (int i = 1; i <= 3; i++) //repeat 3 cycles
    {
        // DutyCycle(D)=85% or D=0.85
        digitalWrite(13, LOW); //
        digitalWrite(12, HIGH); //
        delayMicroseconds(17); // On for 17us

        digitalWrite(13, HIGH); //
        digitalWrite(12, LOW); //
        delayMicroseconds(3); // Off for 3 microseconds
    }

    for (int i = 1; i <= 3; i++) //repeat 3 cycles

```

```

{
// DutyCycle(D)=75% or D=0.75
digitalWrite(13, LOW); //
digitalWrite(12, HIGH); //
delayMicroseconds(15); // On for 15us

digitalWrite(13, HIGH); //
digitalWrite(12, LOW); //
delayMicroseconds(5); // Off for 5 microseconds
}

for (int i = 1; i <= 4; i++) //repeat 3 cycles
{
// DutyCycle(D)=65% or D=0.65
digitalWrite(13, LOW); //
digitalWrite(12, HIGH); //
delayMicroseconds(13); // On for 15us

digitalWrite(13, HIGH); //
digitalWrite(12, LOW); //
delayMicroseconds(7); // Off for 5 microseconds
}

for (int i = 1; i <= 4; i++) //repeat 3 cycles
{
// DutyCycle(D)=55% or D=0.55
digitalWrite(13, LOW); //
digitalWrite(12, HIGH); //
delayMicroseconds(11); // On for 15us
}

```

```

digitalWrite(13, HIGH); //
digitalWrite(12, LOW); //
delayMicroseconds(9); // Off for 5 microseconds
}

for (int i = 1; i <= 14; i++) //repeat 7 cycles
{
// DutyCycle(D)=40% or D=0.4
digitalWrite(13, LOW); //
digitalWrite(12, HIGH); //
delayMicroseconds(8); //

digitalWrite(13, HIGH); //
digitalWrite(12, LOW); //
delayMicroseconds(12); //
}

for (int i = 1; i <= 4; i++) //repeat 3 cycles
{
// DutyCycle(D)=55% or D=0.55
digitalWrite(13, LOW); //
digitalWrite(12, HIGH); //
delayMicroseconds(11); // On for 15us

digitalWrite(13, HIGH); //
digitalWrite(12, LOW); //
delayMicroseconds(9); // Off for 5 microseconds
}

for (int i = 1; i <= 4; i++) //repeat 3 cycles

```

```

{
// DutyCycle(D)=65% or D=0.65
digitalWrite(13, LOW); //
digitalWrite(12, HIGH); //
delayMicroseconds(13); // On for 15us

digitalWrite(13, HIGH); //
digitalWrite(12, LOW); //
delayMicroseconds(7); // Off for 5 microseconds
}

for (int i = 1; i <= 3; i++) //repeat 3 cycles
{
// DutyCycle(D)=75% or D=0.75
digitalWrite(13, LOW); //
digitalWrite(12, HIGH); //
delayMicroseconds(15); // On for 15us

digitalWrite(13, HIGH); //
digitalWrite(12, LOW); //
delayMicroseconds(5); // Off for 5 microseconds
}

for (int i = 1; i <= 3; i++) //repeat 3 cycles
{
// DutyCycle(D)=85% or D=0.85
digitalWrite(13, LOW); //
digitalWrite(12, HIGH); //
delayMicroseconds(17); // On for 17us
}

```

```
digitalWrite(13, HIGH); //
digitalWrite(12, LOW); //
delayMicroseconds(3); // Off for 3 microseconds
}

for (int i = 1; i <= 4; i++) //repeat 4 cycles
{
// DutyCycle(D)=95% or D=0.95
digitalWrite(13, LOW); //
digitalWrite(12, HIGH); //
delayMicroseconds(19); // On for 19us

digitalWrite(13, HIGH); //
digitalWrite(12, LOW); //
delayMicroseconds(1); // Off for 1 microseconds
}

}
```

## **Appendix B**

## List of Publications

M. H. H. Rozlan, M. K. Darwish, A. Sallama & M. Khodapanah 2015, "Low loss inverter circuit based on buck and boost topology", *2015 50th International Universities Power Engineering Conference (UPEC)*, pp. 1.

M. Khodapanah, A. F. Zobaa, M. H. H. Rozlan, & M. Abbod 2015, "Monitoring of power factor for induction machines using estimation techniques", *2015 50th International Universities Power Engineering Conference (UPEC)*, pp. 1.

M. H. H. Rozlan, M. K. Darwish, "A components reduction in switched-capacitor multilevel inverters topologies using resonant switched-capacitor circuit technique", *International Review of Electrical Engineering*, Submitted in May 2017.